

8-2021

SYNTHETIC ESSENTIALITY OF TDO2 IN APC-MUTATED COLORECTAL CANCER

Rumi Lee

Follow this and additional works at: https://digitalcommons.library.tmc.edu/utgsbs_dissertations



Part of the [Medicine and Health Sciences Commons](#)

Recommended Citation

Lee, Rumi, "SYNTHETIC ESSENTIALITY OF TDO2 IN APC-MUTATED COLORECTAL CANCER" (2021). *The University of Texas MD Anderson Cancer Center UTHealth Graduate School of Biomedical Sciences Dissertations and Theses (Open Access)*. 1132.

https://digitalcommons.library.tmc.edu/utgsbs_dissertations/1132

This Dissertation (PhD) is brought to you for free and open access by the The University of Texas MD Anderson Cancer Center UTHealth Graduate School of Biomedical Sciences at DigitalCommons@TMC. It has been accepted for inclusion in The University of Texas MD Anderson Cancer Center UTHealth Graduate School of Biomedical Sciences Dissertations and Theses (Open Access) by an authorized administrator of DigitalCommons@TMC. For more information, please contact digitalcommons@library.tmc.edu.

**SYNTHETIC ESSENTIALITY OF TDO2 IN APC-MUTATED COLORECTAL
CANCER**

by

Rumi Lee, M.S.

APPROVED:

Ronald DePinho, M.D.
Advisory Professor

Guillermina Lozano, Ph.D.

Scott Kopetz, M.D., Ph.D.

Glen Traver Hart, Ph.D.

Y. Alan Wang, Ph.D.

APPROVED:

Dean, The University of Texas
MD Anderson Cancer Center UTHealth Graduate School of Biomedical
Sciences

**SYNTHETIC ESSENTIALITY OF TDO2 IN APC-MUTATED COLORECTAL
CANCER**

A

DISSERTATION

Presented to the Faculty of

The University of Texas

MD Anderson Cancer Center UTHealth

Graduate School of Biomedical Sciences

in Partial Fulfillment

of the Requirements

for the Degree of

DOCTOR OF PHILOSOPHY

by

Rumi Lee, M.S.

Houston, Texas

August 2021

ACKNOWLEDGEMENTS

First, I would like to thank my Ph.D. mentor, Dr. Ron DePinho. I could not end this journey without Dr. DePinho's support and mentoring. He showed me what it is like to have a true mentor and I truly appreciate his tremendous patience in helping me navigate through my study. I am thankful for the opportunity to be trained as a graduate student with him and be part of his lab.

I would also like to express my sincere gratitude for my advisory committee members, Dr. Guillermina Lozano, Dr. Scott Kopetz, Dr. Traver Hart and Dr. Alan Wang. I really appreciate their constructive advice and encouragement for my projects throughout the years. Their endless support really improved my project and knowledge in cancer biology.

I thank the many current and former DePinho lab member that I have had the pleasure of working with over the course of my Ph.D. training. As fellow Ph.D. students and incredible friends, I also would like to thank Dong Joo Rhee, Jiah Yang, and Min Seon Kim who made my life in Houston so much happier. I cannot thank enough for my friends in Korea, Kyung Eun Yeun, Su Jeong Kim, Seung Yun Jo, Hyang Choi, Seung Hwan Gong and Seungh Ho Shin, for always checking up on me whether I am doing fine.

My biggest thanks to my family for all the support you have shown me through years of distance learning. Their support and unconditional love allowed me to pursue my career and dreams.

SYNTHETIC ESSENTIALITY OF TDO2 IN APC-MUTATED COLORECTAL CANCER

Rumi Lee, M.S.

Advisory Professor: Ronald DePinho, M.D.

Inactivation of the adenomatous polyposis coli (APC) tumor suppressor is common genetic event across many cancers and serves a critical initiating event in the majority of sporadic colorectal cancers (CRC). The WNT/APC pathway remains an elusive target for cancer, prompting us to explore orthogonal strategies to identify specific vulnerabilities for APC-deficient CRC and other cancers. Using the concept of synthetic essentiality (SE), we sought to identify essential effectors of APC deficiency with the goal of expanding targetable vulnerabilities in CRC. We identified Tryptophan 2,3-dioxygenase 2 (TDO2) as an SE gene for APC-deficient cancers. Mechanistically, APC loss results in TCF4/ β -catenin-mediated activation of TDO2 gene transcription. TDO2 in turn activates the Kyn-AhR pathway which boosts glycolysis, promotes proliferation, and upregulates CXCL5 which recruits macrophages into the tumor microenvironment (TME). These tumor-associated macrophages not only suppress anti-tumor immunity but serve to support cancer cell survival via their secretion of GAS6 which activates AXL in cancer cells, consistent with heterotypic symbiotic signaling in the TME. Thus, APC-deficiency activates a TCF4-TDO2-AhR-

CXCL5-GAS6-AXL circuit that impacts multiple cancer hallmarks via autonomous and non-autonomous mechanisms, and illuminates new therapeutic targets for APC mutant cancers.

TABLE OF CONTENTS

APPROVAL	i
TITLE.....	ii
ACKNOWLEDGEMENTS	iii
ABSTRACT	iv
TABLE OF CONTENTS	vi
LIST OF ILLUSTRATIONS.....	xi
Chapter 1: Introduction.....	2
1.1 Adenomatous polyposis coli (APC)	2
1.1.1 Overview	2
1.1.2 APC in Wnt signaling.....	4
1.1.3 WNT signaling in colorectal cancers	6
1.1.4 Current cancer interventions for WNT/APC signaling	10
1.2 Synthetic Essentiality	11
1.3. Tryptophan 2,3-Dioxygenase.....	14
1.3.1 Overview	14
1.3.2 Kynurenine pathway.....	15
1.3.3 Aryl hydrocarbon receptor signaling.....	18
1.3.4 IDO/TDO2-Kyn-AhR signaling in cancer	20
1.4. Tumor-associated macrophages	21

1.4.1 Overview	21
1.4.2 Tumor-associated macrophages in cancer	22
1.4.3 Tumor associated macrophages-targeting interventions	23
1.5 Growth arrest specific 6- Axl axis	24
1.5.1 Overview	24
1.5.2 Gas6-Axl axis in Cancer.....	26
Chapter 2: Materials and methods	28
2.1 Mice	29
2.2 Cell Culture	29
2.3 CRISPR-Cas9 Transfection.....	30
2.4 Mouse Colon Organoid Culture and Genome Engineering	30
2.5 Mouse APCmin Organoids	31
2.6 Human Samples	31
2.7 Mutual exclusivity analysis.....	32
2.8 TCGA data computational analysis	32
2.9 Gene stable shRNA/siRNA knockdown and inducible shRNA knockdown	33
2.10 Western blot.....	35
2.11 Hairpin-resistant ORF and cytokine ORF expression.....	36
2.12 Luciferase assay.....	36
2.13 Cytokine array and phospho-RTK array	37

2.14 Immunohistochemistry and immunofluorescence.....	37
2.15 Migration assay.....	37
2.16 Colony formation assay	38
2.17 TDO2 inhibitor and Epacadostat treatment	38
2.18 Mass Cytometry (CyTOF).....	38
2.19 Kyn, 2-DG uptake and lactate secretion measurement.....	39
2.20 LC-MS/MS-Based Targeted Metabolomics	39
2.21 ChIP–sequencing and ChIP-PCR.....	40
2.22 mRNA expression analysis, microarray and RNA sequencing.....	41
2.23 Quantification and statistical analysis	42
Chapter 3: Identification of synthetic essential genes for APC mutations	44
3.1 Introduction and rationale	44
3.2 Results.....	44
3.2.1 Identification of TDO2 as a downstream effector for APC deficiency in cancer	44
3.2.2 TDO2 expression is correlated with WNT activation in CRC	51
3.2.3 APC deficiency upregulates TDO2 expression via transcription factor TCF4	57
Chapter 4: Cancer cell autonomous signaling mediated by TDO2 in APC-mutant CRC cancer.....	64

4.1 Introduction and rationale	64
4.2 Results.....	65
4.2.1 TDO2 depletion specifically impairs growth and survival of APC/ WNT- mutated CRC cells	65
4.2.2 TDO2 depletion specifically impairs tumor growth and survival of APC/ WNT-mutated CRC cells in vivo.....	71
4.2.3 TDO2-Kyn-AhR axis supports APC-deficient cancer cell proliferation, survival, and tumorigenic potential.....	81
4.2.4 TDO2-Kyn-AhR axis regulates glycolysis pathway of APC-mutant CRC cancer cells.	87
Chapter 5: TDO2 regulates infiltration of tumor associated macrophage in APC- mutated CRC.....	96
5.1 Introduction and rationale	96
5.2 Results.....	97
5.2.1 TDO2 depletion inhibits infiltration of tumor associated macrophages	97
5.2.2 TDO2 depletion inhibits infiltration of tumor associated macrophages in human CRC	103
5.2.3 TDO2 modulates TAM infiltration by regulating cytokines	105
5.2.4 TDO2-AhR-CXCL5 modulates TAM infiltration and polarization in APC- mutant CRC	109
5.2.5 TDO2-AhR-CXCL5 in human TCGA datasets	115

Chapter 6: A symbiotic relationship between APC-mutant CRC cells and tumor associated macrophages	119
6.1 Introduction and rationale	119
6.2 Results.....	120
6.2.1 GAS6 is upregulated by CXCL5 in macrophages and promotes cancer cell growth	120
6.2.2 Kyn and CXCL5 upregulate GAS6 in macrophages and polarize them into M2 macrophage phenotype	121
6.2.3 Depletion of Gas6 in macrophages impairs tumor growth in vivo	124
Chapter 7: Conclusions, discussion, and future direction	127
7.1. Conclusions and discussion	127
7.2 Future directions	133
BIBLIOGRAPHY.....	134
VITA.....	150

LIST OF ILLUSTRATIONS

Figure 1: human APC protein structure.....	3
Figure 2: WNT signaling pathway	5
Figure 3: Conceptual frames to discover genetic context-specific cancer vulnerabilities.....	13
Figure 4: Kynurenine pathway.....	17
Figure 5: AhR signaling	19
Figure 6: Roles of TAMs in tumor biology.	23
Figure 7: Mutual exclusive patterns of TDO2 and APC/CTNNB1 in TCGA database of multiple cancer types.....	47
Figure 8: TDO2 as a synthetic essential gene for mutant APC gene in CRC.	49
Figure 9: TDO2 as a synthetic essential gene for mutant APC/CTNNB1 gene in BRCA.	50
Figure 10: Upregulated TDO2 expression in human CRC TMA.	53
Figure 11: Upregulated TDO2 expression in mouse CRC tumors and organoids. ...	55
Figure 12: Analysis of IDO1/2 for mutual exclusive patterns with mutant APC and correlation with WNT pathway in CRC.....	56
Figure 13: Increased TDO2 expression upon APC deletion in human and mouse CRC cell lines.....	59
Figure 14: TCF4/TCF7L2 mediates upregulation of TDO2 in APC-mutated CRC cells.	60
Figure 15: Depletion of TCF4/TCF7L2 decreases TDO2 expression in APC-mutated CRC cells.	62

Figure 16: Depletion of TDO2 leads to impaired colony formation in human APC-mutated CRC cells.	68
Figure 17: TDO2 depletion reduces colony formation ability and increases cell death in murine APC-mutated CRC cells and organoids.	69
Figure 18: TDO2 knockdown impairs tumor growth of human CRC cells in vivo.....	73
Figure 19: TDO2 depletion specifically impairs growth of APC/WNT-mutated murine CRC cells in vivo.	76
Figure 20: Anti-tumorigenic activity of TDO2 inhibitor specifically in APC-deficient CRC tumors.....	80
Figure 21: Upregulated TDO2 activates kynurenine pathway and AhR signaling in APC-mutant CRC cells.....	84
Figure 22: TDO2-Kyn-AhR axis supports APC-deficient cancer cell proliferation, survival, and tumorigenic potential.	86
Figure 23: Glycolysis pathway is increased by APC deficiency and decreased by TDO2 depletion in MC38 cells.....	89
Figure 24: TDO2-AhR axis regulates glycolysis pathway in APC-deleted MC38 cells.	92
Figure 25: Glycolytic flux is regulated by the TDO2-AhR axis.....	93
Figure 26: TDO2 mediates tumor growth by regulating macrophage infiltration.	100
Figure 27: Increased macrophage infiltration mediated by APC deficiency is reversed by TDO2 inhibition in MC38 tumors.	102
Figure 28: TDO2 expression correlates with M2-like macrophage signature expression.	104

Figure 29: Cytokines secreted from APC-deficient CRC cells promote macrophage migration, which is inhibited by TDO2 knockdown.	106
Figure 30: TDO2-AhR-CXCL5 axis regulates macrophage recruitment in APC-mutated CRC tumors.....	108
Figure 31: TDO2-AhR-CXCL5 axis regulates macrophage polarization.....	112
Figure 32: Macrophage depletion or CXCL5 neutralization inhibit APC-deleted tumor growth and improve survival.....	114
Figure 33: CXCL5 expression is correlated with TDO2-AhR pathway and macrophage infiltration in human CRC.	117
Figure 34: APC-deficient CRC cells promote macrophage-derived Gas6, which binds to Axl on tumor cells.	123
Figure 35: Gas6 secreted by macrophages promotes tumor growth.	125
Figure 36: Working model	128

CHAPTER 1: INTRODUCTION

Chapter 1: Introduction

1.1 Adenomatous polyposis coli (APC)

1.1.1 Overview

The discovery of *APC* gene first initiated with the observation that chromosome 5q21 band is deleted in a patient with Garner's syndrome (Herrera et al., 1986), which is a subtype of a subtype of familial adenomatous polyposis (FAP). Family studies with FAP mapped the *APC* gene to 5q51 (Bodmer et al., 1987) and the cloning and identification of *APC* gene were followed (Grodin et al., 1991, Kinzler et al., 1991). Human APC protein has 2,843 amino acid (aa) residues (mouse APC: 2,842 aa) and is comprised of an oligomerization domain, an armadillo repeat-domain, a basic domain, and binding domains for EB1 and disc large (DLG) proteins (Fig. 1) (Fearnhead et al., 2001). The oligomerization domain contains the heptad repeats that allow APC proteins to form helical homodimers (Joslyn et al., 1993). The armadillo domain interacts with IQ-motif-containing GTPase activation protein 1 (IQGAP1) and APC-Stimulated Guanine Nucleotide Exchange Factor (ARHGEF4/29) and activates Cdc42 and Rac1, which in turn modulates cell migration and adhesion by remodeling actin cytoskeleton (Kawasaki et al., 2000, Watanabe et al., 2004). Between the Armadillo domain and the basic domain, multiple 15- and 20- residue repeats and serine-alanine-methionine-proline (SAMP) repeats are located and are able to bind to β -catenin and Axin. Importantly, the mutation cluster region (MCR) consists of several 20-aa repeat motifs is critical for β -catenin turnover and is prone to mutations (Xing et al., 2004, Kohler et al., 2008). The basic region and EB1/DLG-binding domains interact with microtubules and

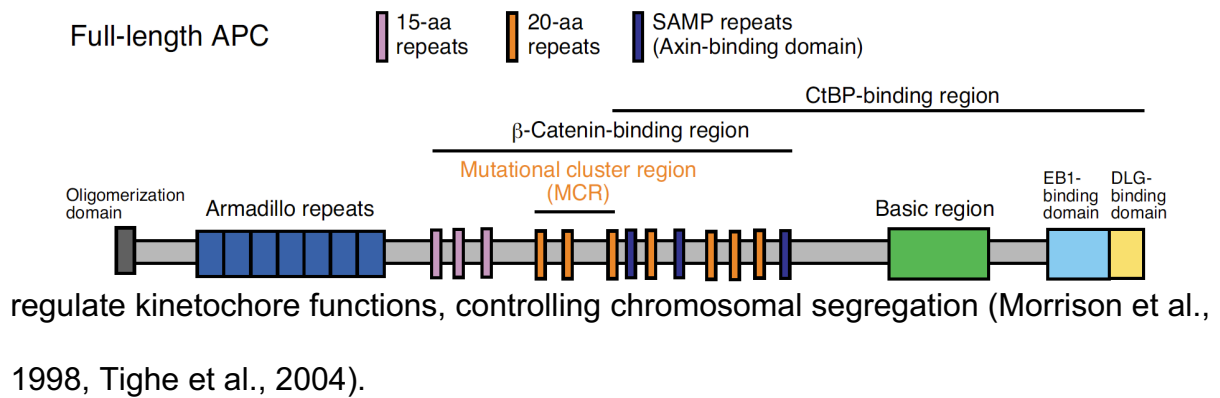


Figure 1: human APC protein structure

Human APC protein contains oligomerization domain and Armadillo repeats in its N-terminal and EB1- and DLG-binding domains in the C-terminal. β -catenin-binding region interacts with β -catenin and mutations of APC mostly occur in the mutational cluster region (MCR).

(Figure is reproduced from Aoki and Taketo, Adenomatous polyposis coli (APC): a multi-functional tumor suppressor gene. *Journal of Cell Science*. 2007; 120, 3327-3335, with permission from Copyright Clearance Center)

APC plays crucial roles in development and cellular homeostasis. In mice, *APC* gene homozygous deletion leads to embryonic lethality at 5.5.d.p.c (Ishikawa et al., 2003, Moser et al., 1995) and heterozygous knockout leads to defective thymic development (Gounari et al., 2005) and FAP phenotype in the intestine (Oshima et al., 1995). In addition, *in vitro* analysis showed that depletion of APC in human and mouse cell lines resulted in chromosomal instability and dysregulated cell migration (Dikovskaya et al., 2007, Kawasaki et al., 2003).

1.1.2 APC in Wnt signaling

Wnt signaling is highly conserved between species and plays a central role in regulating tissue homeostasis and development. Canonical Wnt pathway controls cellular processes through modulating the level of its key effector β -catenin. Phosphorylation and ubiquitin-mediated degradation of β -catenin suppress the activity of Wnt signaling and are regulated by β -catenin destruction complex. The complex is comprised of AXIN, APC, casein kinase 1 (CK1), and glycogen synthase kinase 3 β (GSK3 β) (Fig. 2). When Wnt ligand is absent, GSK3 β and CK1 phosphorylate β -catenin N-terminal and consequently recruited the E3 ligase β -transducin repeats-containing proteins (β -TrCP) ubiquitinates β -catenin. Ubiquitinated β -catenin are subjected to proteasomal-mediated degradation. Conversely, in the presence of Wnt ligand, it binds to the receptor Frizzled (FZD) with co-receptor low-density lipoprotein-related protein 5/6 (LRP5/6) and recruits the destruction complex to the membrane via a scaffold protein Dishevelled (DVL). The

interaction between DVL and AXIN elicits the dissociation of β -TrCP, resulting in intact β -catenin. Accumulated β -catenin translocates to the nucleus and displaces the Wnt repressor Groucho (Gro)/ transducin-like Enhancer of split (TLE) from key Wnt transcription factors T cell factor (TCF)/lymphoid enhancer-binding factor (LEF) and induces downstream Wnt target genes.

1.1.3 WNT signaling in colorectal cancers

Colorectal cancer (CRC) is the second leading cause of cancer-related death in developed countries and responsible for more than 600,000 deaths globally each year. The evolution of CRC from adenoma to adenocarcinoma and ultimately invasive and metastatic disease is governed by the serial acquisition of signature alterations that includes the loss of APC and p53 tumor suppressors and the mutational activation of the KRAS oncogene (Orchard et al., 2013). Up-regulation of the WNT pathway is frequently observed in the consensus molecular subtype 2 (CMS2) subtype of CRC (8), which accounts for nearly 40% of early-stage colorectal tumors. Dysregulated Wnt signaling by mutations in key Wnt player genes leads to dysregulated cell proliferation, survival, and ultimately promote tumorigenesis.

APC gene mutations

The *APC* gene functions as a tumor suppressor gene and loss of *APC* is the critical initiating event which occurs in the vast majority (~90%) of sporadic CRC. Inactivating mutations of the *APC* gene mostly occurs in the MCR region and include deletion, single-base substitutions, and insertions resulting in truncated APC

proteins. It is estimated that above 75% reduction in APC protein level is sufficient to form a polyp (Taketo, 2006). APC multiple intestinal neoplasia (APCMin) mice harboring a heterozygous *APC* gene mutation at codon 850 develop adenomatous polyps mostly in the small intestine (Su et al., 1992). Beyond initiation of neoplasia, CRC mouse models have also established a role of APC in tumor maintenance (Mao et al., 2015).

Germline mutations of *APC* gene predispose an individual to hereditary cancer syndrome FAP. The most frequent *APC* gene loss-of-function germline mutations occurs at codon 1,061 and 1,309, which are located in the MCR (Fig. 1) (Fearnhead et al., 2001). The severity and the number of polyps in FAP are correlated with where the mutations occurred; mutations within the MCR often cause severe polyposis and patients with mutations located at the 5' or 3' of the *APC* gene tend to show less severe FAP phenotype, attenuated adenomatous polyposis coli syndrome (Fearon, 2011). Mutations in genes in DNA repair signaling such as MutL Homolog 1 (*MLH1*) and Post-meiotic Segregation Homolog 2 (*PMS2*) in addition to *APC* germline mutations are found in Turcot's syndrome, which is characterized by multiple polyps in colon with higher risk of CRC and brain cancers (medulloblastomas and glioblastoma) (Fearon, 2011). Interestingly, mutations at codon 1,307I>K and 1,317E>Q, albeit modestly, lead to error-prone replication of *APC* gene and predispose the loss of functional APC proteins (Sieber et al., 2003). Multiple polymorphisms by SNPs in the *APC* genes have been identified (1458T>C, 4479G>A, 5268T>G) but the correlation with the variants to risk of developing FAP or CRC remains to be determined (Chen et al., 2006).

CRC tumors developed from FAP patients often exhibit loss-of heterozygosity (LOH) of *APC* gene and the additional somatic mutations are associated with the germline mutations in the MCR. Somatic mutations of *APC* gene in CRC are mostly frameshift and nonsense mutations and they are usually clustered between codon 1,309 and 1,450 (Novellasmunt et al., 2015). Mutated APC proteins lack the β -catenin and AXIN binding sites, resulting β -catenin accumulation and dysregulated activation of Wnt downstream genes including *C-MYC*, *AXIN2*, matrix metalloproteinase 7 (*MMP-7*), fibroblast growth factor 9 (*FGF9*) and *CD44* (For an extensive list of Wnt signaling target genes; <http://web.stanford.edu/group/nusselab/cgi-bin/wnt/>).

Besides the mutations in the *APC* gene on the genomic level, multiple ways to downregulate the expression of the *APC* gene in cancer cells have been identified. Epigenetic silencing of *APC* gene by hypermethylation of promoter CpG island, mostly in the 1A promoter region, is frequently shown in metastatic CRC and is correlated with worse prognosis (Chen et al., 2005, van Engeland et al., 2011, Liang et al., 2017). In addition, microRNA (miRNA) miR-494 is overexpressed in CRC and negatively regulates the *APC* gene (Zhang et al., 2018) and long intergenic non-coding RNAs (LncRNAs) CACS15 represses the expression of APC via Enhancer Of Zeste 2 Polycomb Repressive Complex 2 Subunit (EZH2) in ovarian cancer (Liu et al., 2019).

Other Wnt pathway genes mutations

CRC tumors often harbor loss of function mutations of multiple components of Wnt signaling, leading to pathway dysregulation. Somatic mutations of *CTNNB1*

gene, which encodes β -catenin protein, are rarely present in *APC* mutation-harboring CRC but can be detected in subsets of CRCs without *APC* mutations (Novellasmunt et al., 2015, Morin et al., 2016). Mutations in the *CTNNB1* gene predominately occurs at the amino acid residues that are phosphorylated by CK1 and GSK3 β in the N-terminal domain, resulting in accumulation of β -catenin (Liu et al., 2002). Scaffold protein AXIN is encoded by *AXIN1* and *AXIN2* and their germline (only found in *AXIN2*) and somatic mutations lead to uncontrolled activation of β -catenin (Fearon, 2011). The *AXIN1* mutations are mostly missense mutations in exon 5 and *AXIN2* mutations are frequently C-terminal domain truncating mutations in exon 7 (Mazzoni and Fearon, 2014). Hypermethylation of *AXIN2* gene is also found in CRC and shows association with initiating events of CRC (Koinuma et al., 2006).

Ring finger protein 43 (RNF43) and Zinc And Ring Finger 3 (ZNRF3) are ubiquitin ligases that are expressed in Lgr5⁺ intestinal stem cells and mediates degradation of Wnt receptor FZD5 via endocytosis, acting as a negative regulator of Wnt signaling (Koo et al., 2012). Hot spots for frameshift mutation in RNF43 gene include codon R117 and G659 which are frequently found in CRC (Giannakis et al., 2014). Interestingly, *RNF43* mutations are mutually exclusive to *APC* mutations in CRC and predominantly present in microsatellite instable-High (MSI-H) subtype of CRC (Giannakis et al., 2014). One of the downstream targets of Wnt signaling R-spondin (RSPO) is a secreted protein and promotes endocytosis-mediated internalization of RNF43/ZNRF3, allowing the Wnt receptor complex to activate the downstream pathway (Fischer and Sigal, 2019, Hao et al., 2012). Genomic analysis

of colon tumors and matched normal colon tissues revealed recurrent *RSPO* gene fusion with Eukaryotic Translation Initiation Factor 3 Subunit E (*EIF3E*) or Protein Tyrosine Phosphatase Receptor Type K (*PTPRK*), further activating Wnt signaling (Seshagiri et al., 2012). Wilms tumor gene on the X chromosome (*WTX*)/*FAM123B* is associated with Wilms tumor and functions as a tumor suppressor gene. *WTX* forms the β -catenin destruction complex with APC, AXIN, β -TrCP2 and regulates turnover of β -catenin (Major et al., 2007) and about 10% of CRC tumors harbor *WTX* truncating mutations (TCGA, Firehose Legacy). In addition, epigenetic silencing by promoter hypermethylation of Wnt negative regulators such as Dickkopf WNT Signaling Pathway Inhibitor 1 (*DKK1*) (Rawson et al., 2011), Secreted frizzled-related protein 1 (*SFRP*) (Suzuki et al., 2004), and WNT Inhibitory Factor 1 (*WIF1*) (Taniguchi et al., 2005) have been identified in CRC.

1.1.4 Current cancer interventions for WNT/APC signaling

Since APC loss and upregulation of Wnt signaling occurs frequently across many other cancer types, motivating efforts to understand more fully the function of APC and its signaling pathway in governing specific hallmarks of cancer and to illuminate therapeutic strategies targeting key pathway components or synthetic lethal interactions. Given its importance in cancer, the therapeutic targeting of this APC signaling cascade remains an important goal for cancer therapy. Currently, the agents targeting WNT pathway include inhibition of WNT ligands, β -catenin degrading complex, TCF/LEF, and Notch and Sonic Hedgehog signaling that crosstalk with WNT. To date, these WNT targeting programs have yet to produce meaningful clinical results.

1.2 Synthetic Essentiality

The concept of synthetic lethality can be exploited to specifically target cancer cells with alterations of tumor suppressor genes (TSGs). A set of genes is considered 'synthetic lethal' when a combination of mutations in two genes leads to cell death, whereas the cell is viable with loss of only one gene (9-11). However, synthetic lethality screens can be limited to in vitro studies, which may not recapitulate the in vivo biology of tumorigenesis and the diversity of human cancer types. To overcome these constraints, DePinho lab developed a novel conceptual frame 'synthetic essentiality (SE)' (12). SE genes are specifically crucial for growth and survival of cancer with TSG deficiency (Fig. 3). These SE genes are rarely mutated or deleted in tumors harboring mutant TSGs, creating mutual exclusive patterns in human genomic data such as TCGA. We reasoned that these genes may be essential for cancer-specific processes and would therefore be potential therapeutic targets in cancers specifically harboring that tumor suppressor deficiency.

To identify SE genes, genome-scale human datasets are analyzed for mutual exclusiveness patterns for mutant TSGs (13). Expression profiles and clinical databases can also be utilized to prioritize SE candidates. Functional validation of putative SE genes involves in vitro assays and in vivo study (i.e. mouse models, drug treatment). This approach uncovered the chromatin helicase DNA-binding factor (CHD1) as an SE gene in PTEN-deleted cancers (14). CHD1 mutation profiles in TCGA prostate cancer datasets exhibit a mutual exclusive pattern with PTEN deletion. Deletion of PTEN leads to failure of CHD1 phosphorylation and its

subsequent ubiquitination, resulting accumulation of CHD1 and increased expression of NF- κ B target genes in prostate cancer cells. This study was followed up by validating the importance of CHD1 mouse model. ICB study. Expanding the concept to other TSGs may provide an opportunity for the discovery of targetable vulnerabilities in cancers with undruggable gene mutations.

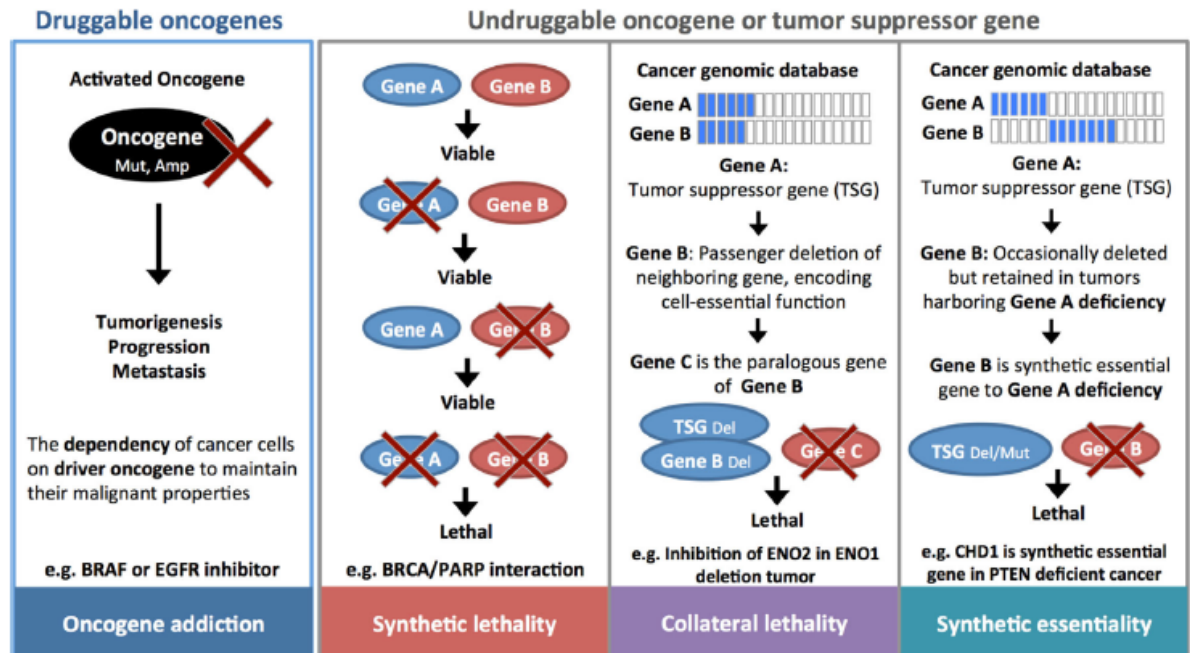


Figure 3: Conceptual frames to discover genetic context-specific cancer vulnerabilities.

Synthetic essentiality (SE) describes an approach to identify synthetic essential genes that are specifically crucial for growth and survival of cancer with tumor suppressor gene deficiency.

(Figure is reproduced from Zhao and DePinho, Synthetic essentiality: Targeting tumor suppressor deficiencies in cancer. Bioessays. 2017; 39, 8, 1700076 with permission from Copyright Clearance Center)

1.3. Tryptophan 2,3-Dioxygenase

1.3.1 Overview

Tryptophan 2,3-Dioxygenase (TDO2) gene is located in chromosome 4q32.1. As one of the enzymes that catalyze the first and rate-limiting step of the kynurenine pathway, TDO2 gene was first mapped and cloned for behavior disorder study (**Comings et al., 1991**) due to its functions in serotonin (5-hydroxytryptamine) metabolism. Mutations in TDO2 gene are associated with pervasive developmental disorder, Tic disorder, and multiple behavioral disorders in human (Comings et al., 1991). TDO2 knockout mice exhibit increased tryptophan (Trp) and 5-HIAA (5-hydroxyindoleacetic acid) plasma levels, anxiety-related behavior, and increased neural progenitor cells in the hippocampus (Kanai et al., 2009).

Human TDO2 protein is a 406nt-long, heme-containing cytosolic protein and is highly conserved in mouse (83.53% similar to human TDO2) (Ball et al., 2014). The protein forms helixes with a flexible loop and is consisted of two substrate binding domains and iron (heme-ligand) binding domain. Usually, TDO2 proteins are tetrameric, and the loops are hypothesized to be induced by substrate binding, especially L-Trp (Kanai et al., 2009). TDO2 protein is known to be interacting with several other proteins, including ASMTL (Acetylserotonin O-Methyltransferase Like), EIF4E (Eukaryotic translation initiation factor 4E), and PRMT6 (Protein Arginine Methyltransferase 6) (Meng et al., 2014). Multiple sites have been identified for TDO2 post-translational modification (PTM) in S23, S155, T200, T212, and S369, in which are all conserved in mouse TDO2 as well (Hornbeck et al., 2015).

Known regulation mechanisms of TDO2 expression can be categorized into three groups: 1) Substrate (L-Trp) and co-factor activation 2) Heme-mediated mechanism 3) Hormone induction. Specifically, expression of TDO2 by hormones is induced when the hormones bind to their responsive elements including glucocorticoid-responsive elements (GREs) for glucagon and estrogen response elements (EREs) for estrogen (Ott et al., 2015).

1.3.2 Kynurenine pathway

Tryptophan (Trp) is an essential amino acid that has a variety of functions within the cell, including synthesis of proteins, muscles, neurotransmitters (Cervenka et al., 2017). Kynurenine pathway (KP) is the major tryptophan (Trp) catabolism pathway in mammals and converts Trp into N- formylkynurenine (Kyn) (Fig. 4). This metabolic pathway produces nicotinamide adenine dinucleotide (NAD⁺) and nicotinamide from Trp in (intrahepatic) and outside the liver (extrahepatic), which regulates systematic Trp levels and its metabolites in the body.

TDO2 and Indoleamine 2,3-dioxygenase (IDO) 1/2 mediate the first and rate-limiting step of the KP. Evolutionally, IDO and TDO2 are not phylogenetically linked but they are an example of functional convergence. In normal tissues, IDO is expressed in tissues throughout the body, whereas TDO2 is predominantly expressed in the liver. In a physiological setting, TDO2 almost solely regulates the intrahepatic Trp conversion and IDO functions as an extrahepatic KP regulator. Interestingly, IDO and TDO2 enzymes, especially in mammals, show differences in substrate selectivity. IDO can be bound to wide range of indole-containing substrates but

TDO2 is specific to the L-Trp enantiomer. Recent studies have shown that the non-redundant roles and differential expression of IDO and TDO2 in cancer cells, raising the possibility of TDO2 inhibition as new therapeutic opportunity.

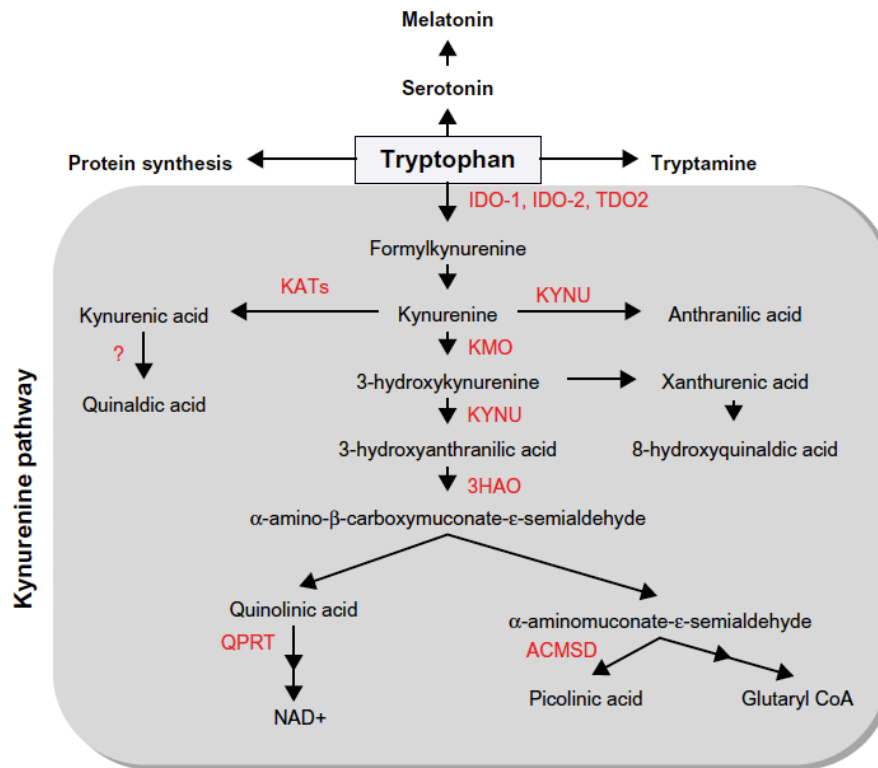


Figure 4: Kynurenine pathway.

Tryptophan metabolism by kynurenine pathway. Red letters indicate enzymes involved in the pathway. IDO, Indoleamine 2,3-dioxygenase; TDO2, Tryptophan 2,3-dioxygenase; KYNU, Kynureninase; KATs, Kynurenine aminotransferases; KMO, Kynurenine 3-monooxygenase; 3HAO, 3-hydroxyanthranilic acid oxygenase; ACMSD, Aminocarboxymuconate-semialdehyde decarboxylase; QPRT, quinolinic acid phosphoribosyltransferase.

(Figure is reproduced from Jones, Guillemin, and Brew, The Kynurenine Pathway in Stem Cell Biology. International Journal of Tryptophan Research. 2013; 6 57–66 with permission from Copyright Clearance Center)

1.3.3 Aryl hydrocarbon receptor signaling

The Aryl hydrocarbon receptor (AhR) belongs to the basic helix-loop-helix/Per-Arnt-Sim (bHLH/PAS) transcription factor superfamily that responds to environmental sensors (Gutierrez-Vazquez and Quintana, 2018), such as planar aromatic (aryl) hydrocarbons and 2,3,7,8 -tetrachlorodibenzo-p-dioxin (TCDD). AhR is activated by ligand binding and regulates xenobiotic-metabolizing enzymes including CYP1A/B1/2 (Cytochrome P450 Family 1 Subfamily A/B Member 1/2) and glutathione S-transferase (Andersson et al., 2002).

AhR harbors nuclear export and localization signal domains and can shuttle nuclear-cytoplasmic compartments. When ligands are absent, AhR is cytoplasm-localized and forms a complex with heat shock protein 90 (HSP90) and HBV X-associated protein 2 (XAP2), which also known as aryl hydrocarbon receptor interacting protein (AIP) (Fig. 5). Upon agonist binding, AhR nuclear translocator (ARNT) displaces HSP90 from the AhR complex and translocates it to the nucleus. The AhR complex binds to the dioxin-responsive element (DRE) and recruit co-activators (Fig. 5).

AhR ligands include indole metabolites, tryptophan metabolites, heme-derived, and arachidonic acid metabolites (Gutierrez-Vazquez and Quintana, 2018). Especially, tryptophan metabolites, as a physiological source of AhR ligands, are majorly produced by KP in the cells and regulate AhR-mediated immune responses and cellular signaling. AhR mediates a myriad of signaling pathways that are not only critical for environmental danger sensing but also energy metabolism, cell proliferation, metabolite synthesis/transport,

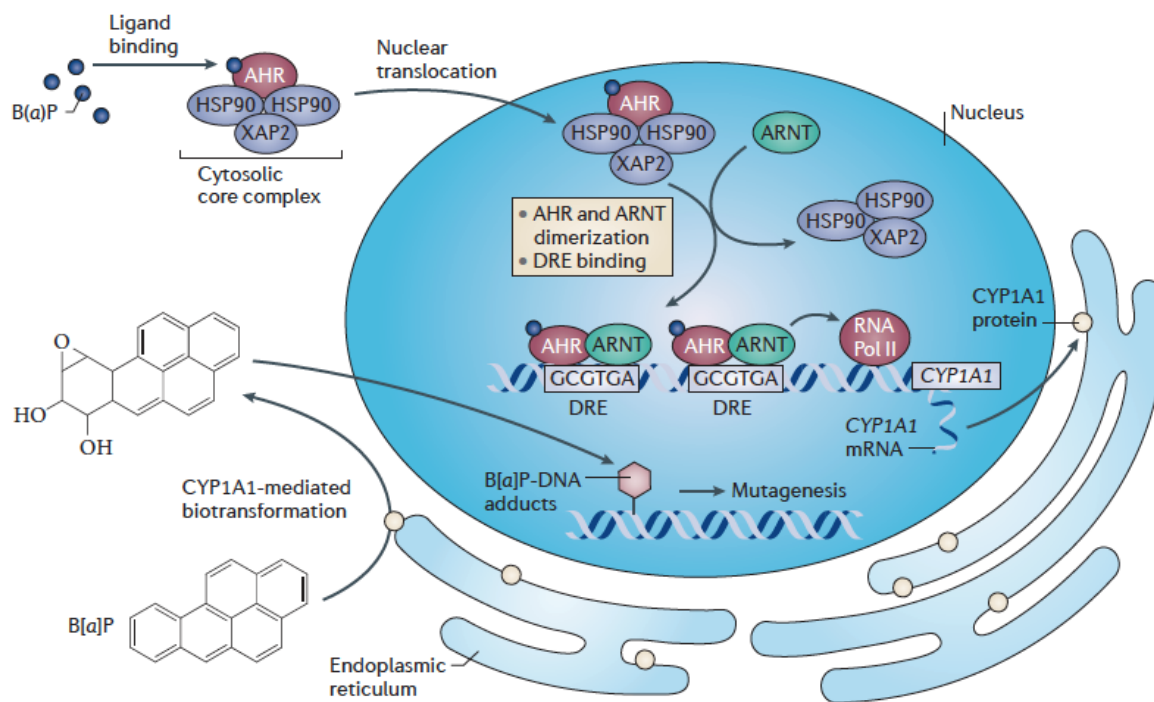


Figure 5: AhR signaling

Regulation of AhR in the presence of AhR ligands. AHRR, AHR repressor; ARNT, AHR nuclear translocator; XRE, xenobiotic response element.

(Figure is reproduced from Murray, Patterson and Perdew, Aryl hydrocarbon receptor ligands in cancer: friend and foe. Nature Cancer Review. 2014; 14, 801-814 with permission from Copyright Clearance Center)

and inflammation. In addition, AhR knockout mice exhibit slower growth, impaired fertility, decreased liver weights, and cardiovascular defects, suggesting the roles of AhR in development.

1.3.4 IDO/TDO2-Kyn-AhR signaling in cancer

It is well established that Trp catabolism plays a critical role in immune suppression and cancer cell proliferation. TDO2 is highly expressed and constitutively active in diverse cancers, such as glioblastoma, colorectal carcinoma, and breast carcinoma (Pilotte et al., 2012). Up-regulated KP by increased TDO2 depletes Trp and accumulates Kyn, creating an immunosuppressive tumor microenvironment (TME). Kyn acts as an agonist for AhR and differentiate naïve CD4⁺ T helper (Th) cells to regulatory T cell (Tregs). In contrast, Kyn-AhR pathway inhibits interleukin-17 (IL-17)-producing Th (Th17) cell differentiation (Prendergast, 2011).

Importantly, AhR directly regulates immune functions of different types of immune cells, further modulating TME. AhR in CD8⁺ T cells, when bound to Kyn, induces programmed cell death protein 1 (PD1) expression and mediates immune evasion (Liu et al., 2018). Activation of AhR in tumor-associated macrophages (TAMs) increases CCR2 expression and promotes infiltration into the tumor site (Takenaka et al., 2019). AhR also regulates proliferation of Tregs and tolerogenic myeloid cells, leading to immune resistance in glioblastoma (Campesato et al., 2020).

Besides the immune modulatory functions of AhR, it can also regulate cancer cell intrinsic signaling and promote tumor initiation and progression. AhR activation inhibits cell-cell adhesion, which leads to unhinged cell proliferation and deregulated migration (Dietrich and Kaina, 2010). Interestingly, upon AhR ligand binding, Src and EGFR pathways crosstalk with AhR downstream signaling to further activate cancer cell proliferation and growth (Ye et al., 2018).

1.4. Tumor-associated macrophages

1.4.1 Overview

Monocyte precursors to macrophages can undergo polarization and differentiation depending on the cellular microenvironment and express specific sets of genes and phenotypic characteristics which determine their functions (Mantovani et al., 2002). Discovery on the distinctive gene expression in macrophages when treated with interleukin (IL)-4 (Nathan et al., 1983, Stein et al., 1992) initiated the classification of macrophages based on their gene expression profiles; M1 (classically activated) and M2 (alternatively activated) (Mantovani et al., 2002). Most well studied cytokines and chemokines that polarize monocytes include interferon-gamma (IFN γ) and lipopolysaccharide (LPS) for M1-type and IL-4 and IL-13 for M2-type macrophages (Pathria et al., 2019). Once polarized, each population express distinctive membrane receptors and effector molecules. M1 macrophages express CD80, CD86, and opsonic receptors such as Fc γ -RI, II, III (CD16, CD32, CD64), whereas M2 express CD163 and non-opsonic receptors such as Fc ϵ -RII (CD23) and mannose receptor (MR) (Brown et al., 2017). Classically activated M1 cells produce pro-inflammatory cytokines, reactive oxygen/nitrogen species to promote Th1

responses and mediate microbicidal functions. Alternatively activated M2 cells, in contrast, produce arginase and anti-inflammatory cytokines, inhibiting tumor immune resistance and regulating tumor progression (Mantovani et al., 2002). Due to the M2 cells' pro-tumorigenic functions, they are also called tumor-associated macrophages (TAMs). However, oversimplified functional grouping which is mostly based on marker expression in the macrophages does not correctly explain the diverse and reversible functions of immune cells. This issue prompted researchers to classify macrophages into more detailed subtypes; M2a, M2b, M2c, and M2d (Roszer, 2015), based on the transcriptional changes upon environmental stimuli.

1.4.2 Tumor-associated macrophages in cancer

Tumor-associated macrophages (TAMs) can directly promote tumor growth by secreting angiogenic factors (VEGF, PDGF), growth factors (EGF, FGF), and cytokines (IFN- β) (Liu and Cao, 2015) (Fig. 6). The secreted factors from TAMs also include Matrix metalloproteinases (MMPs) which are responsible for matrix remodeling, metastasis, and recruitment of more monocytes. TGF- β and CCL2 signal fibroblasts to infiltrate TME and induce fibrosis within the tumor (Pathria et al., 2019).

Importantly, TAMs regulate a variety of immune cell types that play critical role in tumorigenesis by producing cytokines and chemokines and altering the target cell functions or proliferation (Fig. 6). CCL18 from TAMs induces anergy of naïve T cells and CCL22 and CCL17 recruit Th2 cells and Tregs into the tumor site, making TME immunosuppressive (Liu and Cao, 2015).

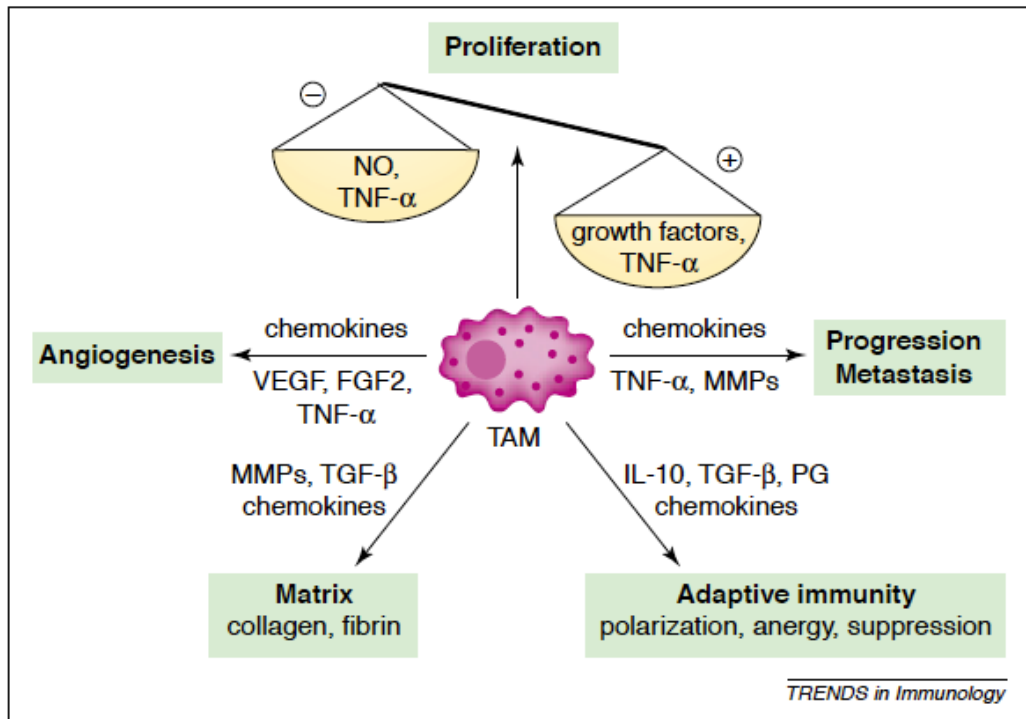


Figure 6: Roles of TAMs in tumor biology.

TAMs not only regulate various cell intrinsic pathways but also modulate immune responses, promoting tumor progression and immune evasion.

(Figure is reproduced from Mantovani, Sozzani, Locati, Allavena and Sica. Macrophage polarization: tumor-associated macrophages as a paradigm for polarized M2 mononuclear phagocytes. *TRENDS in Immunology*. 2002; Vol.23 No.11 with permission from Copyright Clearance Center)

1.4.3 Tumor associated macrophages-targeting interventions

Various ways to target TAMs have been tested in preclinical studies due to multiple functions of TAMs in promoting tumorigenesis. Inhibition of colony stimulating factor 1 receptor (CSF1R), one of the key TAM receptors, comprises the viability of TAMs and this approach has shown promising preclinical results in prostate and GBM cancer models (Stafford et al., 2016, Xu et al., 2013). Blocking phenotype-specific receptors, such as CXCR4 and

CXCR7, to inhibit the cell recruitment showed improved radiation response in multiple mouse tumor models (Domanska et al., 2014, Walters et al., 2014). Antagonizing the secretory factors from TAMs with anti-VEGF and anti-CXCL12 has been also investigated in the preclinical settings (Brown et al., 2017).

1.5 Growth arrest specific 6- Axl axis

1.5.1 Overview

Axl (UFO, ARK, TYRO7), along with Tyro3 (SKY, BRT, DTK, RSE, TIF) and Mer (EYK, NTK, TYRO12), is a part of the TAM receptor tyrosine kinase (RTK) family (Fig. 7) The TAM family members are transmembrane proteins which are consisted of two immunoglobulin-like (IgL) extracellular domains which are connected to tandem fibronectin type III repeats, transmembrane domain, and a cytoplasmic portion that contains kinase domain. The TAM family is unusual RTKs because they have no significant functions in embryonic developmental processes but have shown their roles in mediating cellular signaling and pathological implications such as proliferation, apoptosis, invasion, and immune responses. To the TAM RTKs, growth

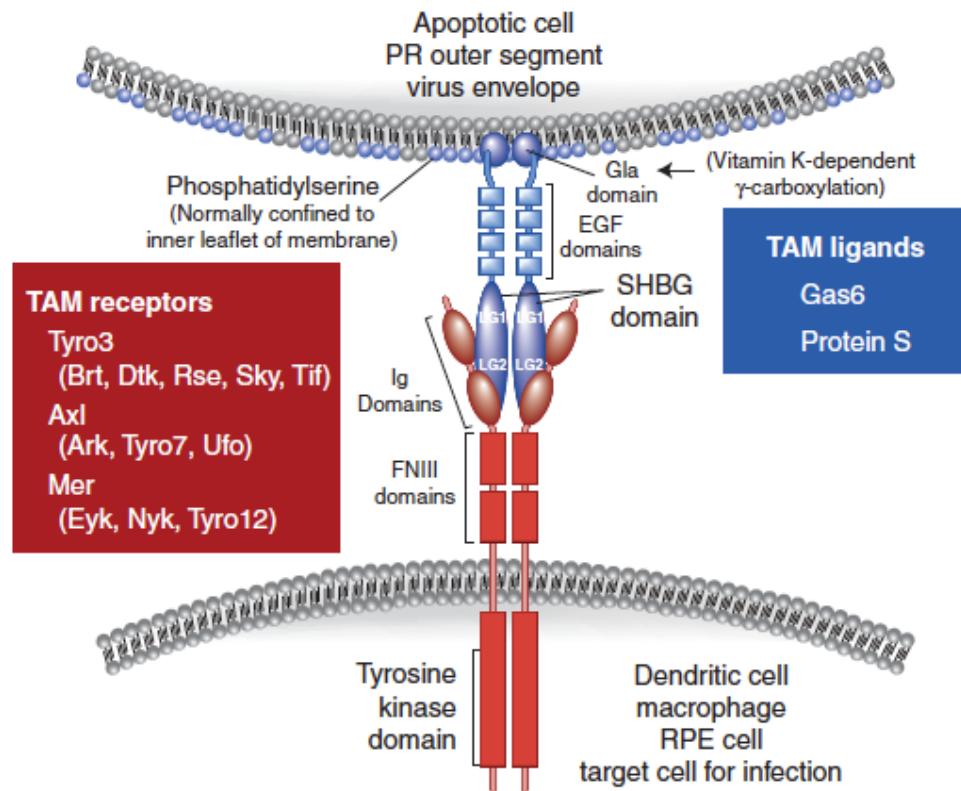


Figure 7: TAM receptors and ligands.

TAM family members (Tyro3, Axl, Mer) and their domains are illustrated. Gas6 and Protein S are most well studied ligands for TAM RTKs.

(Figure is reproduced from Lemke. Biology of the TAM Receptors. Cold Spring Harb Perspect Biol 2013;5:a009076 with permission from Copyright Clearance Center)

arrest specific 6 (Gas6) and Protein S are two major ligands, which are vitamin K-dependent proteins (Fig. 7). Protein S and Gas6 share high sequence homology and have ability to activate the TAM family members. Gas6 was named after an observation of its increased expression after NIH 3T3 cell serum starvation and Protein S contains a thrombin sensitive cleavage site, which mediates the blood coagulation signaling (Schneider et al., 1988).

Axl is ubiquitously expressed in the body and exhibits the highest affinity with Gas6 (Wu et al., 2017). Upon binding of Gas6, Axl forms homodimers of another Axl proteins but it also can form heterodimers with other TAM family members (Brown et al., 2016). Once the receptor forms dimers, trans-autophosphorylation of tyrosine residues occurs and initiate the cascade signaling activation including MAPK signaling, PI3K pathway, and induction of SOCS proteins (Brown et al., 2016).

1.5.2 Gas6-Axl axis in Cancer

Broad downstream pathways that Axl exerts power on indicates the pro-tumorigenic roles of Axl across all the molecular signaling. Axl promotes proliferation, survival, invasion, and metastasis of cancer cells via JNK, PI3K, Ras/ERK pathways (Wu et al., 2017). Axl and phosphorylated Axl are overexpressed in multiple types of cancer and they are correlated with poor prognosis, more advanced tumor stage, and resistance to anti-cancer therapy (Pinato et al., 2016, Wimmel et al., 2001, Martinelli et al., 2015). Small molecule inhibitors for Axl have been developed and tested in preclinical breast cancer, NSCLC, AML, and melanoma models. Specifically, R428 has shown high selectivity

to Gas6/Axl complex and exhibited promising results, providing an insight to target this universal tumor marker (Wu et al., 2017).

Gas6 itself can also promote tumorigenesis by educating monocytes to become TAMs and invading tumor immune surveillance (Loges et al., 2010). Most Gas6 present in the TME is macrophage-derived (Loges et al., 2010), suggesting a synergetic relationship between macrophages and tumor cells. Studies also showed that Gas6 can inhibit the anti-tumorigenic functions of NK cells (Paolino et al., 2014), generating more immunosuppressive TME.

Chapter 2: Materials and methods

Chapter 2: Materials and methods

Content of this chapter is partly based on the following articles:

Lee R, Li J, Chakravarti D, Chen P, Li J., Wu C, Jiang S, LaBella KA, Spring DJ, Wang YA, Zhao D., DePinho RA., Synthetic Essentiality of TDO2 in APC-Mutated Colorectal Cancer, *Submitted*

2.1 Mice

Five mice per cages were maintained under pathogen-free conditions. All animal experiments were performed with the approval of MD Anderson Cancer Center's Institutional Animal Care and Use Committee (IACUC). NSG (NOD.Cg-Prkdcscid Il2rgtm1Wjl/SzJ), C57BL/6J, and BALB/cJ mice were purchased from Jackson laboratory (Stock No: 005557, 000664, 000651). Colorectal orthotopic xenograft tumor models were established by following protocol (Tseng et al., 2007, JoVE). After orthotopic injection of cells, mice that exhibited successful tumor formation were randomized before starting Dox, antibody, or inhibitor treatment for each cell line. Sample size was determined based on previous similar experiments performed in our lab.

2.2 Cell Culture

The CRC cell lines MC38 and its isogenic cells, BMDM and 293T cells were cultured in Dulbecco's Modified Eagle's Medium (DMEM). CCD-841-CoN, RKO, HT-29 and LS180 cells were cultured in Eagle's Minimum Essential Medium (EMEM). HT-29 cells were cultured in McCoy's 5A medium. DLD-1, CT26, and Raw264.7 macrophage cell line was cultured in RPMI 1640 medium (RPMI). All cell lines were

cultured in indicated medium containing 10% Tet System Approved FBS (Clontech) and 100U/ml ampicillin/penicillin. All human cell lines have been validated through fingerprinting by the MD Anderson Cell Line Core Facility. All cells were confirmed to be mycoplasma-free and maintained at 37 °C and 5% CO₂. BMDMs from C57BL/6 mice were cultured as previously described (Chen et al., 2017). Conditioned media were collected from treated or untreated cells as indicated after culturing for 24 h in FBS-free culture medium.

2.3 CRISPR-Cas9 Transfection

sgRNA plasmids targeting human APC gene (sc-400374) were purchased from Santa Cruz Biotechnology. For mouse APC gene, a sgRNA target sequence of TTGAGCGTAGTTTCACTCCG was cloned into pCas-Guide-EF1a-GFP plasmids (Origene Technologies, Inc.). Human RKO and mouse MC38 cells were maintained in 6-well plates to a 70-80% confluency in culture media supplemented with 10% heat-inactivated FBS and 100U/ml ampicillin/penicillin. The plasmids with sgRNA were transiently transfected into using Lipofectamine 2000 according to the manufactory protocol. Cells were harvested 72 h later, and GFP-positive cells were sorted into each well of a 96-well plate as single cell by flow cytometry. At day 10 after cell sorting, the grown cell colonies were expanded in 24-well plates. The knock-out of APC gene in each colony was confirmed by RT-PCR and western blot for APC and β -catenin.

2.4 Mouse Colon Organoid Culture and Genome Engineering

To isolate colonic crypts for organoid culture, a 2 cm piece of distal colon was incubated in PBS containing 5mM EDTA 0.2% FBS at 4°C for 45 min on a shaker. Incubated colon pieces were shaken vigorously to release crypts. Crypts were washed and spun down sequentially at 300g, 200g, and 100g to enrich for intact crypts. Crypts were resuspended in Matrigel and plated in 24-well plates containing 50uL Matrigel per well. 500uL of organoid culture media containing Wnt3a, R-spondin, Noggin, and EGF was added and changed every 2 days.

Knockout of *Apc* was performed via transient transfection of a plasmid expressing Cas9 and a sgRNA targeting *Apc* (*Apc* sgRNA-LentiCRISPRv2; sgRNA sequence: APC-G0-1 – CGCTTGTCTAGATAAGCACG). *Apc*^{-/-} organoids were selected by removal of Wnt and R-spondin from the media.

2.5 Mouse APCmin Organoids

Intestinal polyps from a 18 week-old male APCmin mouse were harvested and the cut tissue were treated with complete chelating solution containing 30mM EDTA for 30 min at 4°C. The tissue pieces were then pipetted gently to dissociate the crypts. These crypts were then seeded in Matrigel (Corning) in the presence of high WNT organoid media in the presence of ROCK inhibitor Y-27632 (STEMCELL Technologies Inc.) for 7-10 days.

2.6 Human Samples

Tissue microarrays (TMA) were obtained from Department of pathology at the University of Texas MD Anderson Cancer Center. The studies related to human

specimens were approved by the MD Anderson Institutional Review Board under protocol Lab09-0373.

2.7 Mutual exclusivity analysis

Mutual exclusivity analysis was performed by the method of Zhao et al., 2017. described by the authors as follows: For the analysis of mutual exclusiveness for APC in colorectal cancer, the genetic alteration of 220 TCGA CRC samples with copy number alterations and sequencing data were downloaded from cBioPortal (<https://www.cbioportal.org/>) ; the gene expression dataset was downloaded from Broad GDAC website (http://gdac.broadinstitute.org/runs/stddata__2016_01_28/data/COAD/20160128/); The detailed method about how to estimate the mutation exclusivity was previously described in (Zhao et al., 2017). Briefly, the rank score (odds ratio score) was calculated to indicate mutual exclusiveness between gene A and gene B deletion. The mean values of gene B expression in all 220 samples and that in gene A deleted samples were calculated and analyzed with student t-test. For APC mutations in CRC datasets, only deletion and mutations with known significance (annotated by OncoKB) cases were considered.

2.8 TCGA data computational analysis

For analysis of human CRC and BRCA data, we retrieved the gene expression and copy number data of TCGA datasets or other available datasets

from cBioPortal: <https://www.cbioportal.org/>. Correlation analysis of TDO2, AhR, and CYP1B1 expression in CRC was performed with R2 platform: <https://r2.amc.nl/>.

2.9 Gene stable shRNA/siRNA knockdown and inducible shRNA knockdown

Mission shRNA hairpins targeting mouse TDO, AhR, and Gas6 were purchased from Santa Cruz and GIPZ shRNA hairpins targeting human TDO were purchased from Horizon. For inducible TDO2 knockdown, SMARTvector Inducible Lentiviral shRNA for mouse TDO2 was purchased from Horizon. The sequences that decreased mRNA and/or protein levels by >80% were chosen. For in vivo bioluminescence imaging, luciferase vector EF1-RFP-T2A-Luciferase (system Biosciences) was used.

Lentiviral infection was performed by the method of Zhao et al. (Zhao et al., 2017) described by the authors as follows: Recombinant lentiviral particles were produced by transient transfection of plasmids into HEK293T cells. In brief, 8 µg of the shRNA plasmid, 4 µg of the psPAX2 plasmid, and 2 µg of the pMD2.G plasmid were transfected using Lipofectamine 3000 into 293T cells plated in 100-mm dishes. Viral supernatant was collected 48 h and 72 h after transfection and filtered. Cells were infected twice in 48 h with viral supernatant containing 8 µg/ml polybrene, and then selected using 2 µg/ml puromycin and tested the expression TDO2, AhR, Gas6, and TCF4 by RT-qPCR. The following shRNA sequences were used.

Human shTDO2 #3: NM_005651: 5'-AATCTGATTCATCACTGCT-3',

Human shTDO2 #6: NM_005651: 5'-AAATCTACAAATACCTTGT-3',

Mouse shTDO2 #2: NM_019911: 5'-
CGGCCAAAGATGAATCCGATCATTCTCGAGA
ATGATCGGATTCATCTTTGGTTTTTG-3',
Mouse shTDO2 #4: NM_019911: 5'-
GGGCGCAAGAACTTCAGAGTGAAGTTCGAGTT
CACTCTGAAGTTCTTGCGCTTTTTTG-3',
Mouse ishTDO2 #3: NM_019911.2: 5'-GGATTTAATTTCTGGGGAA-3',
Mouse shAhR #1: NM_013464: 5'-
CGGCATCGACATAACGGACGAAATCTCGAGAT
TTCGTCCGTTATGTCGATGTTTTTG-3',
Mouse shAhR #2: NM_013464: 5'-
GTACCGGGTCAAGCCTGTTAGCTATATTCTCGA
GAATATAGCTAACAGGCTTGACTTTTTTG-3',
Mouse shGas6 #1: NM_019521: 5'-
CCGGCCTGGCACTGATGGAAATCAACTCGAG
TTGATTTCCATCAGTGCCAGGTTTTTG -3',
Mouse shGas6 #2: NM_019521: 5'-
CCGGGCTGTAATGAAGATCGCGGTACTCGAG
TACCGCGATCTTCATTACAGCTTTTTTG -3'.
Human shTCF4 #1: NM_030756: 5'-
CCGGCCTTTCACTTCCTCCGATTACCTCGAGGTAATCGGAGGAAGTGAAA
GGTTTTTG -3',

Human shTCF4 #2: NM_030756: 5'-
CCGGAGAGAAGAGCAAGCGAAATACCTCGAGGTATTTGCTTGCTCTTCT
CTTTTTTG -3',

For siRNA experiments, Lipofectamine RNAiMAX Transfection Reagent (Thermo Fisher, 13778030) was used and the assay was performed by following manufacturer's protocol. Transfected cells were maintained for three days and knockdown efficiency for TCF4 was measured by western blotting. The following siRNAs (Sigma-Aldrich) were used.

Human siTCF4 #1: NM_030756: SASI_Hs01_00197690

Human siTCF4 #2: NM_030756: SASI_Hs01_00197691

Human siTCF4 #3: NM_030756: SASI_Hs01_00197692

Mouse siTCF4 #1: NM_009333: SASI_Mm01_00142189

Mouse siTCF4 #2: NM_009333: SASI_Mm02_00315891

Mouse siTCF4 #3: NM_009333: SASI_Mm01_00142190

2.10 Western blot

Cell lysates were prepared with RIPA lysis buffer (Roche) with Halt™ Protease and Phosphatase Inhibitor Single-Use Cocktail (Thermo, 78442). Immunoblotting was performed following standard protocol. Antibodies were purchased from the indicated companies, including β -actin, tubulin, vinculin, TDO2, β -catenin, TCF4, cleaved Caspase-3.

2.11 Hairpin-resistant ORF and cytokine ORF expression

To construct hairpin-resistant hTDO2 ORF expression vector to shTDO2 #3, site-directed mutagenesis was performed with human TDO2 ORF gene in pcDNA3.1+/C-(k)DYK vector (GenScript, OHu09674D). Nucleotide mutation was targeted for 1) 1272 T to C, 2) 1275 T to C, 3) 1278 A to G, 4) 1281 A to G and no amino acid was altered. Mutated TDO2 ORF gene insert was subcloned into PS100102 (pLenti-C-mGFP-P2A-BSD Tagged Cloning Vector (Origene, PS10094).

For mutagenesis, following primers were used:

F: 5'-CCTACTTCAGCAGCGACGAGTCGGATTAAAATCG-3'

R: 5'-CGATTTTAATCCGACTCGTCGCTGCTGAAGTAGG-3'

Lentiviral ORF expressing vectors for blank, CXCL5, CXCL7, and CSF3 were purchased from ABM (LV587, LV407122, LV395200, LV455866).

2.12 Luciferase assay

HEK 293T cells were seeded in each well of 24-well plates and transfected with luciferase reporter vectors of pGL3-Basic (Promega, E1751), pGL3-hTDO2 promoter, or pGL3-hTDO2 promoter with a mutated TCF4 binding site with pRL Renilla Luciferase Control Reporter Vector (Promega, E2261) and pLV-beta-catenin Δ N90 (Addgene, 36985) using Lipofectamine 2000 reagent (Thermo, 11668019). pcDNA/Myc DeltaN TCF4 expression vector (Addgene, 16513) was transfected to express dominant negative form of TCF4. Luciferase activity was measured with

Dual-Luciferase reagent (Promega, E1910) and assays were performed according to the manufacturer's instructions.

2.13 Cytokine array and phospho-RTK array

For cytokine array, CRC orthotopic tumors established with ishTDO2 APC-WT and APC-KO MC38 cells were incubated in RIPA buffer with protease/phosphatase inhibitor cocktail and homogenized. Cytokine array was performed with mCytokine Array Kit, Panel A (R&D Systems, ARY006) and the manufacturer's protocol was followed. For phospho-RTK array, ishTDO2 APC-WT and APC-KO MC38 cells were treated with dox for 48hr and the lysates were used for the array. Assays were performed according to the manufacturer's instructions for mPhos RTK Array Kit (R&D Systems, ARY014).

2.14 Immunohistochemistry and immunofluorescence

Immunohistochemistry was performed using standard protocol as we previously described (19). Antibodies specific to TDO2, AhR, β -catenin, Ki67, Cleaved caspase-3, F4/80, CD163, CD206, p-AXL, EpCam were used in this study. For immunofluorescence nuclei staining, DAPI was used. The human and mouse tumor tissue sections were reviewed and scored.

2.15 Migration assay

Assay was performed by the method of Chen et al. (Chen et al., 2019) described by the authors as follows: Macrophages (1×10^4 for Raw264.7 and

BMDM) were suspended in serum-free culture medium and seeded into 24-well Transwell inserts (5.0 μm). Medium with indicated factors or conditioned media was added to the remaining receiver wells. After 24 h, the migrated macrophages were fixed and stained with crystal violet (0.05%, sigma), and then counted with ImageJ.

2.16 Colony formation assay

Colorectal cancer cell proliferation in vitro was assayed through colony formation. 1×10^3 cells were seeded in each well of 6-well plates and cultured for 5-7 days. At the end point, cells were fixed and stained with 0.5% crystal violet in 25% methanol for 1 hr. These experiments were performed in triplicate.

2.17 TDO2 inhibitor and Epacadostat treatment

The structure of the TDO2 inhibitor (PF06845102/EOS20080) was referenced from Schramme et al., 2020 study (Schramme et al., 2020). Institute of Applied Cancer Science (IACS) at MDACC synthesized the TDO2 inhibitor according to the compound structure. TDO2 inhibitor (200mg/kg) was dissolved in 0.5% hydroxypropyl methylcellulose (HPMC) before each injection and administered orally twice daily by oral gavage. For Epacadostat treatment, the compound dissolved in 10% DMSO was further diluted in 90% corn oil and administered orally twice daily at 100mg/kg by oral gavage.

2.18 Mass Cytometry (CyTOF)

Mutual exclusivity analysis was performed by the method of Liao et al. (Liao et al., 2019) described by the authors as follows: Briefly tumors were digested and single cells blocked with FcR were incubated with surface antibody. Cells were then incubated with Cell-ID Cisplatin (Fluidigm, Cat# 201064) and permeabilized for FOXP3 intracellular staining. For nuclei staining, cells were incubated with Cell-ID Intercalator-Ir (Fluidigm, Cat #201192A) while fixing. Samples were analyzed with a CyTOF instrument (Fluidigm) in the Flow Cytometry and Cellular Imaging Core Facility at MD Anderson Cancer Center. Cell numbers and percentages of each cell populations were analyzed with FlowJo (Tree Star) and GraphPad Prism 6 software. CyTOF data were visualized using a dimensionality reduction method viSNE (Amir et al., 2013), which was implemented using the Cytobank (Chen and Kotecha, 2014).

2.19 Kyn, 2-DG uptake and lactate secretion measurement

Kyn concentration was measured by following manufacturer's protocol for Kyn ELISA measurement kit (ImmuSmol, BA-E-2200). 2-DG uptake assay was performed according to manufacturer's protocol for 2-Deoxyglucose Uptake measurement kit (Cosmo Bio, CSR-OKP-PMG-K01TE). For secreted lactate measurement, Lactate Colorimetric/Fluorometric Assay Kit (BioVision, 10186-852) was used and assay was performed by following manufacturer's protocol.

2.20 LC-MS/MS-Based Targeted Metabolomics

Media from cultured cells were harvested and quickly put them into dry ice or -80°C freezer. Cells were washed twice with ice-cold PBS and snap-frozen by putting the flasks on liquid nitrogen. Frozen cells were scraped into 1 mL of -70°C-cooled 80% methanol for collection and quickly stored at -80°C. LC-MS/MS analyses were performed on an AB SCIEX QTRAP 6500 LC-MS/MS system at Pharmacology Core of Karmanos Cancer Institute. Analyst 1.6 software was used for system control and data acquisition, and MultiQuant 3.0 software was used for data processing and quantitation. For statistical analysis, Metaboanalyst (<https://www.metaboanalyst.ca/>) was used.

2.21 ChIP–sequencing and ChIP-PCR

ChIP was performed by the method of Chen et al. (Chen et al., 2019) described by the authors as follows: Chromatin from PFA-fixed cells were cross-linked with 1% PFA and then reactions were quenched using 0.125 M Glycine. Cells were lysed with ChIP lysis buffer [10 mM Tris-HCl (pH 8.0), 140 mM NaCl, 1 mM EDTA (pH 8.0), 1% Triton X-100, 0.2% SDS and 0.1% deoxycholic acid] for 30 min on ice. Chromatin fragmentation was performed using a Diagenode BioruptorPico sonicator (30 s on and 30 s off, 45 cycles) and incubated with the appropriate mixture of antibody and Dynabeads (Life Technologies) overnight. Immune complexes were washed with RIPA buffer (three times), once with RIPA-500 (RIPA with 500 mM NaCl), and once with LiCl wash buffer [10 mM Tris-HCl (pH 8.0), 1 mM EDTA (pH 8.0), 250 mM LiCl, 0.5% NP-40 and 0.5% deoxycholic acid]. Elution and reverse-crosslinking were performed in direct elution buffer [10 mM Tris-HCl (pH 8.0),

5 mM EDTA, 300 mM NaCl, 0.5% SDS] containing proteinase K (20 mg/ml) at 65 °C overnight. Eluted DNA was purified using AMPure beads (Beckman-Coulter), which then was used to generate libraries using NEBNext Ultra DNA Library kit (E7370), or to perform qPCR. Sequencing was performed using an Illumina HiSeq 2500 instrument to generate dataset.

2.22 mRNA expression analysis, microarray and RNA sequencing

Cells were pelleted, and RNA was isolated with RNeasy Mini Kit (Qiagen, 74104). RNA was reverse-transcribed into cDNA by following SuperScript™ III First-Strand Synthesis SuperMix (Invitrogen, 18080400). qRT-PCR was performed using SYBR Green PCR Master Mix (Thermo Fisher Scientific) in a 7500 Fast Real-Time PCR Machine (Applied Biosystems). qRT-PCR primers are listed in Supplementary Table. The expression of each gene was normalized by that of GAPDH or Actin. For microarray, tumors established with ishTDO2 APC-WT and APC-KO MC38 cells was harvested (biological triplicates for control and APC-KO MC38 tumors). RNAs were isolated using Trizol (Invitrogen, 15596-026) and further purified with the RNeasy Mini Kit. Samples were analyzed at the MD Anderson Microarray Core facility using the GeneChip Mouse Clariom D array (Affymetrix) to generate dataset. Genes that were differentially expressed between control and APC-depleted MC38 cells were subjected to gene set enrichment analysis (GSEA). For RNA sequencing, RNAs were isolated from ishTDO2 APC-WT and APC-KO MC38 cells with and without Dox treatment were harvested (biological triplicates per group) using the

RNeasy Mini Kit. Illumina TrueSeq CHIP library was used for Illumina Next Seq 500 Sequencing.

2.23 Quantification and statistical analysis

All statistical analyses were performed with Student's t-test and represented as mean \pm SD. The analysis of TAM IHC staining for the correlation among nuclear β -catenin, TDO2, and CD163 was performed using the chi-squared test. Mouse survival analysis was performed using Log-rank (Mantel-Cox) test (GraphPad Prism 9). The p values were designated as: *, $p < 0.05$; **, $p < 0.01$ and ***, $p < 0.001$; n.s. non-significant ($p > 0.05$).

Chapter 3: Identification of synthetic essential genes for APC mutations

Chapter 3: Identification of synthetic essential genes for APC mutations

Content of this chapter is partly based on the following manuscript:

Lee R, Li J, Chakravarti D, Chen P, Li J., Wu C, Jiang S, LaBella KA, Spring DJ, Wang YA, Zhao D., DePinho RA., Synthetic Essentiality of TDO2 in APC-Mutated Colorectal Cancer, *Submitted*

3.1 Introduction and rationale

Expanding the synthetic essentiality (SE) concept to other tumor suppressor genes may provide an opportunity to discover targetable cancer vulnerabilities with undruggable gene mutations. We embarked on an effort to expand this approach to other tumor suppressors and given the significance of the *APC* gene in regulating CRC tumorigenesis and its prevalent mutation rate in CRC and other cancers. We first screened The Cancer Genome Atlas (TCGA) database and genome scale loss-of-function screening data for genes that are retained in the context of APC loss-of-function mutations.

3.2 Results

3.2.1 Identification of TDO2 as a downstream effector for APC deficiency in cancer

To identify synthetic essential effectors of APC-deficiency in CRC, we first searched for genes showing mutually exclusive mutation/deletion patterns with *APC* mutations or deletion cases in CRC TCGA database. Due to the gatekeeper functions of *APC* gene mutations in CRC initiation process, a majority of CRC cases

(~70%) harbor APC deletion or loss-of-function mutations. To overcome the limitation that only a small fraction of CRC cases are intact for APC, we conducted a pan-cancer analysis which showed consistent retention of TDO2 in APC deleted/mutated cancers including CRC, breast cancer, prostate cancer, lung cancer, head and neck squamous cell carcinoma and sarcoma (Fig. 7). We also included the mutation cases of *CTNNB1*, which encodes β -catenin that functions as a downstream effector of APC/WNT signaling. We found that TDO2 showed mutual exclusive patterns to CTNNB1 as well, which further showing the mutual exclusivity of TDO2 to WNT signaling.

Recognizing the limited sample size and low frequency of these genomic events, we triangulated these genomic results with (i) hits from genome wide loss-of-function screens designed to identify genes that are consistently retained in cancer cells bearing APC loss-of-function mutations (Rosenbluh et al., 2012) and (ii) unbiased transcriptomic analyses to identify genes with positive correlations of WNT pathway activation signature (Van der Flier et al., 2007) and HALLMARK_WNT_BETA_CATENIN_SIGNALING (Subramanian et al., 2005). These intersections yielded 5 potential SE genes for APC-deficient tumors (TDO2, C3, MAFB, CAB39L, PPFIA2) with TDO2 as the top hit (Fig. 8A).

We performed a similar analysis using the same datasets with statistical cutoffs for each dataset and TDO2 is the highest ranked gene identified by the triangulation. Specifically, triangulation identified 5 genes (TDO2, C3, MAFB, CAB39L, PPFIA2) with cutoffs of $p < 0.01$ and $FDR \leq 0.01$; and identified 13 genes (IRS1, TDO2, C3, MAFB, CAB39L, PPFIA2, SORCS2, COL6A3, CPZ, CTSO,

GAMT, GLRB, SPOCK3) with less stringent cutoffs of $p < 0.05$ and $FDR \leq 0.05$. When we applied a FDR cutoff ($FDR < 0.3$) in addition to the p value for RNAi dataset narrowed down the RNAi dataset number to 81 and triangulation with WNT signature correlation and mutual exclusivity datasets identified only TDO2.

Finally, we performed similar *in silico* analysis with TCGA breast cancer dataset (BRCA) to evaluate whether synthetic essential roles of TDO2 are CRC-specific or they are applicable to other types of cancer. Similar to the CRC analysis, we triangulated the genome-scale loss-of-function screen data with (i) TCGA BRCA mutual exclusive dataset for *APC/CTNNB1* genes (ii) TCGA BRCA genes that exhibit higher expression in *APC/CTNNB1*-mutant BRCA tumors compared to *APC/CTNNB1*-WT BRCA. This analysis revealed three potential SE genes for *APC/CTNNB1*-mutant BRCA (TDO2, YES1, UCHL5), further strengthens our findings of the correlation of TDO2 with WNT signaling and specific essentiality in APC-mutant tumors (Fig. 9).

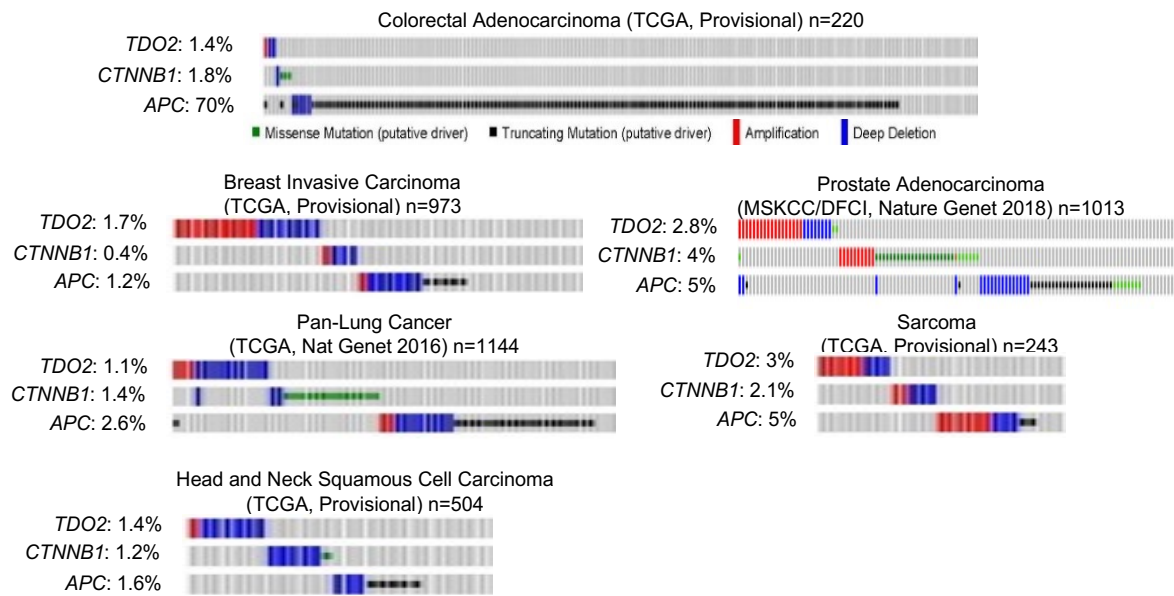


Figure 7: Mutual exclusive patterns of TDO2 and APC/CTNNB1 in TCGA database of multiple cancer types.

The percentages of alteration in each gene are indicated.

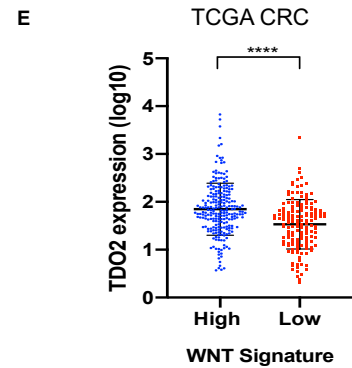
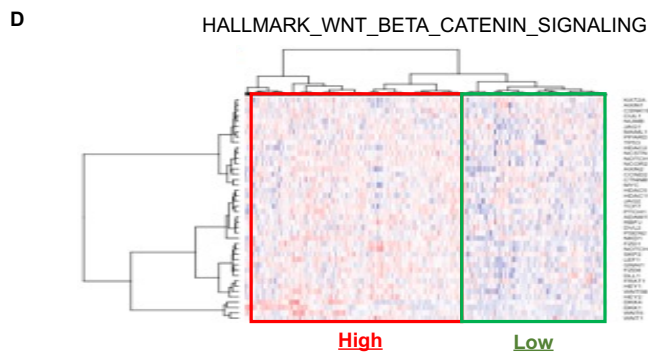
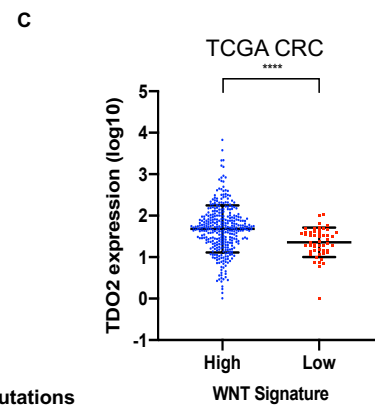
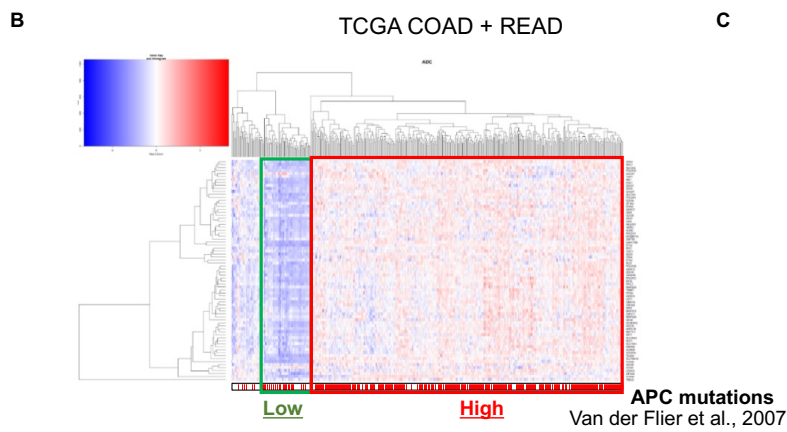
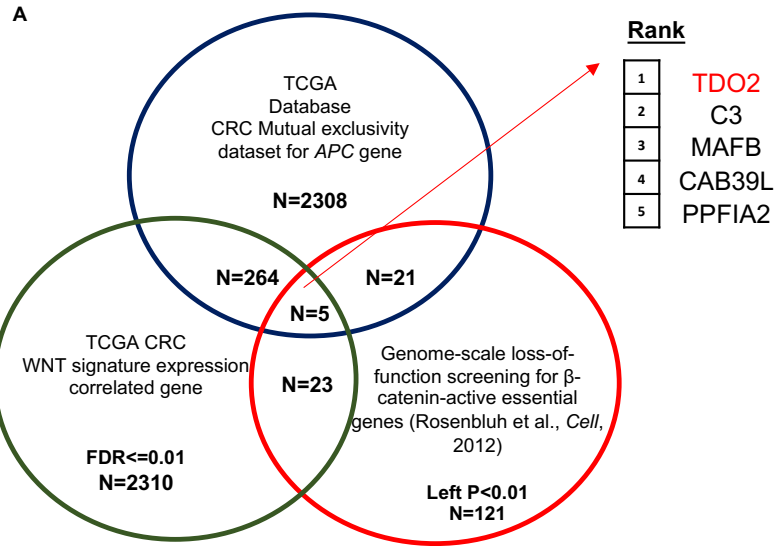


Figure 8: TDO2 as a synthetic essential gene for mutant APC gene in CRC.

(A) Venn diagram representing synthetic essential gene analysis using three different datasets identified TDO2 as a top potential SE gene for mutant APC gene. (B) Representation of clustering of TCGA COAD and READ dataset based on the expression of WNT signature genes (Van der Flier et al., 2007). APC mutation status is shown on the bottom. (C) Expression of WNT signature genes are correlated with TDO2 expression in TCGA CRC (COAD + READ, Provisional) patient samples (n=433). ****P<0.0001 (D) Representation of clustering of TCGA COAD and READ dataset based on the expression of hallmark WNT gene sets (HALLMARK_WNT_BETA_CATENIN_SIGNALING). (E) Expression of hallmark WNT genes are correlated with TDO2 expression in TCGA CRC (COAD + READ, Provisional) patient samples (n=433). ****P<0.0001

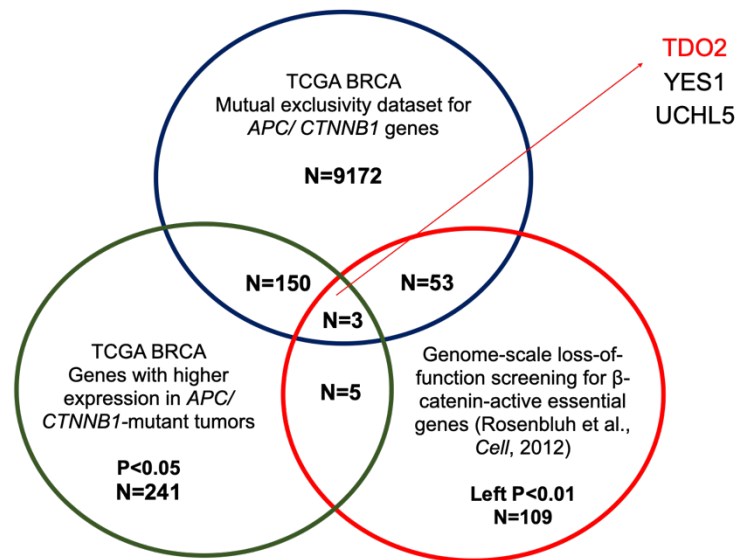


Figure 9: TDO2 as a synthetic essential gene for mutant APC/CTNNB1 gene in BRCA.

Venn diagram representing synthetic essential gene analysis using three different datasets identified TDO2 as one of the potential SE genes for mutant APC/CTNNB1 gene in BRCA.

3.2.2 TDO2 expression is correlated with WNT activation in CRC

We performed expression analysis using two different WNT signature gene sets: one from GSEA pathway hallmark geneset and the other from a study that identified colorectal cancer-specific WNT activation markers. Analysis of human TCGA CRC datasets (COAD and READ) revealed that TDO2 gene expression indeed correlates positively with WNT pathway activation signature genes (Fig. 8, B-D). Correspondingly, tumor microarray analysis of human CRC samples showed coincident increased signal for TDO2 and for nuclear β -catenin and c-Myc, which are indicative WNT pathway activation (Fig. 10, A-E). We utilized iAP ($APC^{mut}/TP53^{mut}$) and iKAP (inducible $Kras^{mut}$ with $APC^{mut}/TP53^{mut}$) (Boutin et al., 2017) murine models for further validation. iAP GEMMs develop colorectal adenoma and/or adenocarcinoma upon 4-hydroxytamoxifen (4-OHT) induction and iKAP mice produce metastasis when KRAS mutation is induced by 4-OHT and Dox administration. CRC tumors of iAP and iKAP mice showed that TDO2 expression tracks closely with nuclear β -catenin and Ki67 signals in tumors (Fig. 11A).

Moreover, baseline TDO2 expression is slightly elevated in the small intestine of $Apc^{Min/+}$ mice relative to C57BL/6J WT controls (Fig. 11B), consistent with haploinsufficiency for *APC*. Finally, $Apc^{Min/+}$ small intestinal organoids and CRISPR/Cas9-mediated *APC*-KO colon organoids showed significantly increased TDO2 expression compared to *APC*-WT organoids (Fig. 11, C and D).

In contrast, another KP enzyme that has the same rate-limiting roles of KP as TDO2, IDO1 did not exhibit mutual exclusive patterns with *APC* and *CTNNB1* mutations in TCGA CRC nor correlate with WNT pathway activation (Fig. 12, A and

B). We did not observe increase IDO1 expression in APC-deficient CRC tumors or isogenic *APC*-KO cell lines. IDO2 expression exhibited a correlation with WNT signaling, although its baseline expression level is extremely low (Fig. 12, A and C). Collectively, APC-deficiency correlates with increased IDO2 expression in normal and malignant intestinal epithelium in humans and mice.

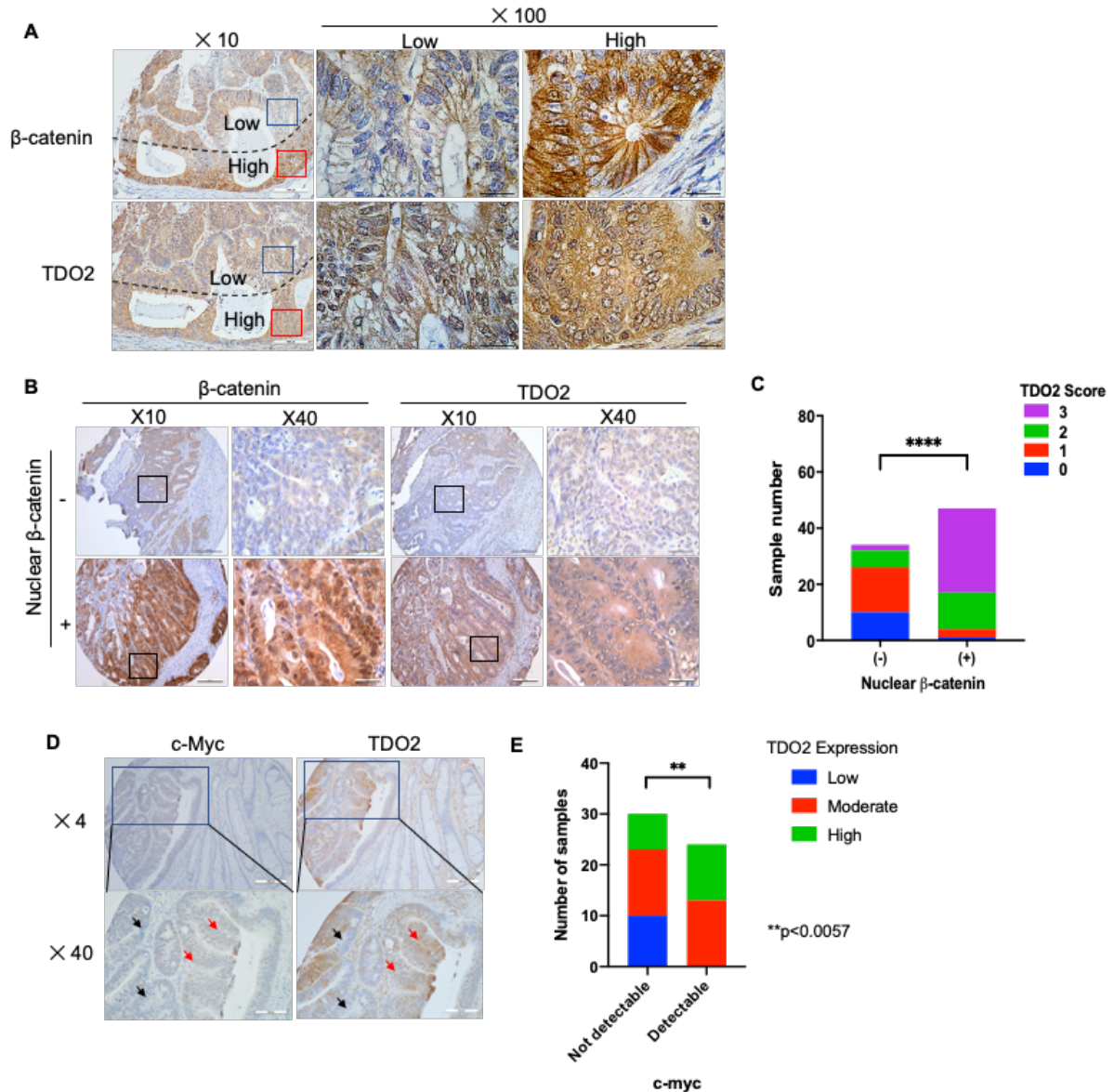


Figure 10: Upregulated TDO2 expression in human CRC TMA.

(A) IHC staining for β -catenin and TDO2 in CRC TMA slides. Dotted lines separate high expression (below) and low expression (above) areas. Areas indicated by blue and red boxes are shown in higher magnification. Scale bars, $\times 10$ (200 μ m) and $\times 100$ (20 μ m) (B) Representative images of IHC staining for TDO2 in human CRC tumors with negative (n=34) and positive nuclear β -catenin (n=47). Scale bars, $\times 10$

(200 μ m) and $\times 40$ (50 μ m). (C) CRC tumors with nuclear β -catenin showed higher TDO2 expression (TDO2 staining score: 0-3). Pearson Correlation Coefficient =42.342, ****P<0.0001. Chi-squared test. (D) Representative images of IHC staining for c-Myc and TDO2 in human CRC TMA slide. Black arrows indicate low MYC/low TDO2 regions and red arrows indicate high MYC/high TDO2 regions. Scale bars, $\times 4$ (500 μ m) and $\times 40$ (50 μ m) (E) Correlation analysis of quantified staining intensity of TDO2 and c-MYC in CRC TMA. Chi-square value, df = 10.35, 2, **P<0.01, Chi-square test

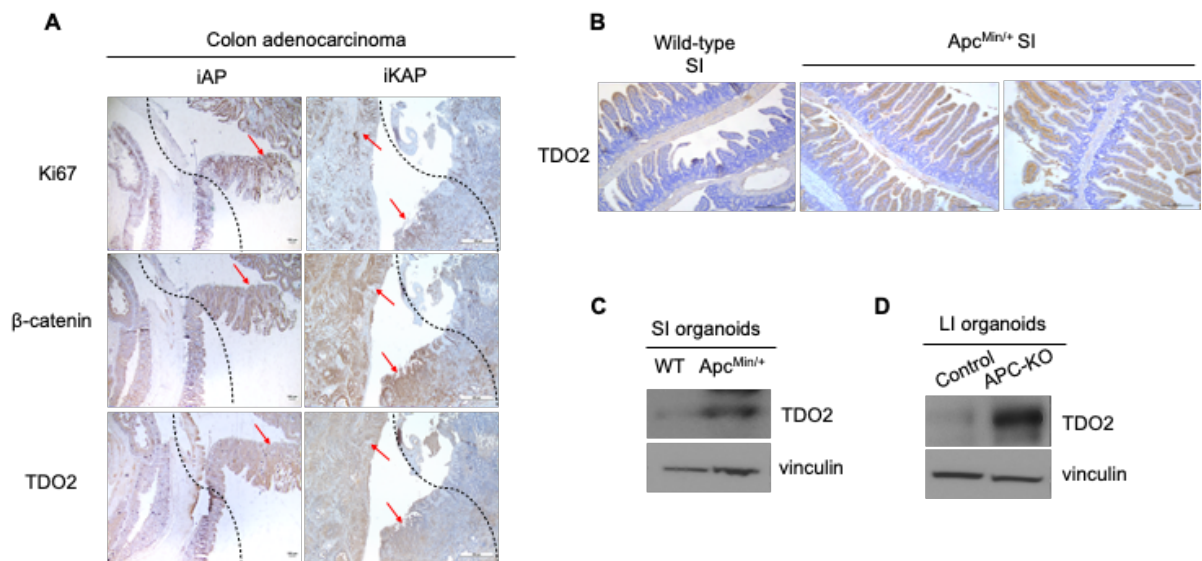


Figure 11: Upregulated TDO2 expression in mouse CRC tumors and organoids.

(A) IHC analysis of CRC tumors from iAP and iKAP mice for nuclear β -catenin, Ki67, and TDO2. Scale bar, 100 μ m for iAP and 500 μ m for iKAP. (B) IHC staining for TDO2 in the small intestines from C57BL/6J wild-type and $Apc^{Min/+}$ mice. Scale bars, $\times 10$ (200 μ m) (C) Immunoblotting for TDO2 in small intestine organoids isolated from C57BL/6J ileum and $Apc^{Min/+}$ mice (D) Immunoblotting for TDO2 in wild-type and APC-null colon organoids

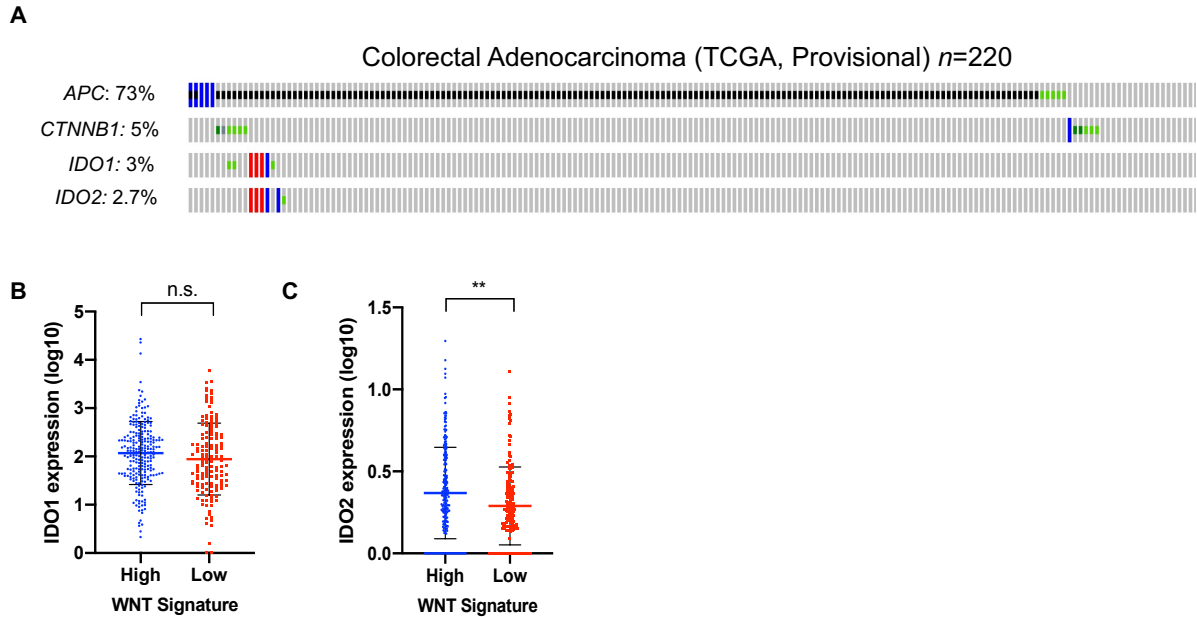


Figure 12: Analysis of IDO1/2 for mutual exclusive patterns with mutant APC and correlation with WNT pathway in CRC.

(A) Mutual exclusive patterns of IDO1/2 to APC and CTNNB1 in TCGA CRC (COAD + READ, Provisional) dataset ($n=220$). (B) IDO1 mRNA expression is not correlated with expression of WNT signature genes in TCGA CRC (COAD + READ, Provisional) patients ($n=433$). n.s. $P>0.05$ (C) IDO2 mRNA expression shows correlation with expression of WNT signature genes in TCGA CRC (COAD + READ, Provisional) patients ($n=433$). $**P<0.01$

3.2.3 APC deficiency upregulates TDO2 expression via transcription factor

TCF4

To validate the positive correlation between the expression of TDO2 and WNT pathway activation in CRC cell lines, we generated multiple isogenic APC-KO MC38 clones to compare CRC cells with APC wild type status to APC null cells and confirmed the status of TDO2 expression (Fig. 13A). Each of the APC-KO clones showed higher TDO2 expression relative to uncloned control cells and APC-WT clones. Human WNT-inactive CRC cell line RKO and CRISPR/Cas9-mediated APC-KO counterparts were also showed elevated TDO2 expression when APC is deficient (Fig. 13B). TDO2 mRNA levels in the human and mouse CRC isogenic cell lines corresponded to the TDO2 protein levels (Fig. 13C). In APC-WT RKO cells, TDO2 expression was higher compared to a normal colon epithelial cells CCD-841-CoN, but APC-KO showed significantly higher TDO2 expression (Fig. 13C).

Increased TDO2 mRNA levels upon *APC* deletion in isogenic prompted examination of the human and mouse *TDO2* gene promoter region for transcription factors. We used the robust JASPAR database, which models transcription factor DNA-binding preferences in multiple species for the analysis. JASPAR aligns binding sites for transcription factors and generates a position frequency matrix (PFM), in which the probability of each base at each position is calculated from the alignment and this database provides scores which are based on the PFMs (Stormo, 2013). Upstream/promoter by 2kb and 5' UTR exons regions of human and mouse *TDO2* genes were scanned for WNT-related transcription factors, especially TCF/LEF family. This analysis identified multiple binding sites for TCF7L2/TCF4 in

the promoter region of *TDO2* gene but failed to reveal prediction sites for other TCF/LEF family members.

We further analyzed for evolutionarily conserved sites between human and mouse by aligning two sequences and identified one conserved site. A conserved WNT pathway transcription factor binding element for TCF4/TCF7L2 was identified immediately upstream of the human and mouse *TDO2* transcription start site (Fig. 14A). CHIP-seq analysis in the APC-KO MC38 cell line shows a positive peak corresponding to the conserved TCF4 site in the promoter of *TDO2* gene, but not APC-WT, MC38 cells (Fig. 14B).

In the human APC-null DLD1 cell line, ChIP-PCR also documented TCF4 binding to the promoters of *TDO2* and the classical WNT target genes *AXIN2* and *MYC*, but not *GAPDH* promoter which served as a negative control (Fig. 14C). Furthermore, a luciferase reporter driven by the human *TDO2* promoter showed increased reporter activity upon transduction of constitutively active β -catenin (CTNNB1 $\Delta 90$), which mimics WNT pathway activation. (Fig. 14D). Conversely, dominant-negative TCF4 expression or TCF4 binding motif mutation abrogated reporter activity (Fig. 14, E and F). Finally, TCF4 depletion or WNT inhibitor XAV-939 treatment, which destabilizes β -catenin decreased *TDO2* levels in multiple independent WNT-activated cells (Fig. 15, A-H). Thus, APC loss activates WNT- β -catenin resulting in TCF4-mediated upregulation of *TDO2* gene transcription.

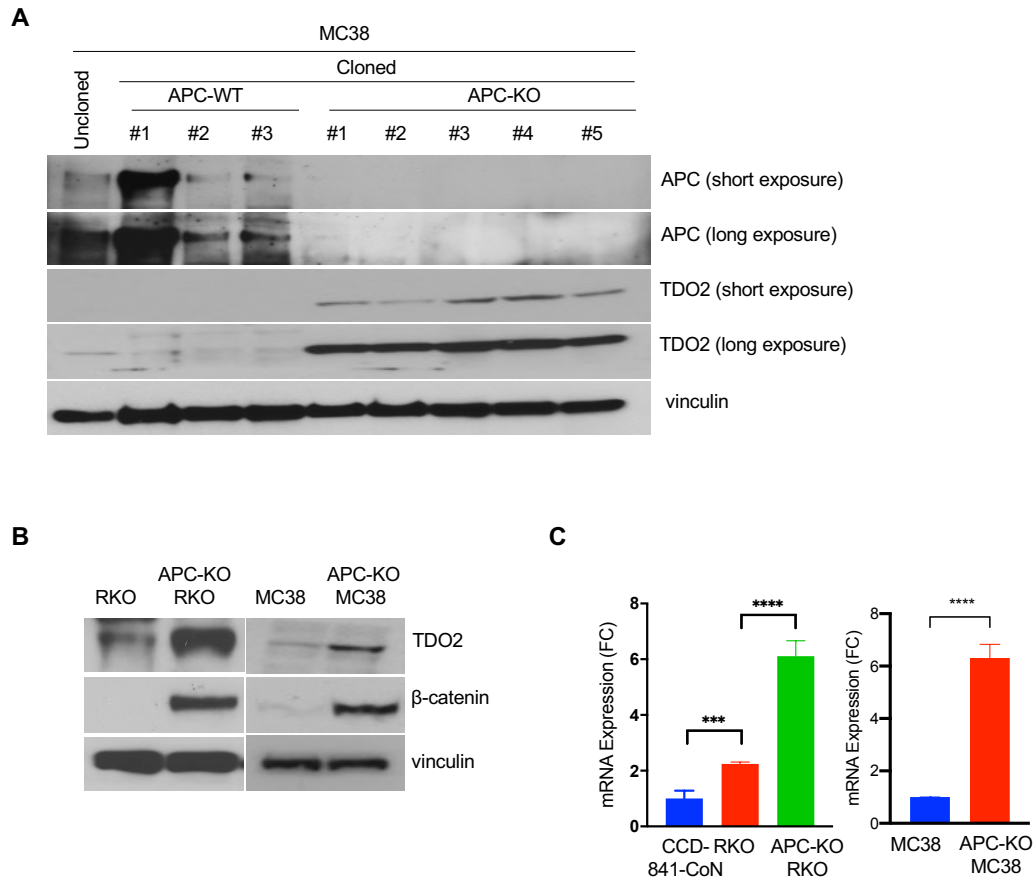


Figure 13: Increased TDO2 expression upon APC deletion in human and mouse CRC cell lines.

(A) Immunoblotting of APC and TDO2 in uncloned MC38 cells, APC-positive clones, and APC-deleted clones of MC38 cells (B) Immunoblots for TDO2 and β -catenin in CRC cell lines RKO (human) and MC38 (Mouse) with their isogenic APC-KO counterparts. (C) RT-qPCR shows APC-deleted RKO and MC38 cell lines exhibit increased TDO2 mRNA expression. **** $P < 0.0001$

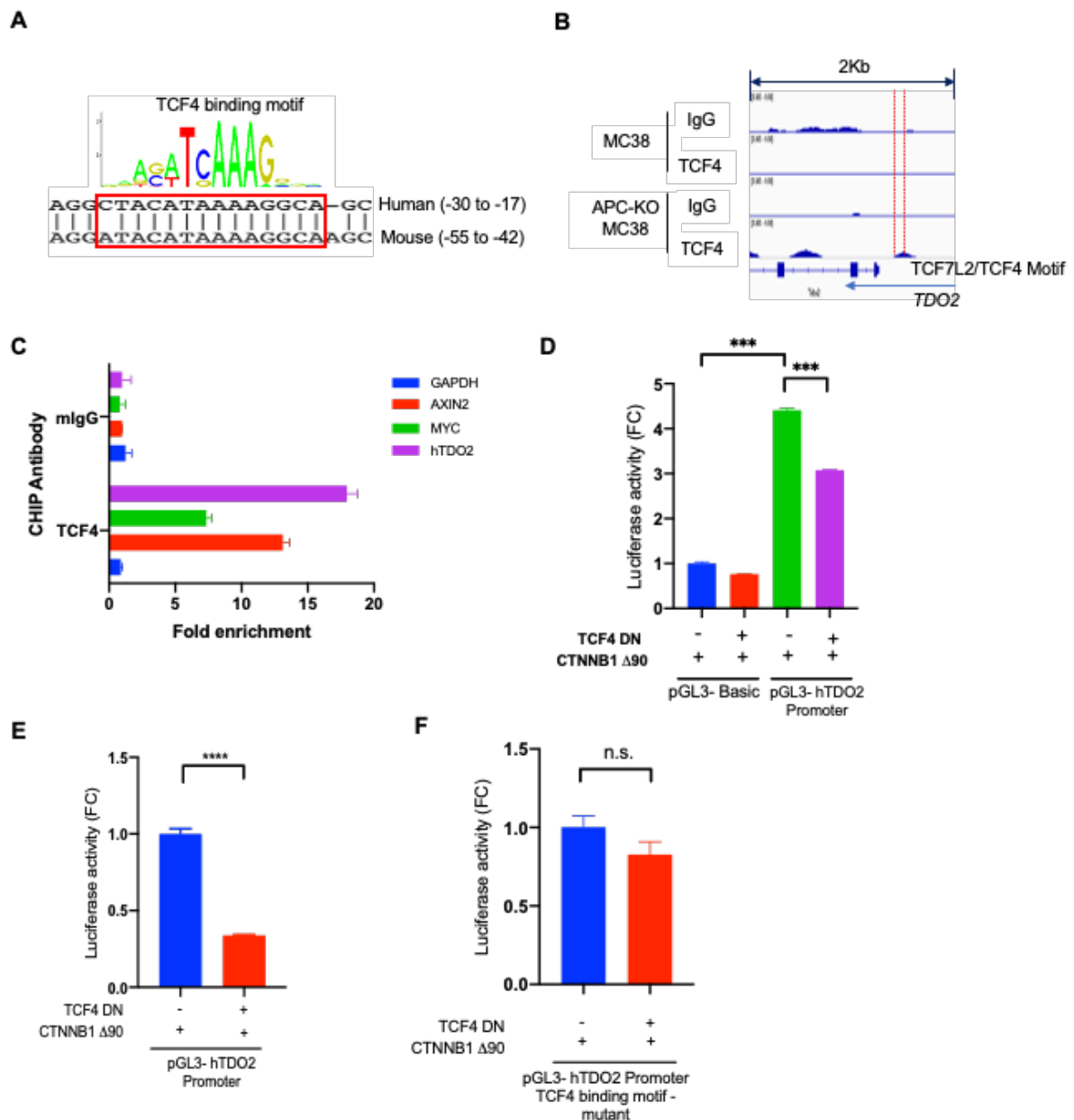


Figure 14: TCF4/TCF7L2 mediates upregulation of TDO2 in APC-mutated CRC cells.

(A) DNA sequence binding motif for transcription factor TCF4/TCF7L2. Promoter regions of human and mouse TDO2 gene harbor TCF4 binding motifs near transcription starting site. The motif sequence is conserved in human and mouse

genes. (B) ChIP-seq in APC-WT and APC-KO MC38 cells showed binding peaks for TCF4 on the promoters of TDO2 gene. (C) ChIP-PCR using TCF4 antibody showed enriched binding to the promoter regions of TDO2 gene in DLD-1 cells. GAPDH as a negative control; MYC and AXIN2 as positive controls. (D) Luciferase activity of hTDO2 promoter in HEK 293T cells with constitutively active form of β -catenin ($\Delta 90$) with or without dominant negative (DN) TCF4. *** $P < 0.001$. (E) Luciferase activity of hTDO2 promoter in HEK 293T cells with constitutively active form of β -catenin ($\Delta 90$) and dominant negative (DN) TCF4. **** $P < 0.0001$. (F) Luciferase activity of mutant TCF4 binding motif hTDO2 promoter in HEK 293T cells with constitutively active form of β -catenin ($\Delta 90$) and dominant negative (DN) TCF4. n.s. $P > 0.05$

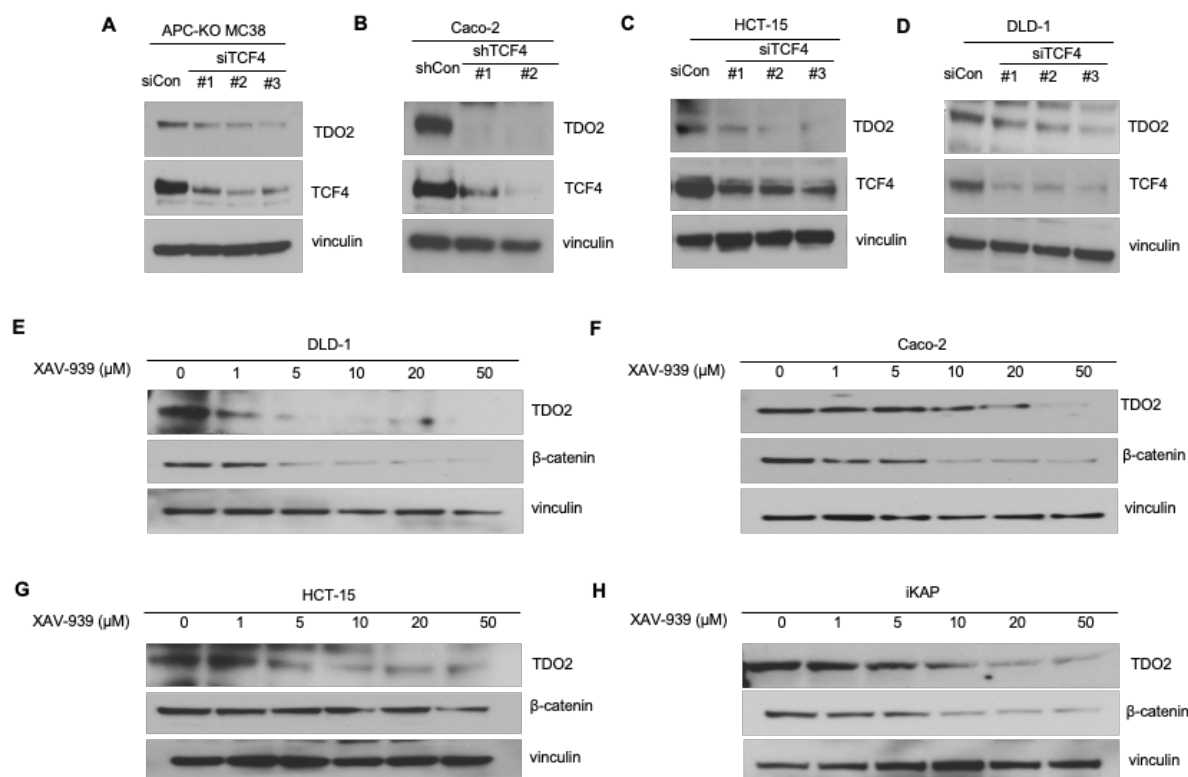


Figure 15: Depletion of TCF4/TCF7L2 decreases TDO2 expression in APC-mutated CRC cells.

(A-D) Immunoblots for TDO2 and TCF4 in APC-KO MC38 cell, HCT-15, and DLD-1 cell lysates after transfecting with siControl or three siTCF4s. Caco-2 cells were infected with shControl or two different shTCF4 constructs. (E-H) Immunoblots for TDO2 and β -catenin upon XAV-939 treatment in DLD-1, Caco-2, HCT-15, and iKAP cell lines at indicated doses for 36hr.

Chapter 4: Cancer cell autonomous signaling mediated by TDO2 in APC-mutant CRC cancer

Chapter 4: Cancer cell autonomous signaling mediated by TDO2 in APC-mutant CRC cancer

Content of this chapter is partly based on the following manuscript:

Lee R, Li J, Chakravarti D, Chen P, Li J., Wu C, Jiang S, LaBella KA, Spring DJ, Wang YA, Zhao D., DePinho RA., Synthetic Essentiality of TDO2 in APC-Mutated Colorectal Cancer, *Submitted*

4.1 Introduction and rationale

Inhibition or depletion of synthetic essential (SE) genes carry context-dependent vulnerabilities in cancers harboring specific tumor suppressor gene mutations. SE genes can be initially identified by examining mutual exclusive patterns in cancer genome data, which can be further triangulated with multiple other datasets. Subsequently, potential SE genes should be validated using in vitro experiments, in vivo models, expression profiles, and survival analysis. We identified TDO2 as a prospective SE gene for mutated APC gene and its positive correlation with Wnt signaling in CRC and other cancers. To validate whether TDO2 confers specific sensitivity to CRC with mutant APC, we utilized CRISPR/Cas9-mediated isogenic cell lines, intestinal organoid system and CRC and BRCA orthotopic mouse models as well as TCGA cancer genomic database. Given the previously studied roles of TDO2 in KP signaling and its downstream AhR pathway, we aimed to understand the cancer cell-intrinsic mechanisms mediated by TDO2 and the relationship between TDO2-AhR axis and mutant APC-driven upregulated Wnt signaling in CRC.

4.2 Results

4.2.1 TDO2 depletion specifically impairs growth and survival of APC/ WNT-mutated CRC cells

To assess TDO2 essentiality as a function of APC status, the biological impact of TDO2 depletion or pharmacological inhibition was tested across multiple murine and human models. We utilized a human normal colon epithelial cell line CCD-841-CoN and multiple CRC cell lines that have either wild type or mutated *APC/CTNNB1* genes (Fig. 16A). Using validated TDO2 shRNAs (Fig. 16B), we found that TDO2 depletion had no impact on colony formation of human *APC*-WT RKO cells yet impaired colony formation of isogenic CRISPR/Cas9-generated *APC*-null RKO controls (Fig. 16, C and D). Similarly, all human *APC/CTNNB1*-mutant CRC lines (DLD1, HT-29, LS180, Caco-2) showed markedly reduced colony formation upon TDO2 depletion (Fig. 16, C and D). Correspondingly, TDO2-specific inhibitor 680C91 (Pilotte et al., 2012) treatment impaired the growth and survival of *APC*-deficient but not *APC*-WT cancer cells including CCD-841-CoN cells (Fig. 16, E and F).

In murine models, TDO2 depletion impaired the growth and cell death of *APC*-null MC38 cells but not the parental *APC*-WT controls (Fig. 17, A-C). Pharmacological inhibition of TDO2 showed increased sensitivity to 680C91 in *APC*-KO MC83 cells compared to *APC*-WT cells (Fig. 17D). We generated dox-inducible shTDO2 *APC*-WT and *APC*-KO MC38 cell lines and examined cell death upon TDO2 depletion. Elevated cleaved caspase-3 was observed only in *APC*-KO cells

but not in APC-WT cells (Fig. 17, E and F). Similarly, TDO2 depletion induced cell death in cultured $Apc^{Min/+}$ intestinal organoids (Fig. 17G).

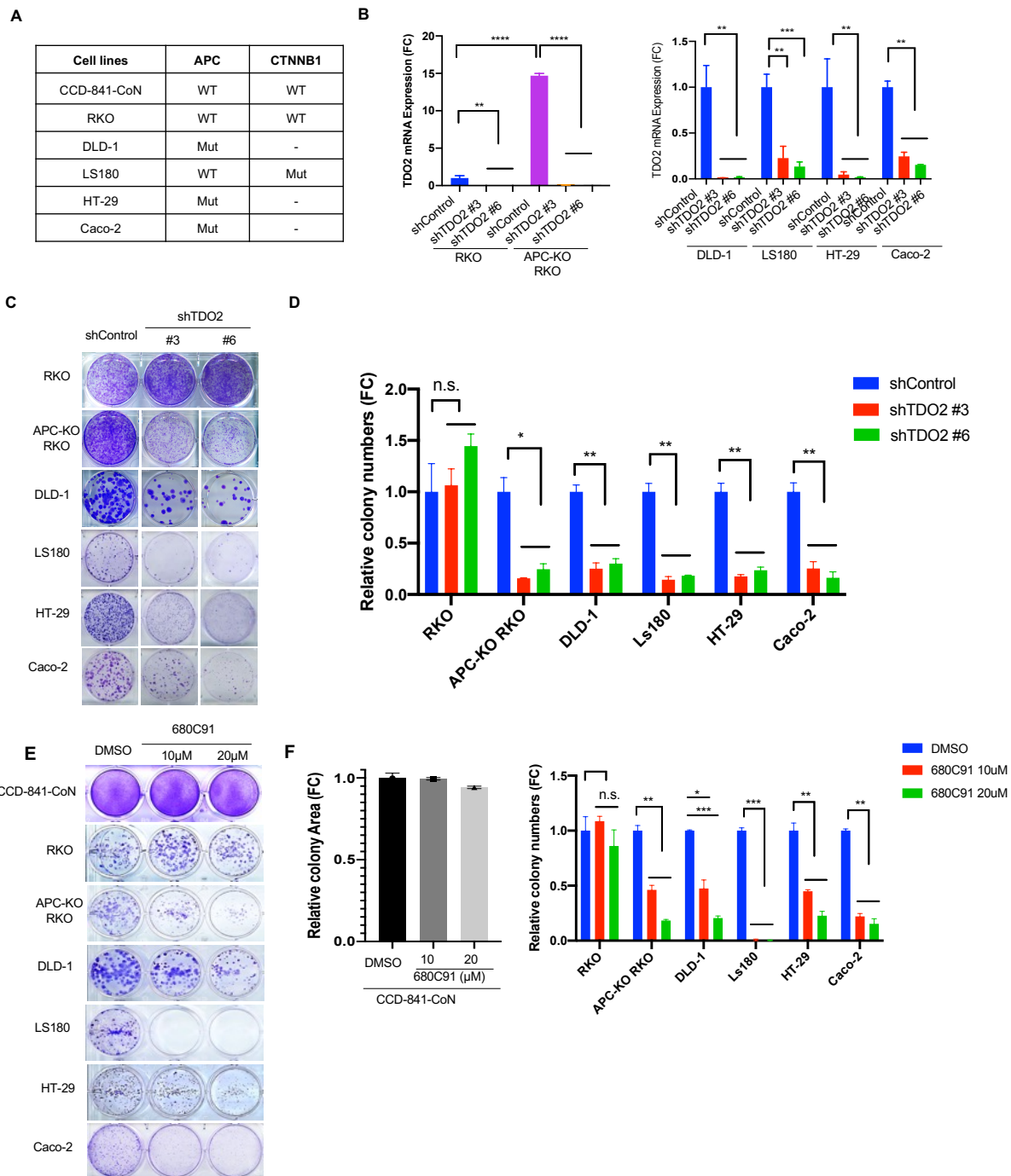


Figure 16: Depletion of TDO2 leads to impaired colony formation in human APC-mutated CRC cells.

(A) Mutation Status of *APC* and *CTNNB1* in human normal and CRC cell lines used in this study. **(B)** RT-qPCR shows TDO2 shRNA knockdown efficiency in isogenic *APC*-WT and *APC*-KO RKO as well as DLD-1, LS180, HT-29, and Caco-2 cell lines. **(C and D)** Representative images and a quantification graph of colony formation assay of human CRC cell lines expressing shControl and two shTDO2 constructs **(E and F)** Representative images and a quantification graphs of colony formation assay of human CRC cell lines upon 680C91 treatment at indicated doses for 48 hr.

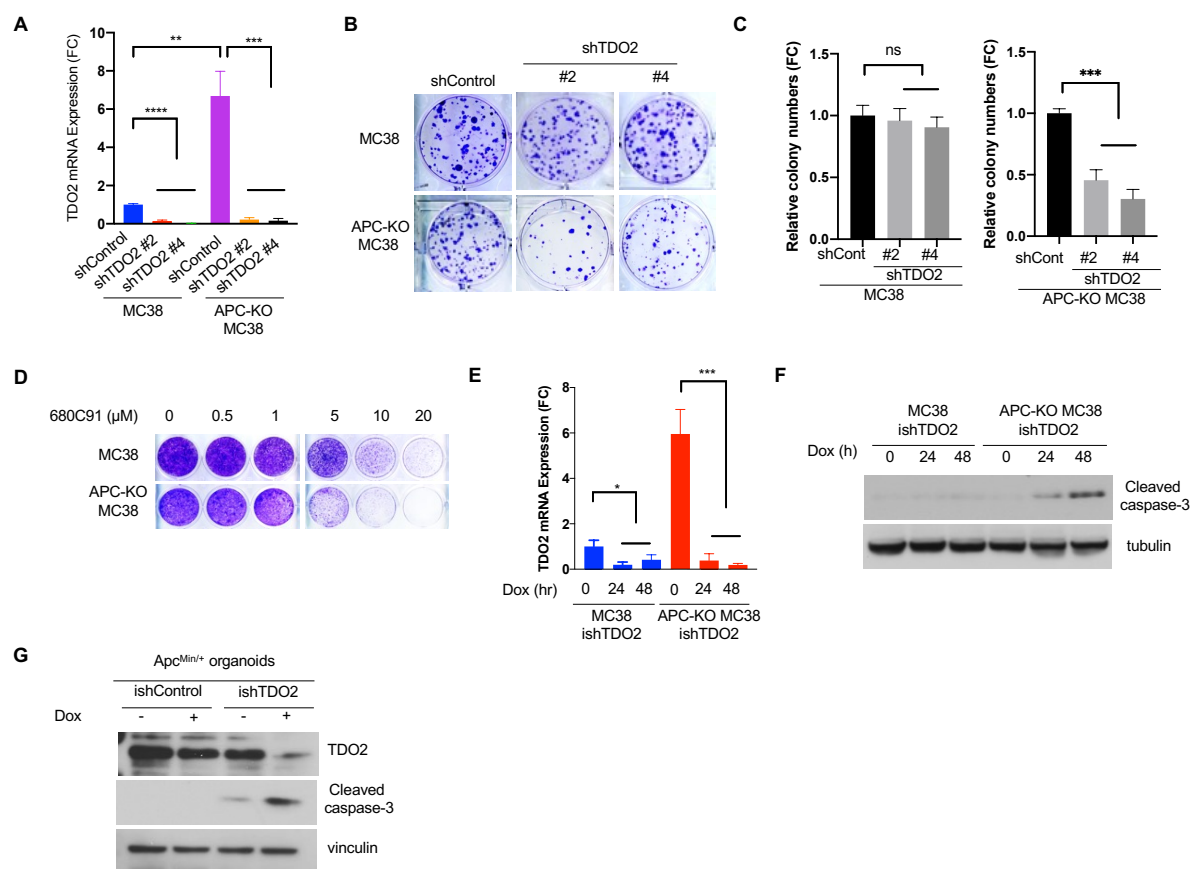


Figure 17: TDO2 depletion reduces colony formation ability and increases cell death in murine APC-mutated CRC cells and organoids.

(A) RT-qPCR shows TDO2 inducible shRNA knockdown efficiency in APC-WT and APC-KO MC38 cell lines. (B) Representative images of colony formation assay of APC-WT and APC-KO MC38 cell lines expressing shTDO2. n=3 biological replicates. (C) Quantification of Panel (D) Representative images of crystal violet staining of APC-WT and APC-KO MC38 cell lines after treating 680C91 in a dose-dependent manner for 48 hr. (E) RT-qPCR shows TDO2 inducible shRNA knockdown efficiency in APC-WT and APC-KO MC38 cell lines. (F) Immunoblots of cleaved Caspase-3 in APC-WT and APC-KO MC38 cell lines with ishTDO2 after

doxycycline (Dox) treatment. **(G)** Immunoblots for TDO2 and cleaved Caspase-3 in $Apc^{Min/+}$ ishControl and ishTDO2 organoid cell lysates after Dox treatment for 48h.

4.2.2 TDO2 depletion specifically impairs tumor growth and survival of APC/WNT-mutated CRC cells *in vivo*

In CRC orthotopic xenograft models that were established by cecal wall injection, APC deletion in RKO cells showed accelerated tumor growth *in vivo* compared to APC-WT RKO cells, which was expected observe considering the roles of APC in activating WNT signaling and subsequent cell proliferation (Fig. 18A). TDO2 depletion decreased growth of orthotopic APC-null RKO tumors in immune deficient NSG mice but not in APC-WT tumors (Fig. 18A). Similarly, TDO2 depletion decreased growth of APC-null DLD-1 tumors which was rescued by enforced expression of a hairpin-resistant TDO2 ORF (Fig. 18B). Pathological analysis of these TDO2-depleted RKO and DLD-1 tumors revealed decreased cancer cell proliferation (Ki67) and increased apoptosis (cleaved Caspase-3) (Fig. 18, C and D). Rescuing the TDO2 expression in DLD-1 cells elevated Ki67 expression and decreased apoptosis, indicating that TDO2 drives these cancer cell-intrinsic hallmarks (Fig. 18D).

We performed similar experiments using immune competent C57BL/6J mice and syngeneic MC38 cells to 1) examine whether murine CRC cells also show impaired tumor growth *in vivo* and 2) investigate if immune responses are also regulated by TDO2. Similar to the tumors in NSG mice, TDO2 depletion impaired CRC orthotopic tumor growth (Fig. 19, A and B). Overall survival of mice was also prolonged by TDO2 knockdown specifically in murine APC-KO MC38, but not APC-WT controls (Fig. 19C). Immunohistochemistry staining of derived tumors showed decreased cancer cell proliferation and increased cancer cell apoptosis (Fig. 19D).

Interestingly, in immune-deficient mice, *APC*-KO MC38 tumors produced similar survival curves to those in immune competent mice but showed reduced survival benefit from induction of TDO2 depletion (Fig. 19E), consistent with cancer cell intrinsic and immune modulatory roles for TDO2 specifically in *APC*-null cancers.

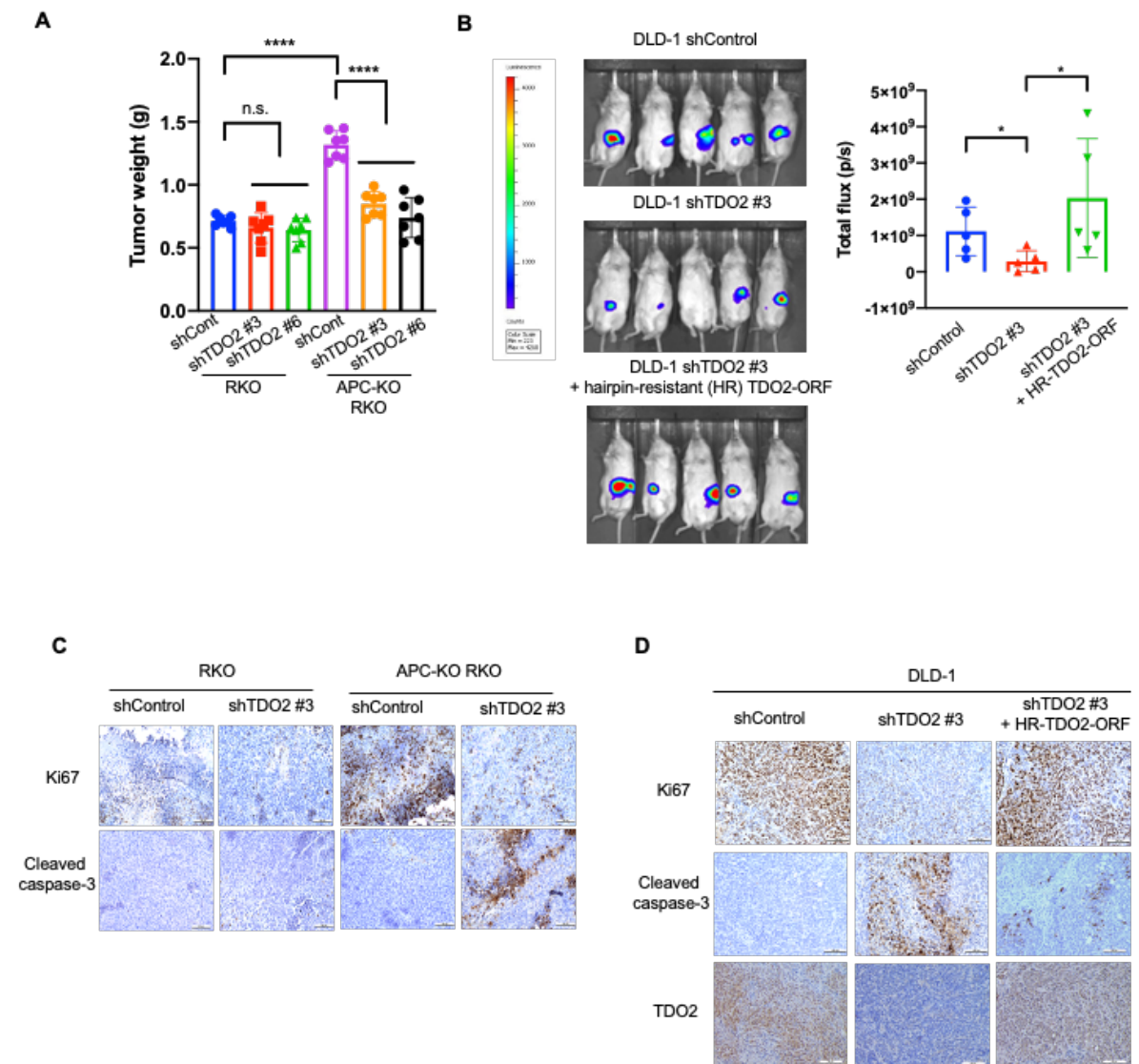


Figure 18: TDO2 knockdown impairs tumor growth of human CRC cells in vivo.

(A) Measured tumor weight in NSG mice injected with *APC*-WT and *APC*-KO RKO cell lines expressing shControl or two shTDO2 constructs. Tumors were harvested from at day 25 post- subcutaneous injection (n=7 per group) n.s. $P>0.05$,

**** $P<0.0001$. two-tailed t-test. **(B)** Measurement of orthotopic tumor growth of TDO2

knockdown and hairpin-resistant (HR) TDO2-ORF expressing DLD-1 cell lines in nude mice (5×10^5 cells per injection). n = 5 per group. Total flux measurement of tumors is shown. *P<0.05, two-tailed t-test. **(C)** IHC of Ki67 and caspase-3 in tumors tissues generated from samples shown in panel **(A)**. Scale bar, 100 μ m. **(D)** IHC of Ki67 and caspase-3 in tumors tissues generated from samples shown in panel **(B)**. Scale bar, 100 μ m.

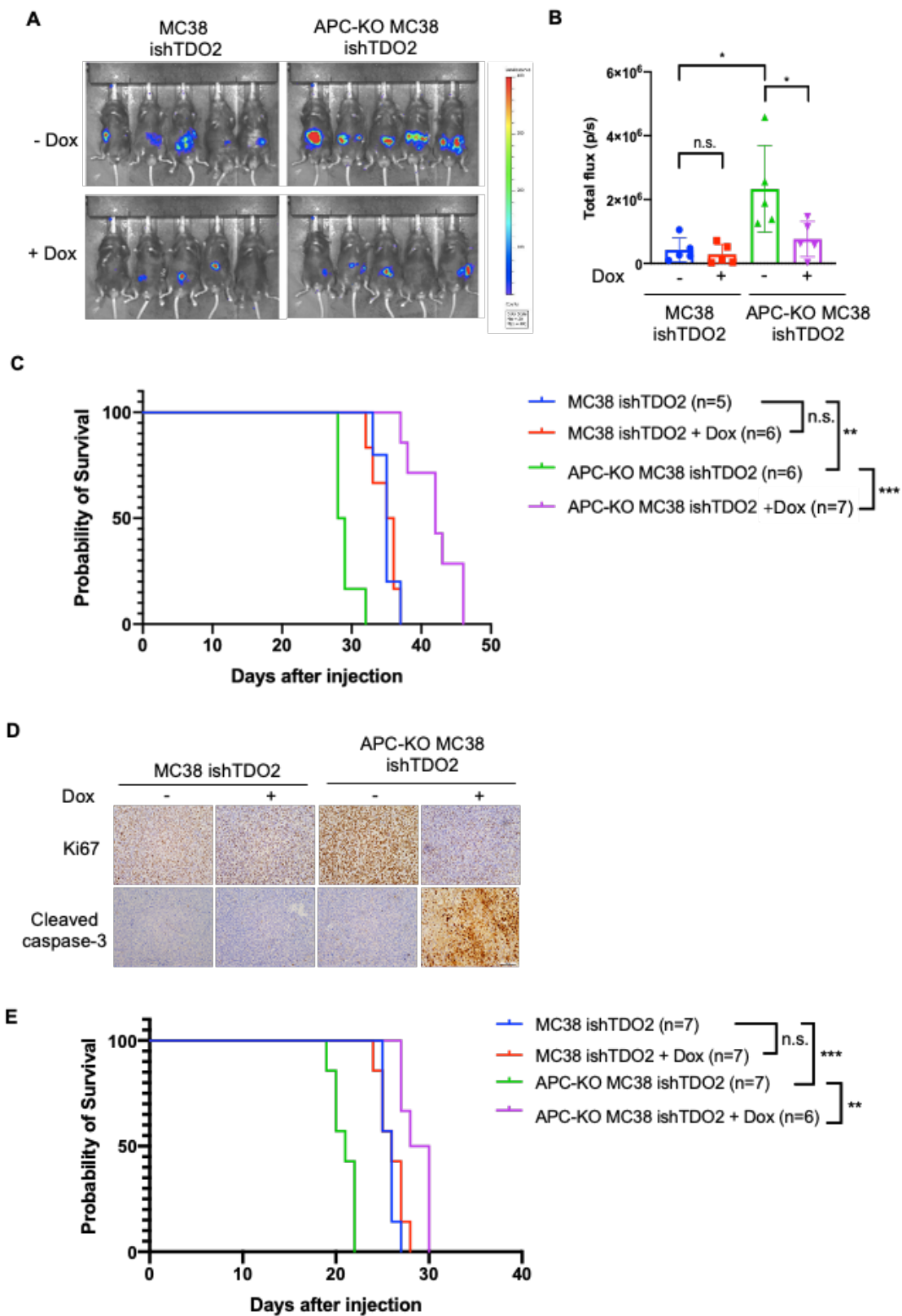


Figure 19: TDO2 depletion specifically impairs growth of APC/WNT-mutated murine CRC cells in vivo.

(A) Representative *in vivo* bioluminescence-based images of C57BL/6J mice at day 21 post-orthotopic injection of ishTDO2 *APC*-WT and *APC*-KO MC38 cell lines (2×10^5 cells). Dox food was provided at day 5 after injection to induced TDO2 knockdown in vivo (n=5 per group). **(B)** Total flux measurement of tumors in panel **(A)**. n.s.P>0.05, *P<0.05 **(C)** Survival curves of C57BL/6J mice orthotopically implanted with ishTDO2 *APC*-WT and *APC*-KO MC38 cell lines (2×10^5 cells). Dox food was supplied at day 5 post-orthotopic injection to induce TDO2 knockdown in n.s.P>0.05, **P<0.01, ***P<0.001. Log-rank (Mantel-Cox) test. **(D)** IHC of Ki67 and caspase-3 in tumors tissues generated from samples in panel **(A)**. Scale bar, 100 μ m **(E)** Survival curves of NSG mice orthotopically implanted with ishTDO2 *APC*-WT and *APC*-KO MC38 cell lines (2×10^5 cells). Dox food was applied at day 5 post-orthotopic injection to induce TDO2 knockdown *in vivo*. n.s.P>0.05, ***P<0.001, ****P<0.0001. Log-rank (Mantel-Cox) test.

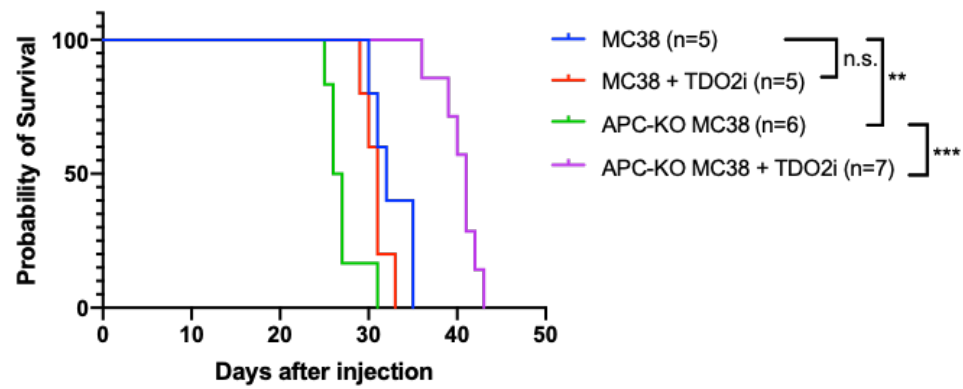
The recent failure of the IDO inhibitor in clinical trials which tested the IDO1 inhibitor Epacadostat combined with anti-PD-1 in advanced melanoma patients (Muller et al., 2019) prompted us to compare the efficacy of TDO2 and IDO inhibition. We tested the impact of TDO2 inhibition in our model system *in vivo* using a small molecule TDO2 inhibitor. The recently developed validated TDO2 inhibitor PF06845102/EOS200809 (Schramme et al., 2020) showed increased Trp and decreased Kyn levels in serum when treated in mice via oral gavage. Interestingly, the growth of tumors established with TDO2-overexpressing CT26 cells in Balb/C mice were inhibited significantly when combined with anti-CTLA4 treatment (Schramme et al., 2020).

TDO2 inhibitor was administrated by oral gavage to mice bearing *APC*-WT or *APC*-KO MC38 orthotopic tumors twice daily and, consistent with the IDO inhibitor failures, Epacadostat did not show anti-tumor activity in mice bearing either *APC*-WT or KO MC38 CRC orthotopic tumors. TDO2 inhibitor treatment improved the survival of mice bearing *APC*-KO MC38 tumors but not *APC*-WT controls despite their inherently more malignant nature compared with parental *APC*-WT MC38 tumors (Fig. 20A).

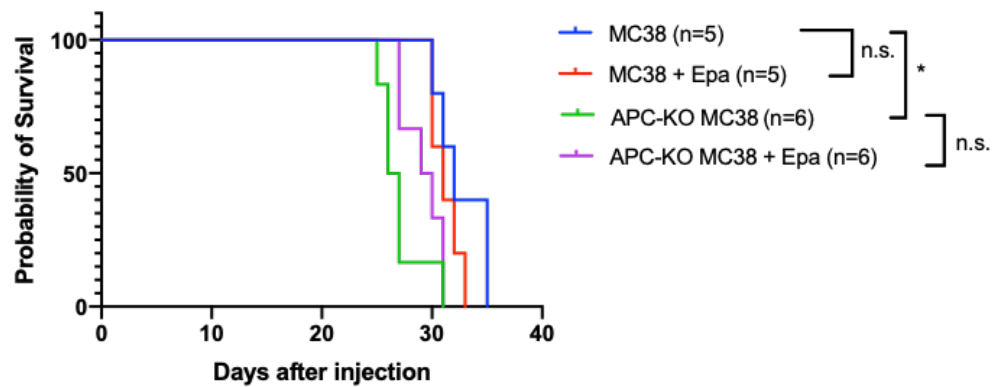
From a pharmacodynamic standpoint, histopathology showed that TDO2 inhibitor treatment decreased Ki67 and increased cleaved caspase-3 specifically in the *APC*-KO MC38 tumors (Fig. 20C). Consistent with the IDO inhibitor failures, the IDO inhibitor, Epacadostat, did not exhibit anti-tumor activity in mice bearing either *APC*-WT or *APC*-KO MC38 CRC orthotopic tumors (Fig. 20, B and C).

These results, together with the observation that the TDO2 inhibitor was well tolerated (no signs of liver toxicity or weight loss), underscore the translational potential of our work. In conclusion, these data support that TDO2 plays a prominent role in supporting cancer cell survival and suppressing anti-tumor immunity specifically in the setting of APC loss and WNT pathway activation.

A



B



C

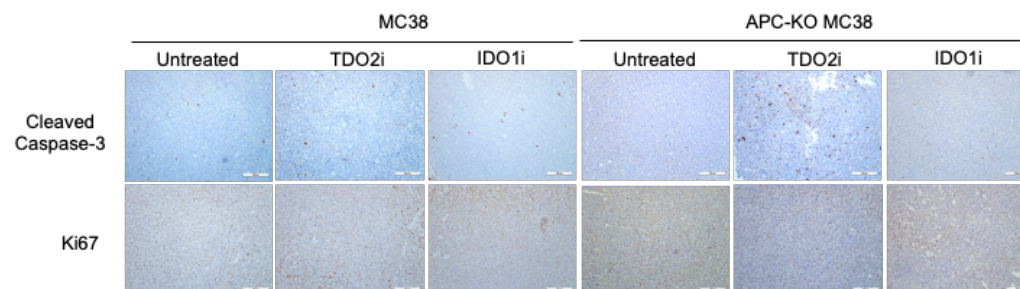


Figure 20: Anti-tumorigenic activity of TDO2 inhibitor specifically in APC-deficient CRC tumors.

(A) Survival curves of C57BL/6J mice orthotopically implanted with *APC*-WT and *APC*-KO MC38 cell lines (2×10^5 cells). TDO2 inhibitor treatment (100mg/kg) was initiated at day 5 post-injection twice a day by oral gavage. n.s. $P > 0.05$, ** $P < 0.01$, *** $P < 0.001$. Log-rank (Mantel-Cox) test. **(B)** Survival curves of C57BL/6J mice orthotopically implanted with *APC*-WT and *APC*-KO MC38 cell lines (2×10^5 cells). Epacadostat (100mg/kg) was initiated at day 5 post-injection twice a day by oral gavage. n.s. $P > 0.05$, * $P < 0.05$. Log-rank (Mantel-Cox) test. **(C, D)** IHC of Ki67 and caspase-3 in tumors tissues generated from samples in panels **(A)** and **(B)**. Scale bar, 200 μ m.

4.2.3 TDO2-Kyn-AhR axis supports APC-deficient cancer cell proliferation, survival, and tumorigenic potential.

As noted previously, TDO2 mediates the first and rate-limiting step of KP that metabolizes Trp to produce Kyn which in turn activates AhR to upregulate genes governing myriad cellular functions. Gene Set Enrichment Analysis (GSEA) of RNA-seq data from the isogenic *APC*-KO and *APC*-WT MC38 cell lines showed that Dox-induction of inducible shTDO2 decreased signatures of tryptophan metabolism as well as xenobiotic metabolism, patterns consistent with the main functions of AhR pathway (Fig. 21A). Correspondingly, expression of AhR and its target gene CYP1B1 correlated positively with TDO2 levels in TCGA COAD dataset (Fig. 21B). CRC tumors from iAP and iKAP also showed that AhR expression strongly tracks with nuclear β -catenin and Ki67 (Fig. 21C) which is similar to TDO2. Moreover, the *APC*-TDO2-KP connection was verified in the *APC*-KO MC38 model system via Kyn ELISA by measuring Kyn concentration in the conditioned media harvested from the APCmin organoids or cell lines. The ELISA analysis documented elevated Kyn secretion relative to *APC*-WT controls (Fig. 21D) and TDO2 depletion in *APC*-KO cells and *Apc*^{Min/+} organoids reduced Kyn levels (Fig. 21, D and E). Finally, gene expression analysis with qRT-PCR showed upregulated AhR and its downstream genes CYP1A1 and CYP1B1 in *APC*-KO MC38 cells compared to *APC*-WT MC38 cells, which was reversed upon TDO2 depletion in *APC*-KO MC38 cells and DLD1 cell lines (Fig. 21, F and G).

To validate Kyn and AhR in mediating TDO2-regulated biology in *APC*-KO context, we assayed the impact of Kyn treatment or AhR depletion in colony

formation assays using the *APC*-KO MC38 ishTDO2 cell lines and *APC*-KO MC38 shAhR cell lines. In *APC*-KO MC38 cells, reduced colony formation upon induction of TDO2 depletion or pharmacological inhibition (680C91) was partially rescued by Kyn treatment (Fig. 22, A-E). In *APC*-WT MC38 cells, TDO2 inhibition and supplementation of Kyn had no effect on the cell death (Fig. 22E). In the iKAP model system, Kyn treatment to a cell line derived from iKAP tumors also decreased 680C91-induced cell death (Fig. 22F), further validating the cell autonomous activity of the TDO2-AhR axis.

Finally, AhR depletion in *APC*-KO MC38 tumors resulted in increased survival compared to the control tumors (Fig. 22G). Correspondingly, AhR-depleted *APC*-KO MC38 tumors showed decreased proliferation (Ki67) and survival (Caspase-3) in the cancer cells (Fig. 22H) as shown in TDO2-depleted *APC*-KO tumors. Together, these findings are consistent with a key role for Kyn and AhR as mediators of TDO2 in *APC*-null cancer cell proliferation, survival, and tumorigenic potential.

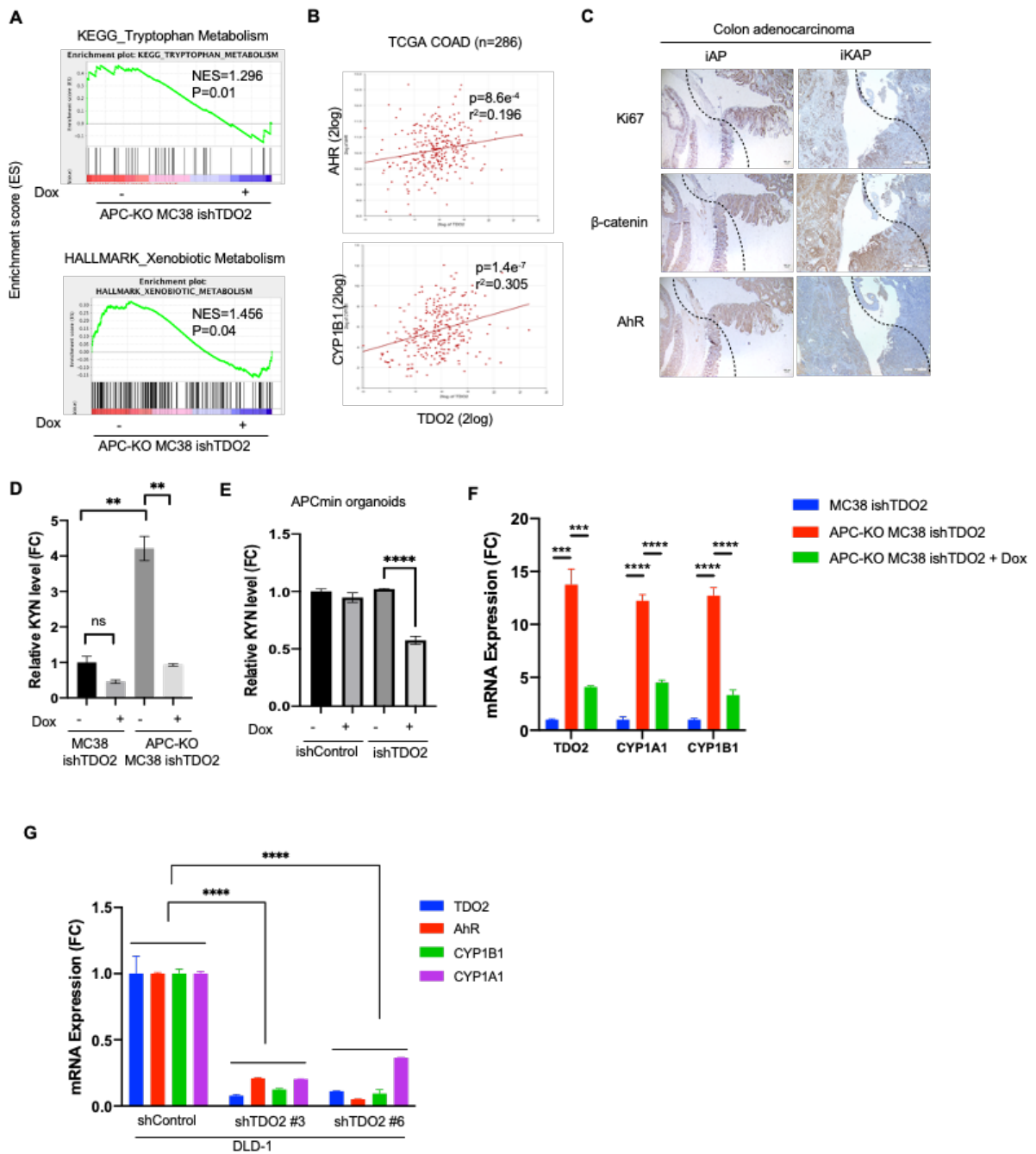


Figure 21: Upregulated TDO2 activates kynurenine pathway and AhR signaling in APC-mutant CRC cells.

(A) GSEA graphs of Tryptophan metabolism and Xenobiotic metabolism with alternatively expressed genes in TDO2 depleted *APC*-KO MC38 cells. Normalized enrichment score (NES) and nominal P value are shown. **(B)** Positive correlation of TDO2 expression to AhR and CYP1B1 expression in TCGA COAD database (n=286). P values and R-squares value are shown. **(C)** IHC analysis for AhR in CRC tumors from iAP and iKAP mice tracks with Ki67 and β -catenin staining. **(D)** Relative kynurenine levels in ishTDO2 *APC*-WT and *APC*-KO MC38 cell lines upon TDO2 depletion. **(E)** Relative kynurenine levels in *Apc*^{Min/+} organoids infected with ishControl and ishTDO2 constructs. **(F)** RT-qPCR shows TDO2 knockdown decreased the expression of AhR downstream target genes in *APC*-KO MC38 cell lines. *** $P < 0.001$, **** $P < 0.0001$. **(E)** RT-qPCR shows decreased expression of AhR, CYP1B1 and CYP1A1 in DLD-1 shTDO2 cells compared to shControl cells. **** $P < 0.0001$

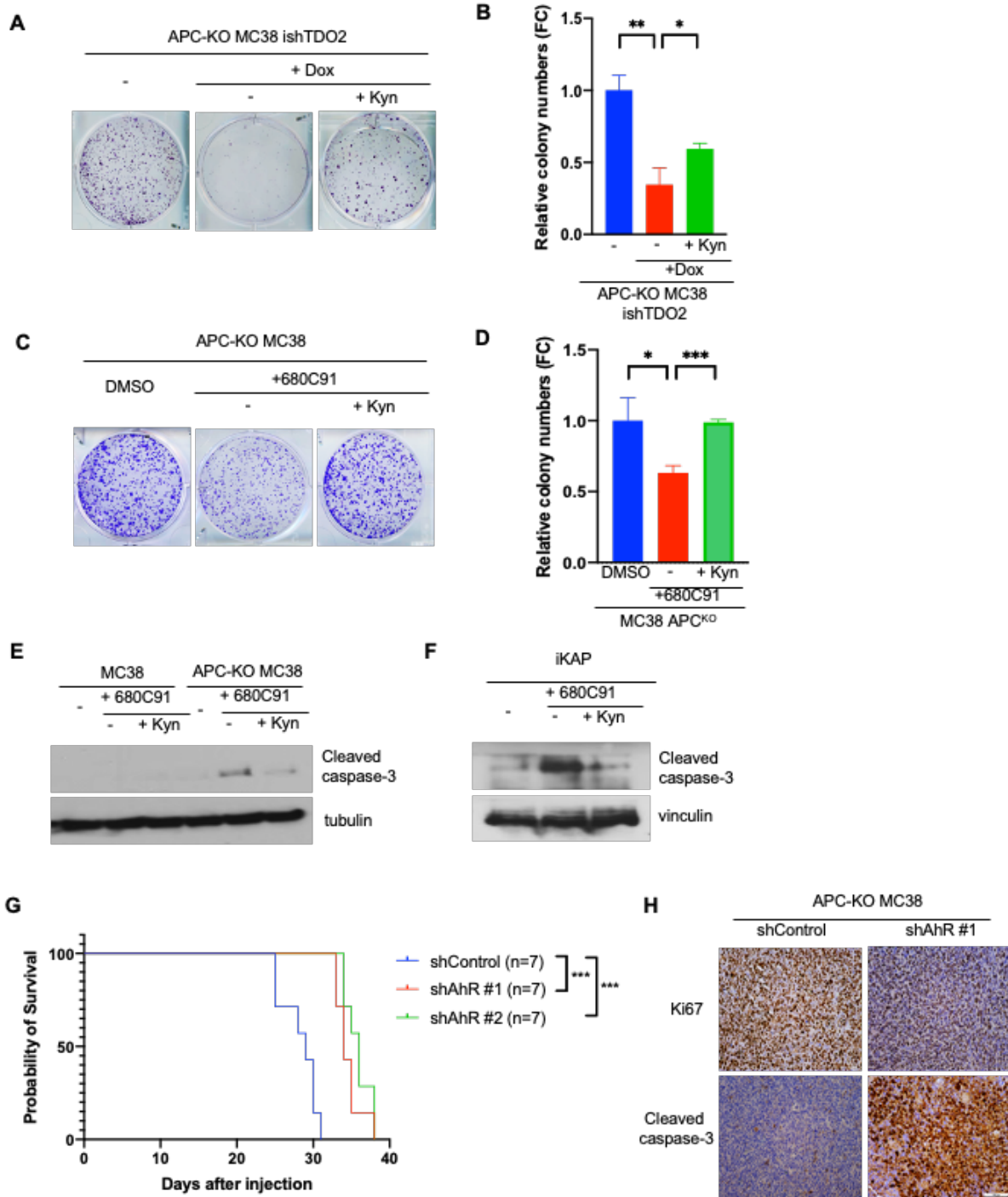


Figure 22: TDO2-Kyn-AhR axis supports APC-deficient cancer cell proliferation, survival, and tumorigenic potential.

(A and B) Representative images and a quantification graph of colony formation assay of ishTDO2 *APC*-KO MC38 cell lines after Dox alone or Dox/Kyn co-treatment. **(C and D)** Representative images and a quantification graph of colony formation assay of ishTDO2 *APC*-KO MC38 cell lines after 680C91 alone or 680C91/Kyn co-treatment. **€** Immunoblots for cleaved Caspase-3 in *APC*-WT and *APC*-KO MC38 cells treated with 680C91 alone or 680C91/Kyn co-treatment. **(F)** Immunoblots for cleaved Caspase-3 in iKAP treated with 680C91 alone or 680C91/Kyn co-treatment. **(G)** Survival curves of C57BL/6J mice orthotopically implanted with *APC*-KO MC38 cells with two different shAhR constructs (2×10^5 cells). *** $P < 0.001$. Log-rank (Mantel-Cox) test. **(H)** Representation of IHC staining for Ki67 and cleaved Caspase-3 in CRC orthotopic tumor tissues established with shControl and shAhR #1 *APC*-KO MC38 cell lines. Scale bars, 100 μ m.

4.2.4 TDO2-Kyn-AhR axis regulates glycolysis pathway of APC-mutant CRC cancer cells.

To discern the cancer hallmarks regulated by TDO2, we performed the pathway analysis using two different sets of samples to analyze the cell-autonomous and immune pathways. Using RNA-seq data from APC-KO MC38 ishTDO2 cell lines and tumor microarray datasets from the tumors established by the cell lines in C57BL/6J mice were, we overlapped these pathways and further narrowed down the list using the pathways that are upregulated by APC deletion to identify the pathways regulated both by WNT pathway and TDO2.

GSEA was conducted on *APC-KO* MC38 cell lines and derivative tumors following TDO2 depletion and consistent with known cancer cell intrinsic functions of the APC/WNT pathway (Pate et al., 2014), hypoxia and glycolysis pathways were up-regulated in *APC-KO* cells (Fig. 23, A and B). Correspondingly, *APC-KO* MC38 cells exhibited higher sensitivity to the GLUT1 inhibitor STF-31 than *APC-WT* controls (Fig. 23C) and showed increased glucose uptake and lactate secretion, which were reversed by TDO2 depletion (Fig. 23, D and E).

RT-PCR analysis confirmed up-regulation of key glycolysis genes (SLC2A1, HK1/2, and PFKL), which were down-regulated upon TDO2 or AhR depletion (Fig. 24, A and B). Metabolite analysis of cell lysates and conditioned media from *APC-KO* MC38 cells showed decreased levels of glycolysis pathway-related metabolites upon TDO2 depletion (Fig. 24C). To further link TDO2 to the regulation of metabolic pathways, we examined multiple elements in the GCN2 and mTOR pathways in MC38 *APC-WT* and *APC-KO* cells containing an inducible shTDO2 construct (Fig.

24D). APC deletion increased the level of phosphorylated eIF2, and this increase was reversed upon TDO2 depletion in the APC null cells. In addition, TDO2 depletion decreased phosphorylated mTOR, only in the APC null cells.

We measured the modified glycolytic function induced by TDO2 via Seahorse XF Glycolysis Stress Test analyses of MC38 APC-WT cells with empty versus TDO2 expression vectors (Fig. 25, A and B). Enforced TDO2 expression increased the key parameters of glycolytic flux which are glycolysis, glycolytic capacity, glycolytic reserve, as well as non-glycolytic acidification, relative to the MC38 empty vector controls, reinforcing the role of TDO2 in promoting glycolysis (Fig. 25C). Finally, and conversely, Seahorse experiments were performed on the MC38 APC-WT and APC-KO ishTDO2 cells to assess the impact of TDO2 depletion on glycolytic flux in real time. As expected, APC deletion was associated with increased glycolysis, glycolytic capacity and glycolytic reserve only in the MC38 APC-KO lines (Fig. 25, D and E). The most significantly changed parameter was glycolytic reserve, which shows 'the cell's potential to respond to an energetic demand as well as how close the glycolytic function is to the cell's theoretical maximum'. Furthermore, the glycolytic flux was also measured with MC38 APC-KO cells expressing two independent AhR shRNAs, showing decreased overall flux upon AhR depletion (Fig. 25, F and G), again confirming the metabolic regulatory role of the TDO2-AhR axis. Together, these experiments show that TDO2-AhR signaling plays a key role in promoting cancer cell glycolysis.

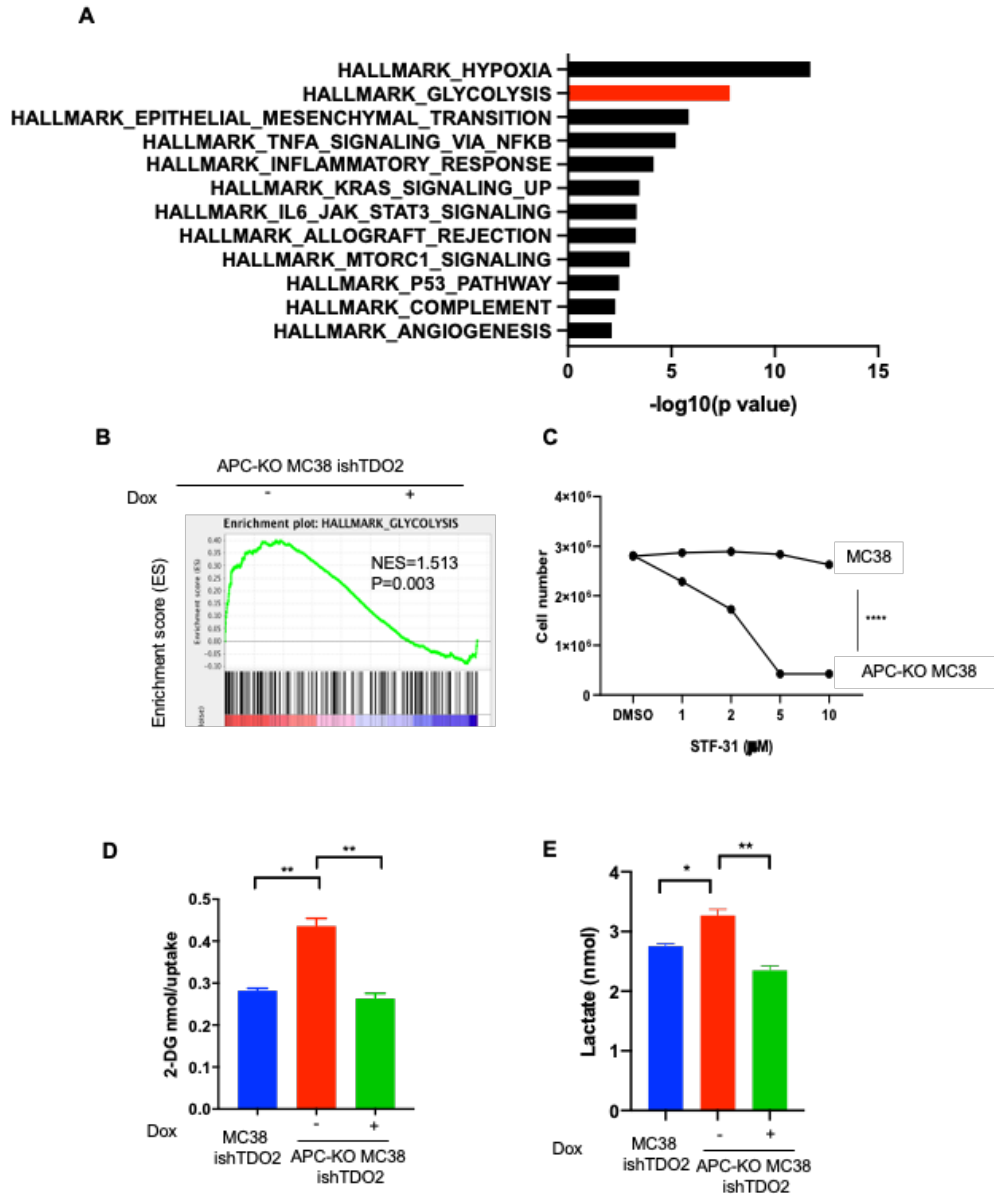
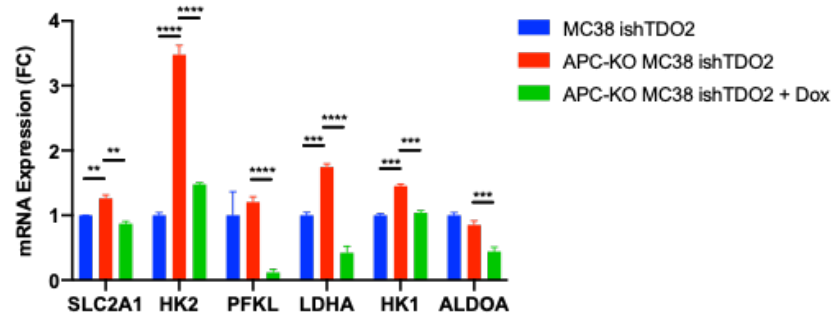


Figure 23: Glycolysis pathway is increased by APC deficiency and decreased by TDO2 depletion in MC38 cells.

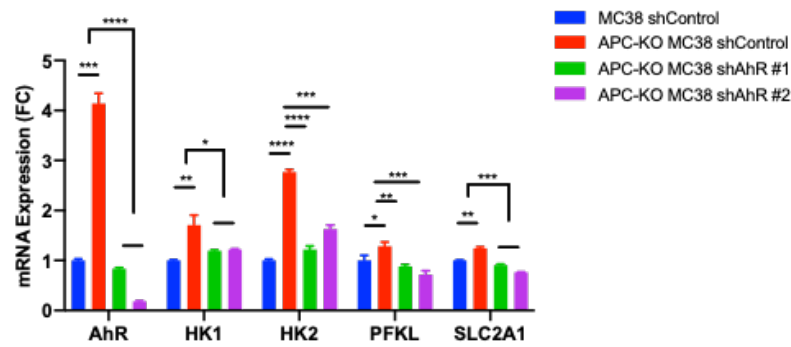
(A) GSEA analysis (Hallmark gene sets) on genes that overlap between RNA-seq datasets of ishTDO2 APC-KO MC38 cell lines (No dox vs. 48hr dox, n=3) and microarray datasets of allograft tumors established with ishTDO2 APC-KO MC38 cell lines (No dox vs. dox treated, n=3). **(B)** GSEA correlation of glycolysis with

altered gene expression in TDO2 depleted *APC*-KO MC38 cells. Normalized enrichment score (NES) and nominal P value are shown. **(C)** Cell viability assay of *APC*-WT and *APC*-KO MC38 cells treated with STF-31 for 24hr in a dose-dependent manner. Six replicates per group. *** $P < 0.001$, two-tailed t-test. **(D)** 2-DG uptake assay with ishTDO2 *APC*-WT and *APC*-KO MC38 cell lines with and without dox treatment. ** $P < 0.01$, *** $P < 0.001$, two-tailed t-test. **(E)** Measurement of secreted lactate with condition media from ishTDO2 *APC*-WT and *APC*-KO MC38 cell lines with and without dox treatment. * $P < 0.05$, ** $P < 0.01$, two-tailed t-test.

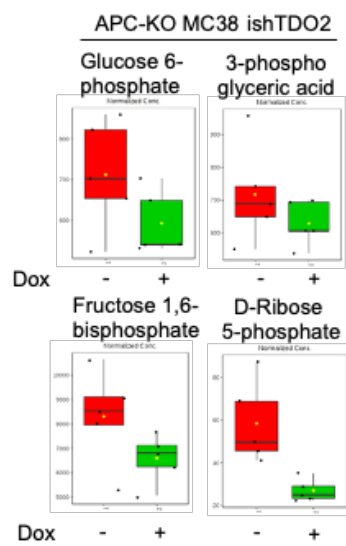
A



B



C



D

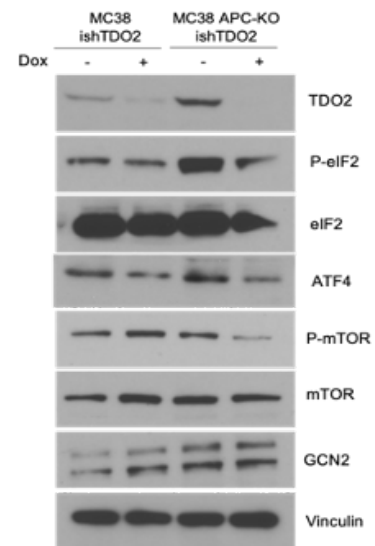


Figure 24: TDO2-AhR axis regulates glycolysis pathway in APC-deleted MC38 cells.

(A) RT-qPCR analysis of glycolysis pathway genes in ishTDO2 *APC*-WT and *APC*-KO MC38 cell lines. ** $P < 0.01$, *** $P < 0.001$, **** $P < 0.0001$, two-tailed t-test. **(B)** RT-qPCR analysis of glycolysis pathway genes in *APC*-WT and *APC*-KO MC38 cell lines expressing shControl or two shAhR constructs. * $P < 0.05$, *** $P < 0.001$, **** $P < 0.0001$, two-tailed t-test. **(C)** Changes in concentration of key glycolysis metabolites in ishTDO2 *APC*-KO MC38 cell line lysates. The red bars indicate cells without dox treatment and the green bars indicate dox-treated cells. $n = 5$ per biological replicates. **(D)** Western blot images of GCN2 and mTOR pathway components in ishTDO2 *APC*-WT and *APC*-KO MC38 cells.

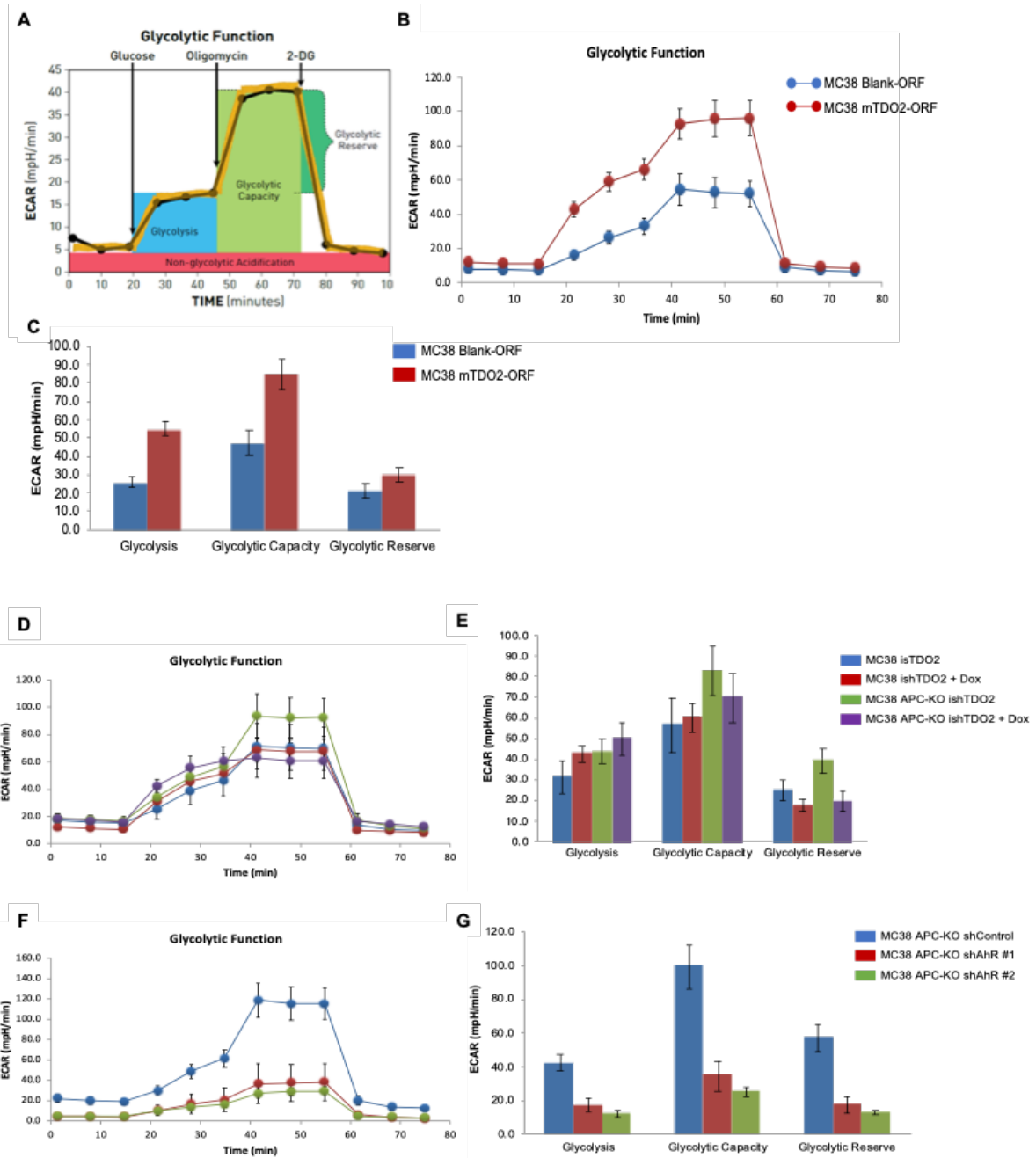


Figure 25: Glycolytic flux is regulated by the TDO2-AhR axis.

(A) Representation of key parameters of glycolytic flux measured by Seahorse experiment. **(B and C)** Measured extracellular acidification rate (ECAR) in MC38 Blank-ORF and mouse TDO2-ORF expressing cell lines. **(D and E)** Measured extracellular acidification rate (ECAR) in MC38 APC-WT and APC-KO ishTDO2 cell lines with and without Dox treatment. **(F and G)** Measured extracellular acidification rate (ECAR) in MC38 APC-KO cell lines with shControl or two different shAhR constructs (#1 and #2).

Chapter 5: TDO2 regulates infiltration of tumor associated macrophage in APC-mutated CRC.

Chapter 5: TDO2 regulates infiltration of tumor associated macrophage in APC-mutated CRC.

Content of this chapter is partly based on the following manuscript:

Lee R, Li J, Chakravarti D, Chen P, Li J., Wu C, Jiang S, LaBella KA, Spring DJ, Wang YA, Zhao D., DePinho RA., Synthetic Essentiality of TDO2 in APC-Mutated Colorectal Cancer, *Submitted*

5.1 Introduction and rationale

Immunosuppressive roles of kynurenine generated from KP signaling are mediated by regulating functions of immune cells in the TME; activation and recruitment of Tregs, inhibiting proliferation and effector functions of CD8-presenting T cells, recruitment of MDSCs (Campesato et al., 2020, Liu et al., 2018, Takenaka et al., 2019). However, whether the functions of KP signaling are at variance depending on the genetic context of the tumor has not been studied.

Considering the low immune infiltration in CRC tumors, so called ‘cold tumors’, and consequent disappointing efficacy of immuncheckpoint blockade therapy in CRC, it is imperative to understand the signaling circuits that contribute to immune evasive TME. Our comparative survival analysis with immune-compromised NSG mice and B6 immuno-competent mice which were injected with isogenic APC-WT and APC-Mut MC38 cell lines orthotopically alluded significant roles of immune system in modulating TDO2-mediated tumor growth in APC-mutant CRC.

In addition, pathway analysis from both RNA-seq data from APC-KO MC38 ishTDO2 cell lines and tumor microarray datasets from the tumors established by the cell lines in C57BL/6J mice showed several immune-related signaling as top

modified pathways by TDO2 depletion, which prompted us to examine the immune modulatory roles of TDO2.

5.2 Results

5.2.1 TDO2 depletion inhibits infiltration of tumor associated macrophages

Pathway analysis using RNA-seq data from APC-KO MC38 ishTDO2 cell lines and tumor microarray datasets from the MC38 tumors established in C57BL/6J mice showed, in addition to cancer cell-intrinsic processes, that APC status (APC-KO versus APC-WT MC38) or TDO2 depletion in APC-deficient cancer cells and tumors resulted in prominent representation of immune signaling signatures such as TNFA signaling, inflammatory response, IL-6_JAK_STAT, allograft rejection, and complement (Fig. 26, A and B). These *in silico* observations prompted immunoprofiling of orthotopic tumors generated from isogenic APC-KO and APC-WT MC38 cells with and without TDO2 depletion.

Cytometry by time of flight (CyTOF) analysis was performed using APC-WT and APC-KO MC38 CRC orthotopic tumors developed in immunocompetent mice to identify subsets of immune cells that are regulated by APC and TDO2. viSNE plots of CyTOF data showed that APC deficiency resulted in significantly increased macrophage abundance, which decreased upon TDO2 depletion (Fig. 26C). Decreased macrophages by TDO2 depletion was not observed in APC-WT MC38 tumors, confirming the APC-deficient context specific immune responses regulated by TDO2. We also observed changes in Tregs and neutrophils, but infiltration of macrophages exhibited the most significant changes. Quantification of F4/80

positive cells (total macrophages) and CD206^{high} M2-like cells in CD45-positive population confirmed enrichment of macrophages in *APC*-KO tumors and their reduction upon TDO2 depletion (Fig. 26D). Immunohistochemistry staining of F4/80 and CD163 in these tumors aligned with the aforementioned CyTOF data (Fig. 27, A and B). *APC*-WT and *APC*-KO MC38 orthotopic tumors treated with the TDO2 inhibitor PF06845102/EOS200809 were also examined for macrophage infiltration, exhibiting similar results to the TDO2-depleted tumors. In contrast, Epacadostat treatment did not increase infiltration of total and M2-like macrophages. (Fig. 27B). Importantly, TDO2 inhibition also increased the number of infiltrating CD8-positive cells only in *APC*-KO MC38 tumors, but Epacadostat-treated tumors showed no changes in the number of CD8-expressing cells (Fig. 27, C and D), suggesting the roles of TDO2 in adaptive immunity.

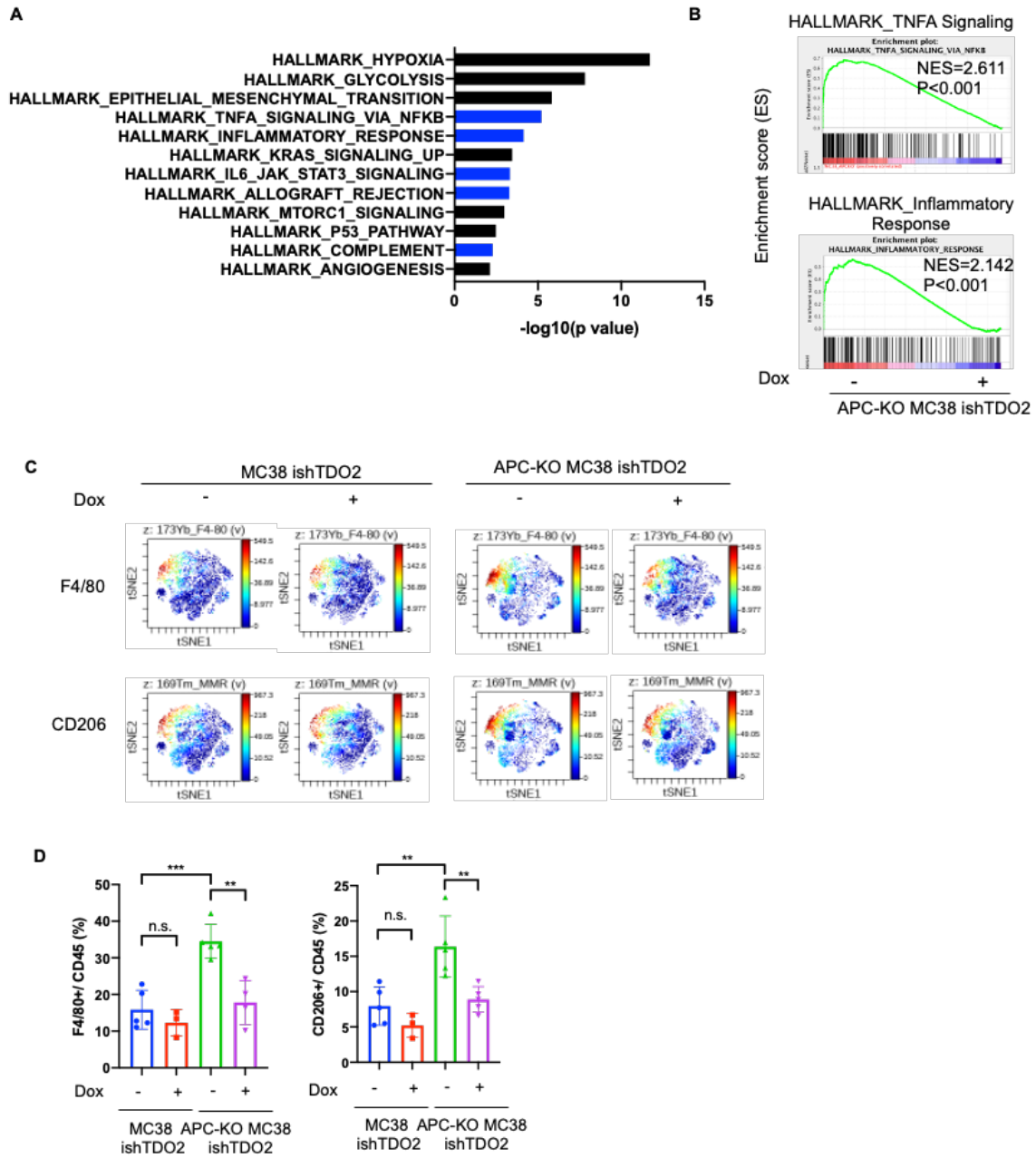


Figure 26: TDO2 mediates tumor growth by regulating macrophage infiltration.

(A) GSEA analysis (Hallmark gene sets) on genes that overlap between RNA-seq datasets of ishTDO2 *APC*-KO MC38 cell lines (No dox vs. 48hr dox, n=3) and microarray datasets of allograft tumors established with ishTDO2 *APC*-KO MC38 cell lines (No dox vs. dox treated, n=3). The blue bars indicate immune response-related pathways. **(B)** GSEA correlation of TNFA signaling and inflammatory response with alternatively expressed genes in TDO2-depleted *APC*-KO MC38 cells. Normalized enrichment scores (NES) and nominal P values are shown. **(C)** viSNE analysis of F4/80+ and CD206+ immune cells assessed by CyTOF from CRC orthotopic ishTDO2 *APC*-WT and *APC*-KO MC38 tumors. **(D)** Quantification of macrophages (F4/80+) and M2 macrophages (CD206+) in tumors shown in panel **(C)**. CyTOF data were analyzed by FlowJo. Data represent mean \pm s.d. *P<0.05, **P< 0.01. two-tailed t-test.

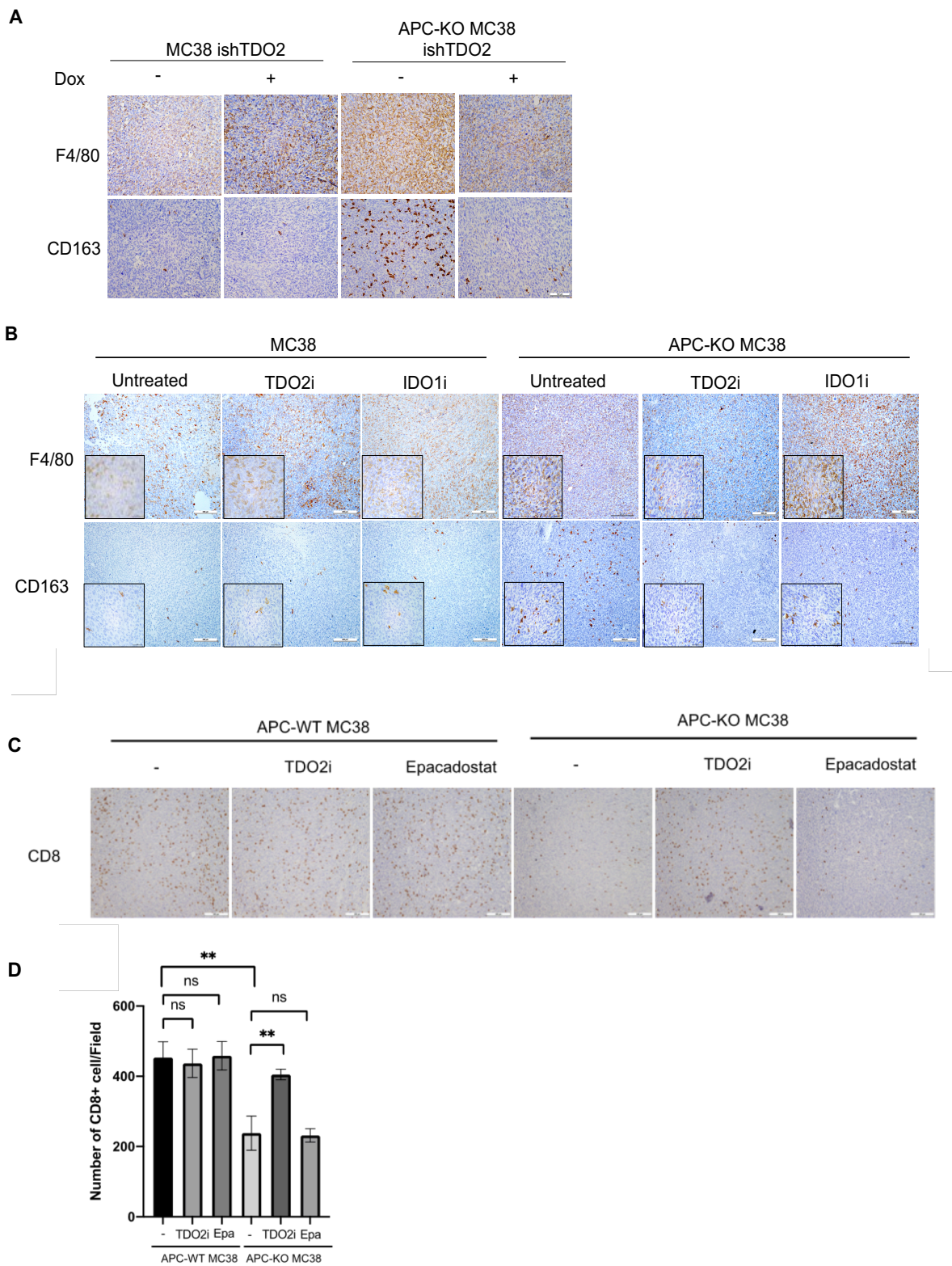


Figure 27: Increased macrophage infiltration mediated by APC deficiency is reversed by TDO2 inhibition in MC38 tumors.

(A) Representation of IHC staining for F4/80 and CD163 in CRC orthotopic tumor tissues established with ishTDO2 *APC*-WT and *APC*-KO MC38 cell lines. Scale bars, 100 μ m. **(B)** Representation of IHC staining for F4/80 and CD163 in no-treatment, TDO2 inhibitor-treated, and Epacadostat-treated *APC*-WT and *APC*-KO MC38 CRC orthotopic tumor tissues. Scale bars, 200 μ m. **(C and D)** Representation of IHC staining for CD8-positive cells in no-treatment, TDO2 inhibitor-treated, and Epacadostat-treated *APC*-WT and *APC*-KO MC38 CRC orthotopic tumor tissues with a quantification graph. Scale bars, 200 μ m.

5.2.2 TDO2 depletion inhibits infiltration of tumor associated macrophages in human CRC

To corroborate TDO2-mediated TME modulation, specifically focusing on macrophage infiltration and polarization, TCGA CRC datasets were examined for correlation between the expression of macrophage (total and M2) and TDO2. It showed that CRC tumors with high total and M2-like macrophage marker expression is positively correlated with TDO2 expression (Fig. 28, A and B). Interestingly, Tregs and MDSC markers also showed strong positive correlations between the degree of TDO2 expression levels (Fig. 28, C and D).

This WNT-TDO2-macrophage correlation was further validated by human CRC tumor microarray (TMA) analyses. Cancer cells with nuclear β -catenin signal exhibited higher CD163 expression in the TME (Fig. 28E). Quantified data of the stained CRC TME showed a significant positive correlation between nuclear β -catenin and infiltrated CD163-expressing/ M2-like macrophages (Fig. 28F). Together, these findings support the model that activated WNT-driven upregulation of TDO2 expression in turn activates the AhR network which functions to recruit immune suppressive TAMs into the TME.

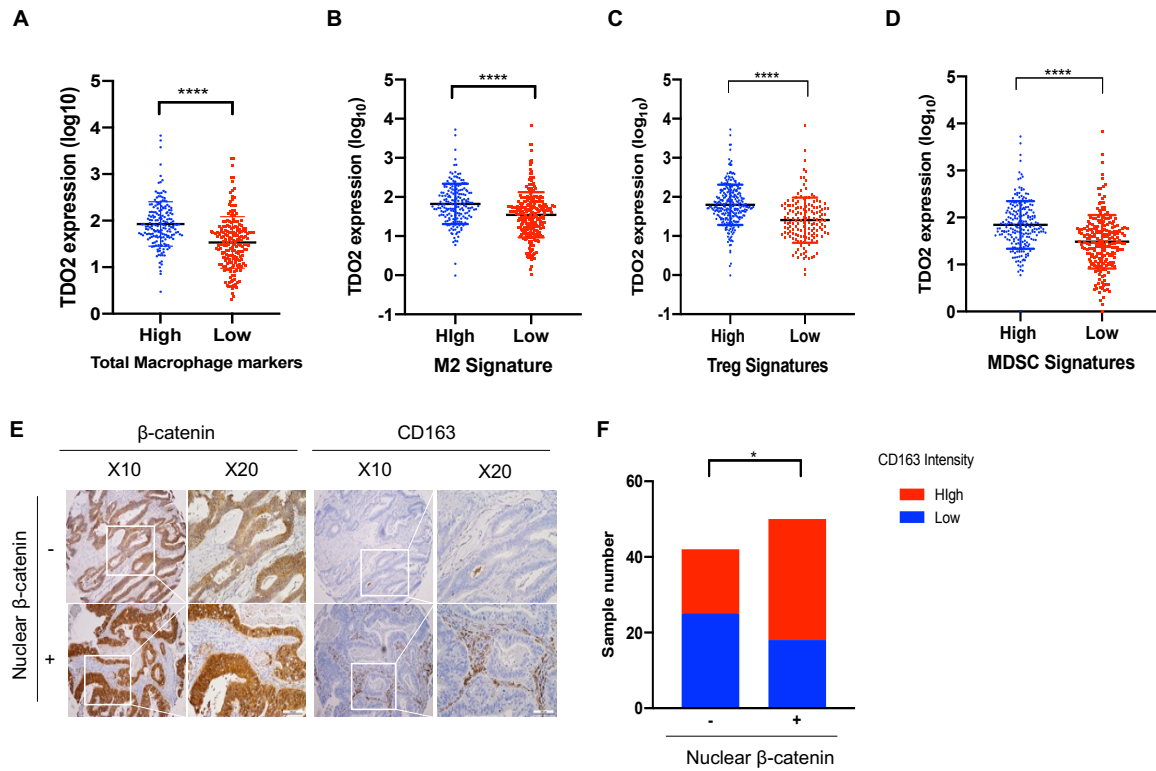


Figure 28: TDO2 expression correlates with M2-like macrophage signature expression.

(A - D) TDO2 mRNA expression is significantly correlated with expression of total macrophage, M2 macrophage, regulatory T cells, and MDSC markers in TCGA CRC (COAD + READ, Provisional) patients (n=433). ****P<0.0001. two-tailed t-test. **(E)** Representative images of IHC staining for CD163 in human CRC tumors with negative (n=42) and positive nuclear β-catenin (n=50). Scale bars, ×10 (200μm) and ×20 (100μm). **(F)** CRC tumors with nuclear β-catenin showed higher CD163 expression. Pearson Correlation Coefficient = 5.074, P =0.0243. Chi-squared test.

5.2.3 TDO2 modulates TAM infiltration by regulating cytokines

To identify WNT-TDO2-AhR-regulated downstream factors that may recruit TAMs into the tumor sites, we performed cytokine array profiling of conditioned media (CM) from *APC*-KO MC38 ishTDO2 cells. Induction of TDO2 depletion reduced secretion of classical macrophage cytokines including G-CSF, GM-CSF, CXCL2 (Fig. 29A) and other cytokines (see below). Correspondingly, transwell migration assays using bone marrow-derived macrophages (BMDM) showed that CM from *APC*-KO MC38 ishTDO2 cultures increased macrophage migration which was nullified upon TDO2 depletion (Fig. 29, B and C).

Next, to more fully vet the most highly regulated cytokines in our system, we identified, and qRT-PCR validated the top ranked genes in the RNA-seq dataset and found that CXCL5, CXCL7 (PPBP), CSF3 (G-CSF), CXCR2, CXCL2, CXCL10, CCL2, and CXCL1 showed the most significant expression changes associated *APC* deletion or TDO2 depletion (Fig. 30A). To further identify the target cytokines of TDO2, cell lines that express ORFs of the top three genes from RNA-seq data -- CXCL5, CXCL7 (PPBP), and CSF3 -- were generated in *APC*-KO MC38 ishTDO2 cells and monitored for tumor growth to identify genes that rescue the impaired proliferation by TDO2 knockdown. Enforced expression of CXCL5, which showed the highest fold changes, was most active in rescuing the decreased tumor growth mediated by TDO2 depletion (Fig. 30B). Moreover, CyTOF analysis of CXCL5-overexpressing *APC*-KO tumors showed increased TAMs in the presence of shTDO2 (Fig. 30, C-E).

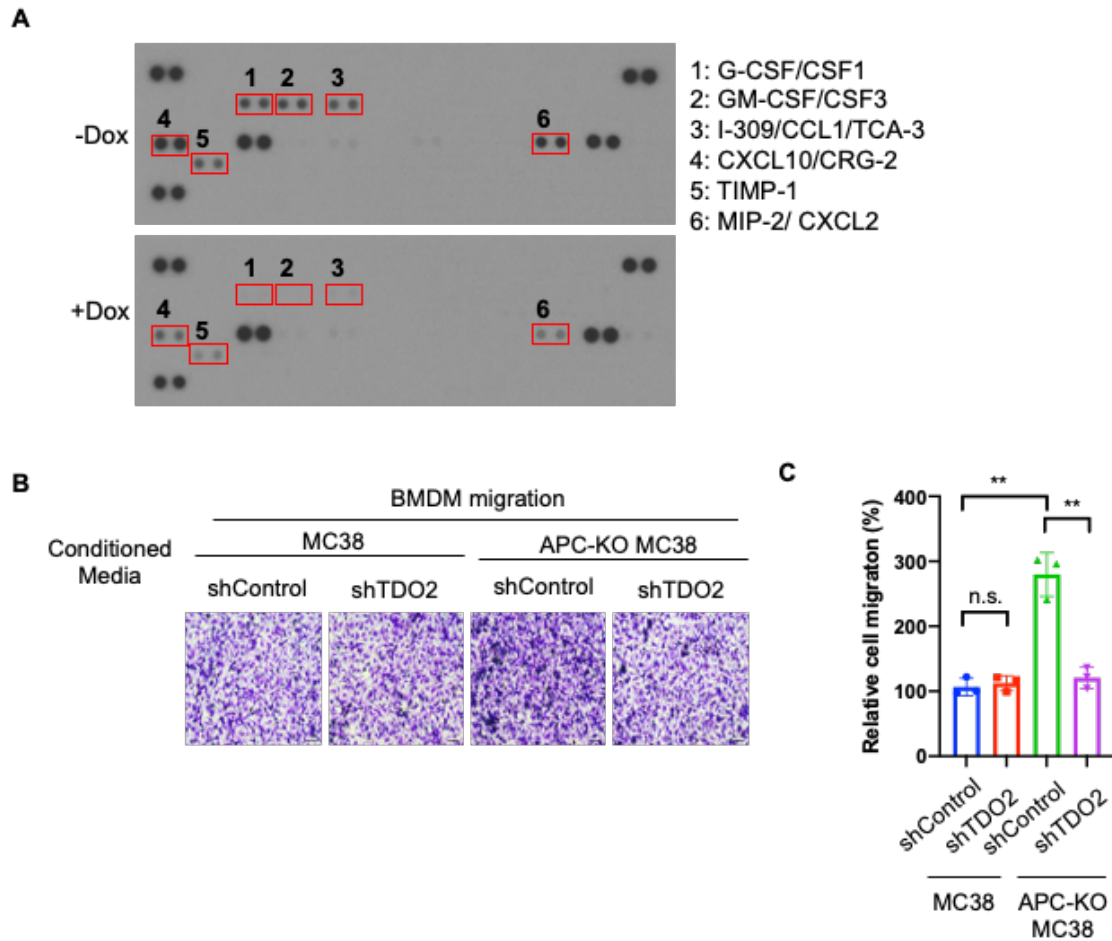


Figure 29: Cytokines secreted from APC-deficient CRC cells promote macrophage migration, which is inhibited by TDO2 knockdown.

(A) Cytokine array of condition media from ishTDO2 APC-KO MC38 cells with and without dox treatment. The red boxes (labeled as 1-6) indicate cytokines that significantly decreased after TDO2 knockdown. **(B and C)** Representation of migrated BMDM cultured in condition media from APC-WT and APC-KO MC38 cell lines expressing shControl or shTDO2. Scale bars, 50 μ m. The graph shows the quantified data ** $P < 0.01$, two-tailed t-test.

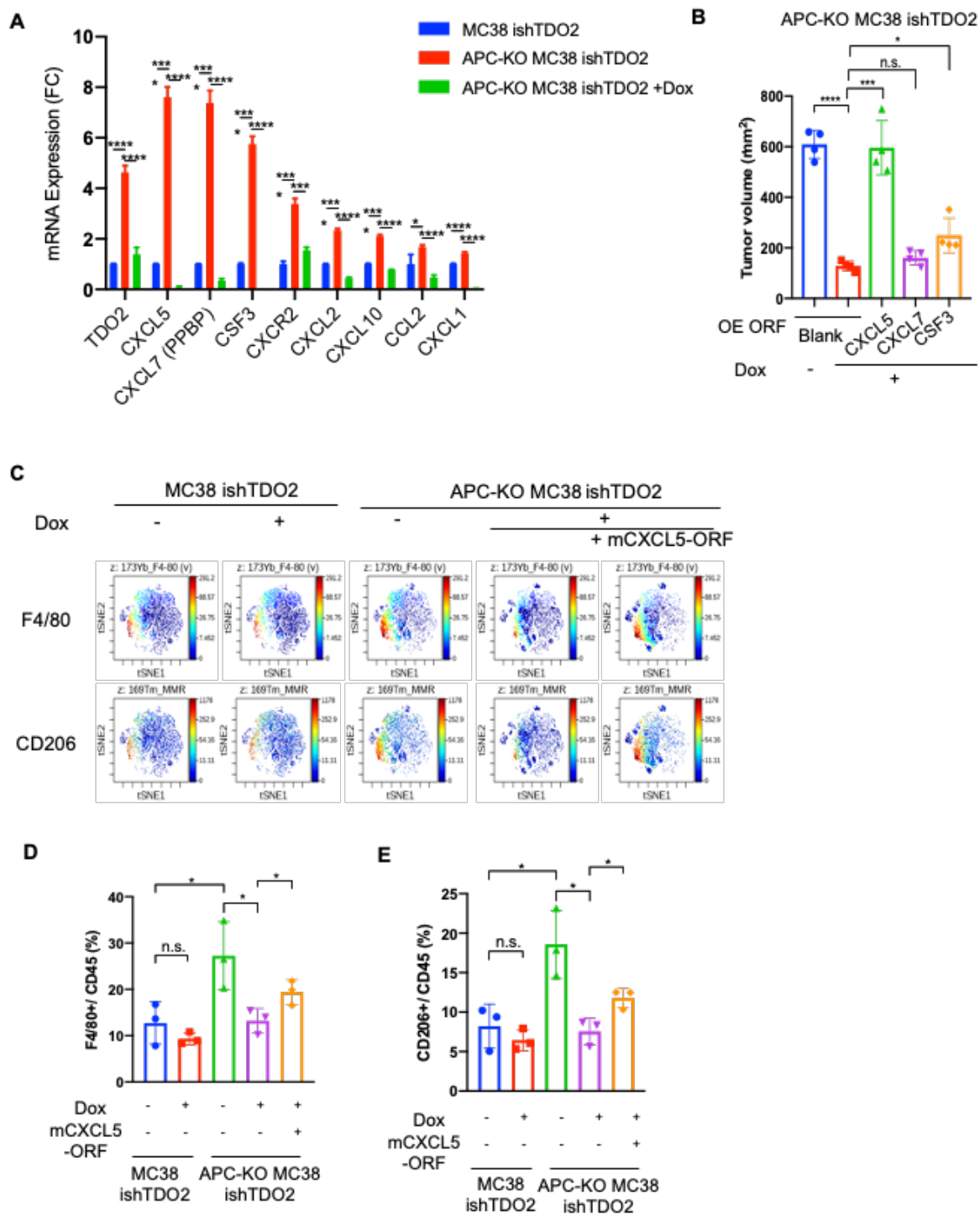


Figure 30: TDO2-AhR-CXCL5 axis regulates macrophage recruitment in APC-mutated CRC tumors.

(A) Expression of immune response-related genes identified in RNA-seq analysis and TDO2 were validated by RT-qPCR using ishTDO2 *APC*-WT and *APC*-KO MC38 cell lines. n=3 biological replicates. *P<0.05, ***P<0.001, ****P<0.0001. two-tailed t-test. **(B)** Volume of tumors established with ishTDO2 *APC*-KO MC38 cell lines expressing Blank, CXCL5, CXCL7, and CSF3. Dox food was supplied at day 5 post-orthotopic injection to induce TDO2 knockdown in vivo. n = 4 per group. n.s.P>0.05, *P<0.05, ****P<0.001, ****P<0.0001. two-tailed t-test. **(C)** viSNE analysis of F4/80+ and CD206+ immune cells assessed by CyTOF from CRC orthotopic ishTDO2 *APC*-WT and *APC*-KO MC38 tumors and CXCL5-ORF expressing *APC*-KO MC38 with TDO2 depletion. **(D and E)** Quantification of macrophages (F4/80+) and M2 macrophages (CD206+) in tumors shown in (E). CyTOF data were analyzed by FlowJo. Data represent mean \pm s.d., n = 3 per group. *P<0.05, **P< 0.01. two-tailed t-test.

5.2.4 TDO2-AhR-CXCL5 modulates TAM infiltration and polarization in APC-mutant CRC

To test whether CXCL5 can promote migration of macrophages, we performed migration assays using recombinant CXCL5 proteins. APC-KO MC38 cells CM significantly promoted Raw 264.7 macrophage cell migration compared to APC-WT CM and APC-KO TDO2-depleted CM decreased the migration (Fig. 31A). Supplementing CXCL5 rescued macrophage recruitment when cultured with either APC-WT and APC-KO CM. SX-682 is an inhibitor of CXCR1/2, where CXCL5 binds and co-treatment of SX-682 abrogated the rescue by CXCL5 supplementation (Fig. 31A). Inhibiting CXCR1/2 not only blocks the binding of CXCL5 but also the binding of other critical cytokines such as CXCL1-3, CXCL6, CXCL7, and CXCL8 that mediates monocytes/macrophages infiltration as well (Olson and Ley, 2002). which resulted in nullifying CXCL5 supplementation effects in APC-WT CM cultured macrophage cells as well. In addition, AhR inhibitor treatment (CH223191) profoundly decreased CXCL5 expression in APC-Wt and APC-KO MC38 cells in a dose-dependent manner (Fig. 31B), which directly shows that CXCL5 expression is regulated by AhR.

Moreover, CM from APC-KO MC38 cells upregulated several M2 macrophage markers (CD206, YM1, YM2, Arg1) in Raw264.7 cells, which were decreased by TDO2 knockdown and rescued by CXCL5 supplementation (Fig. 31C). Similarly, BMDMs co-cultured with Kyn or CXCL5 showed increased M2 macrophage marker expression while CSF1 serves as a positive control. Interestingly, CSF1 and CXCL5 did not increased the expression of a M1-like

macrophage marker iNOS, Kyn upregulated iNOS expression in BMDM, which suggests multi-faceted roles of Kyn in regulating monocyte education. These results support a role for the TDO2-AhR axis in promoting TAM polarization (Fig. 31D).

Immunohistochemical analysis of total and M2-like macrophage markers showed increased infiltration of macrophages in tumors with enforced CXCL5 expression despite the TDO2 depletion (Fig. 32A). Finally, allograft mice with *APC*-KO MC38 cells showed increased survival upon TDO2 depletion (inducible shTDO2) or macrophage depletion by Clodronate liposomes (Fig. 32B). CXCL5 overexpression in *APC*-KO MC38 cell lines with TDO2 depletion significantly shortened the survival of mice, which was reversed by depleting macrophages (Fig. 32B). Finally, *APC*-KO MC38 cells treated with anti-CXCL5 neutralizing antibody also showed prolonged survival (Fig. 32C). These results suggest the roles of the TDO2-AhR-CXCL5 axis in regulating TAM infiltration and polarization in *APC*-KO CRC tumors.

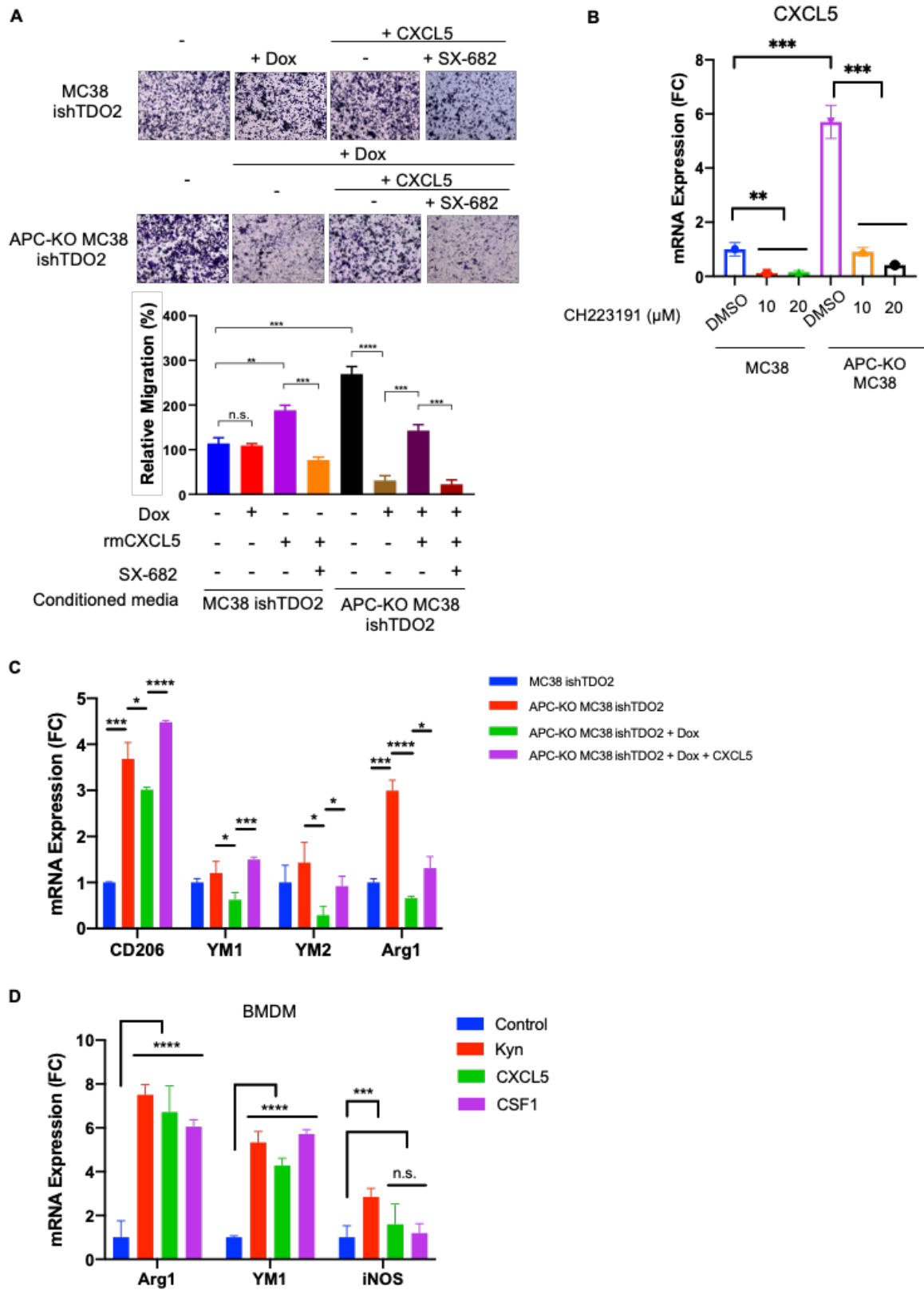


Figure 31: TDO2-AhR-CXCL5 axis regulates macrophage polarization.

(A) Representative images of migrated Raw264.7 cells cultured with ishTDO2 *APC*-WT and *APC*-KO MC38 conditioned media in transwell assay. Recombinant CXCL5 protein (50 ng) and SX-682 (1 μ M) were added to harvested conditioned media for 36 hr. Scale bar, 100 μ m. n=3 biological replicates. Quantification: n.s. $P>0.05$, *** $P<0.001$, **** $P<0.0001$. two-tailed t-test. **(B)** RT-qPCR analysis for CXCL5 expression in *APC*-WT and *APC*-KO MC38 cells upon CH223191 treatment for 36hr. *** $P<0.001$ **(C)** RT-qPCR analysis of M2 macrophage signature genes in Raw264.7 cells incubated with conditioned media from ishTDO2 *APC*-WT and *APC*-KO MC38 cells for 30h. n=3 biological replicates. **(D)** RT-qPCR analysis of M2 macrophage signature genes Arg1 and YM1 and M1 macrophage signature gene iNOS in BMDM treated with CSF1 (50ng), CXCL5 (50ng), and Kyn (1mM) for 24hr n.s. $P>0.05$, **** $P<0.0001$. two-tailed t-test.

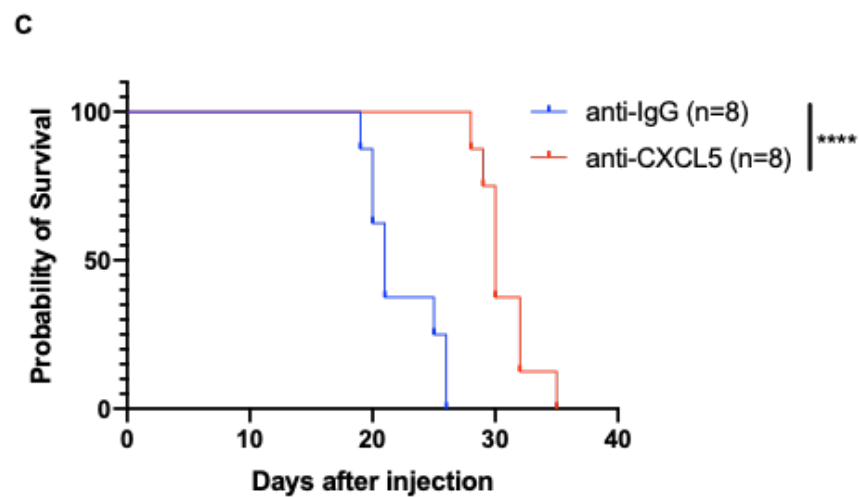
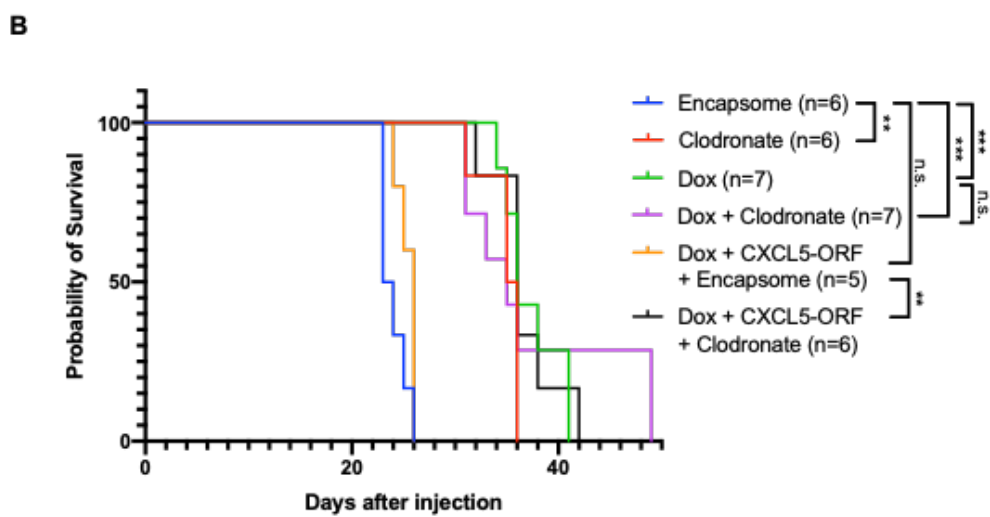
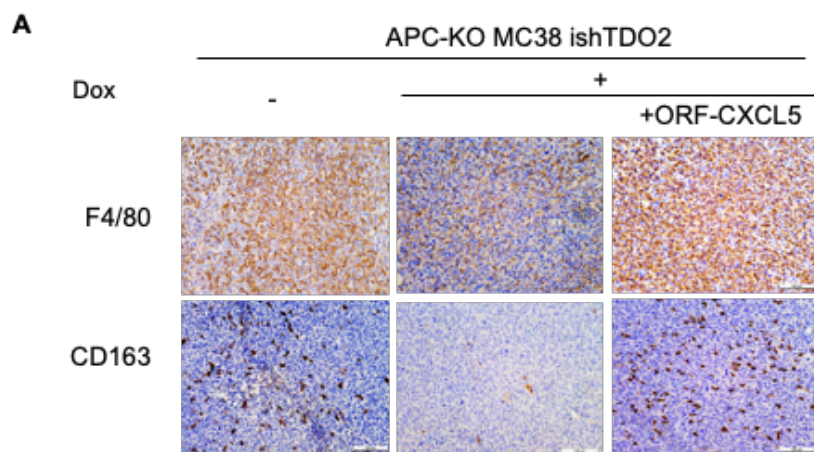


Figure 32: Macrophage depletion or CXCL5 neutralization inhibit APC-deleted tumor growth and improve survival.

(A) Representation of IHC staining for F4/80 and CD163 in CRC orthotopic tumor tissues established with ishTDO2 and ishTDO2/CXCL5-ORF APC-KO MC38 cell lines. Scale bars, 100 μ m. **(B)** Survival curves of C57Bl/6J mice orthotopically implanted with ishTDO2 and ishTDO2/CXCL5-ORF APC-KO MC38 cell lines (5×10^5 cells). Clodronate liposomes or control Encapsome liposomes were given intraperitoneally (100 μ l) at day 2 post-orthotopic injection and three times a week. (Encapsome and Clodronate groups, n = 6; Dox and Dox + Clodronate groups, n = 7; Dox + CXCL5-ORF + Encapsome, n = 5; Dox + CXCL5-ORF + Clodronate, n = 6). n.s.P>0.05, **P<0.01, ***P<0.001. Log-rank (Mantel-Cox) test. **(C)** Survival curves of C57Bl/6J mice orthotopically implanted with APC-KO MC38 cell lines (5×10^5 cells) treated with 200 μ g control rat IgG2b or neutralizing CXCL5 antibodies every three days post injection. ****P<0.0001. Log-rank (Mantel-Cox) test.

5.2.5 TDO2-AhR-CXCL5 in human TCGA datasets

To further validate the positive relationship between the TDO2-AhR-CXCL5 axis and TAM abundance in human CRC, TCGA CRC (COAD and READ) dataset was clustered based on CXCL5 expression and analyzed for correlated immune populations. These analyses revealed that TAM abundance correlated positively with high CXCL5 expression (Fig. 33A). We also observed positive correlation between CXCL5 expression and macrophage infiltration in TCGA BRCA dataset (data not shown). Types of immune cells that showed positive correlation identified macrophages as one of the immune cell subsets (Fig. 33B). Interestingly, T cell showed the most significant positive correlation with CXCL5 expression level, further suggesting the roles of CXCL5 in regulating adaptive immune responses in CRC.

In addition, CXCL5 expression correlated positively with increased tryptophan metabolism (TDO2 as top pathway signature gene) and xenobiotic metabolism in TCGA CRC (Fig. 33, C-E). Together, these data establish that TDO2-AhR signaling upregulates CXCL5 which recruits TAMs to promote tumor growth; conversely, neutralization of the TDO2-AhR-CXCL5 pathway is a validated anti-tumor strategy.

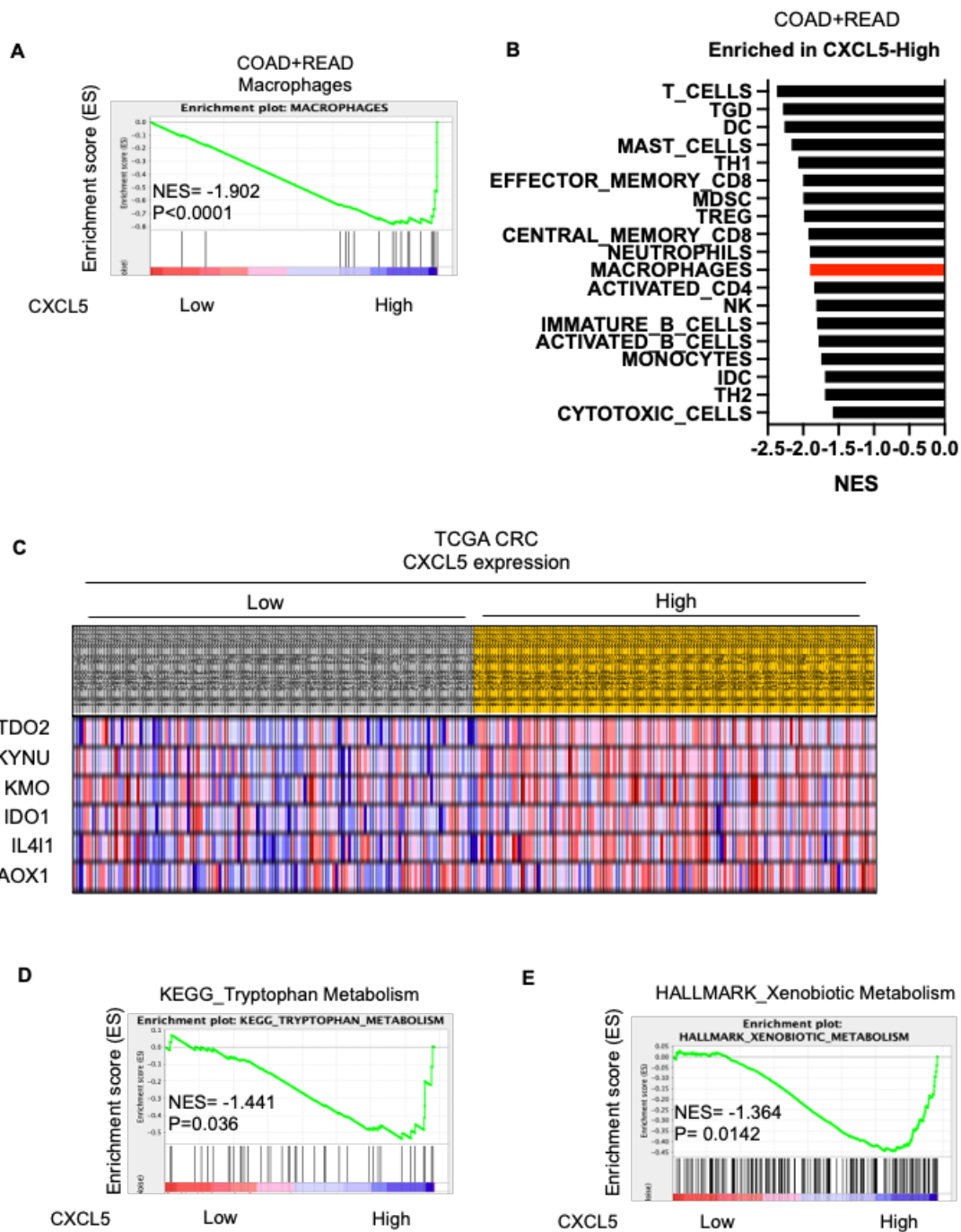


Figure 33: CXCL5 expression is correlated with TDO2-AhR pathway and macrophage infiltration in human CRC.

(A) GSEA correlation of macrophage populations with CXCL5-High tumors in TCGA CRC database. NES and nominal P value are shown. **(B)** List of immune populations positively correlated with CXCL5 expression in TCGA CRC (n = 254) tumors. The red bar indicates macrophages. NES values are shown. **(C)** Representative images of clustered TCGA CRC patient samples based on CXCL5 expression and expression of correlative top six tryptophan metabolism-associated genes (*TDO2*, *KYNU*, *KMO*, *IDO1*, *IL4I1*, and *AOX1*) in ranked order (CXCL5 high, n = 127, CXCL5 low, n = 127). **(D and E)** GSEA correlation of tryptophan metabolism and xenobiotic metabolism with CXCL5-High TCGA CRC tumors. Normalized enrichment score (NES) and nominal P value are shown.

Chapter 6

: A symbiotic relationship between APC-mutant CRC cells and tumor associated macrophages

Chapter 6: A symbiotic relationship between APC-mutant CRC cells and tumor associated macrophages

Content of this chapter is partly based on the following manuscript:

Lee R, Li J, Chakravarti D, Chen P, Li J., Wu C, Jiang S, LaBella KA, Spring DJ, Wang YA, Zhao D., DePinho RA., Synthetic Essentiality of TDO2 in APC-Mutated Colorectal Cancer, *Submitted*

6.1 Introduction and rationale

To further understand the role of CXCL5-recruited TAMs in regulating tumor growth, we considered the possibility that, in addition to their classical immunosuppressive functions, infiltrating macrophages may also provide trophic support for cancer cells as we have recently reported in GBM (Chen et al., 2019). To that end, we examined the receptors on *APC*-KO cells that bind to macrophage-derived ligands which may promote cancer cell growth. From a phospho-tyrosine kinase (RTK) receptors assay, we identified that Axl and Gas6 plays an important role in promoting heterotypic interactions between tumor cells and infiltrated tumor-associated macrophages.

Axl is one of the members of TAM RTKs which are consisted of Tyro3, Axl and Mer. Their ligands include Gas6 and Protein S. When Gas6 binds to Axl, Axl gets phosphorylated and mediates proliferation and migration through multiple signal transduction including MAPK, NOTCH, PI3K pathways (Brown et al., 2016). Axl is over-expressed in many types of cancer and its expression is associated with metastasis and adverse prognostic factor. Previous findings on Gas6 showed that it

is expressed abundantly in macrophages and DC, especially in tumor context. And treatment of Gas6 to cancer cells promoted proliferation (Loges et al., 2010). They showed that tumor cells can program the infiltrating monocytes to produce Gas6 which accelerates the tumor growth (Loges et al., 2010).

6.2 Results

6.2.1 GAS6 is upregulated by CXCL5 in macrophages and promotes cancer cell growth

To further understand the role of CXCL5-recruited TAMs in regulating tumor growth, we hypothesized that in addition to their classical immunosuppressive functions, infiltrating macrophages may also provide some trophic support for cancer cells. We examined the receptors on APC-KO cells that bind to macrophage-derived ligands which may promote cancer cell growth. Receptor tyrosine kinase phospho-array analysis revealed increased phosphorylated Axl in *APC-KO* cells which was decreased upon TDO2 depletion only in the *APC-KO* cell lines (Fig. 34A).

Gas6 is a ligand of the Axl receptor tyrosine kinase and secreted mainly by TAMs in the TME (Loges et al., 2010). To assess whether macrophage-derived Gas6 might activate Axl to support the growth of APC-deficient cancer cells, we first validated that orthotopic *APC-KO* MC38 tumors showed increased phosphorylated Axl in cancer cells (indicated by EpCam staining) which was reduced upon TDO2 depletion and rescued upon enforced CXCL5 expression in TDO2-depleted *APC-KO* MC38 tumors (Fig. 34B).

6.2.2 Kyn and CXCL5 upregulate GAS6 in macrophages and polarize them into M2 macrophage phenotype

We evaluated whether secreted factors from cancer cells might amplify Gas6 expression in macrophages by utilizing mouse BMDMs. BMDMs were incubated with conditioned media from MC38 cell lines and the expression of Gas6 were measured with qRT-PCR. Conditioned media from *APC*-KO MC38 cell lines significantly increased the Gas6 mRNA levels in macrophages compared to *APC*-WT cell lines (Fig. 34C). TDO2 depletion in *APC*-KO MC38 cells resulted in decreased Gas6 expression in BMDMs (Fig. 34C).

In addition, while CSF1 is known to upregulate Gas6 in macrophages (serves as a positive control) (Loges et al., 2010), Kyn and CXCL5 also increased Gas6 expression in BMDM. Interestingly, the Gas6 itself also increased the Gas6 expression in macrophages, suggesting establishment of a positive feedback loop between cancer cells and macrophages. (Fig. 34D).

A

Mouse RTK Phospho-Array

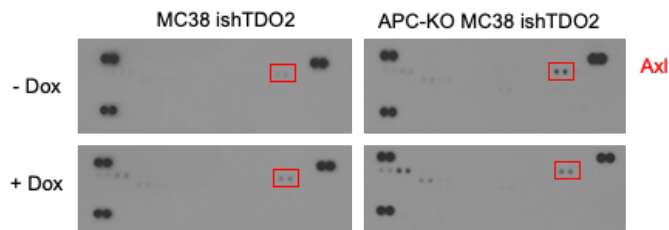
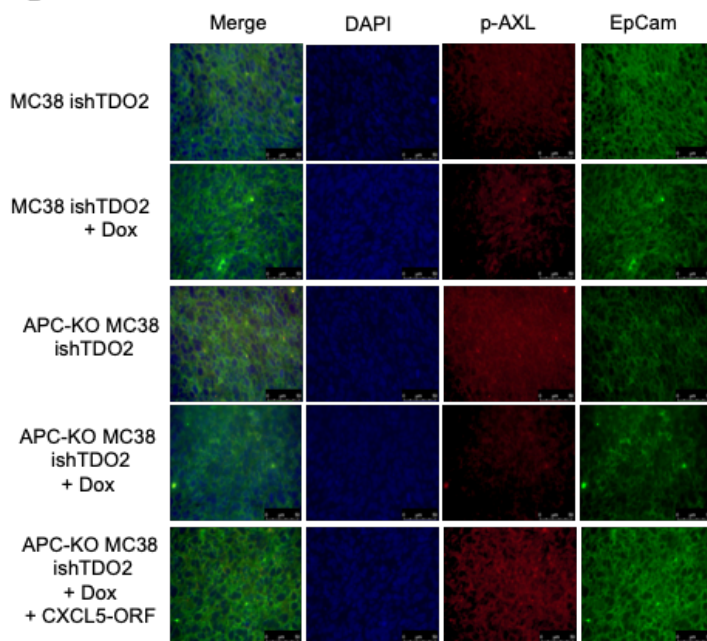
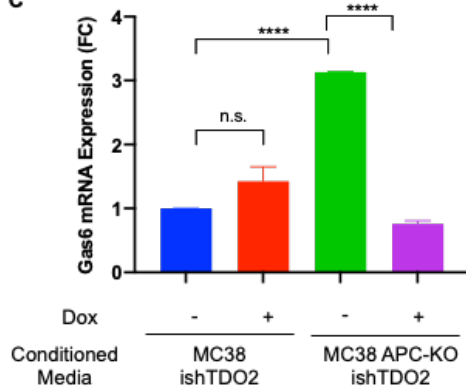
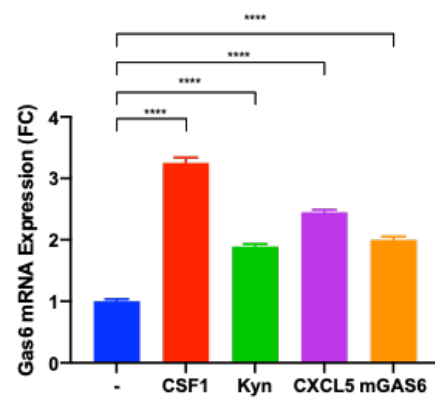
**B****C****D**

Figure 34: APC-deficient CRC cells promote macrophage-derived Gas6, which binds to Axl on tumor cells.

(A) Mouse RTK phospho-array of lysates from ishTDO2 *APC*-WT and *APC*-KO MC38 cell lines before and after dox treatment. The red box indicates Axl. **(B)** Immunofluorescence staining of phosphorylated Axl (RFP) in CRC orthotopic tumors established by injecting *APC*-WT and *APC*-KO MC38 cells into C57BL/6J mice. Epithelial cells are stained with EpCam and indicated by GFP. Blue is DAPI staining. $\times 63$ magnification. **(C)** RT-qPCR analysis of Gas6 expression in BMDM cultured in conditioned media from ishTDO2 *APC*-WT and *APC*-KO MC38 cell lines. $n=3$ biological replicates. $n.s.P>0.05$, $****P<0.0001$. two-tailed t-test. **(D)** RT-qPCR analysis of Gas6 expression in BMDM treated with CSF1 (50 ng), Kyn (1 mM), CXCL5 (50 ng) and Gas6 (25 ng) for 24 hr. $n=3$ biological replicates. $****P<0.0001$. two-tailed t-test.

6.2.3 Depletion of Gas6 in macrophages impairs tumor growth *in vivo*

Finally, to validate the roles of Gas6 in promoting tumor growth *in vivo*, we first established shGas6 Raw 264.7 macrophage cell lines with two independent shRNAs (Fig. 35A). CT26 murine CRC cell lines were utilized for the co-injection experiments in order to match the origin of mouse strain (BalB/cJ) for Raw 264.7 cells. shControl and shGas6 macrophage cells and CT26 tumor cells were co-injected into syngeneic BalB/cJ mice and tumor burden was measured which showed that the mice injected with Gas6-depleted macrophages showed reduced tumor growth (Fig. 35B),

Reversely, macrophages pre-treated with recombinant CXCL5 proteins before the injection promoted the growth of CT26 cells significantly (Fig. 35C). Collectively, these data reveal a symbiotic heterotypic signaling circuit between cancer cells and macrophages mediated by the CXCL5-Gas6-Axl axis.

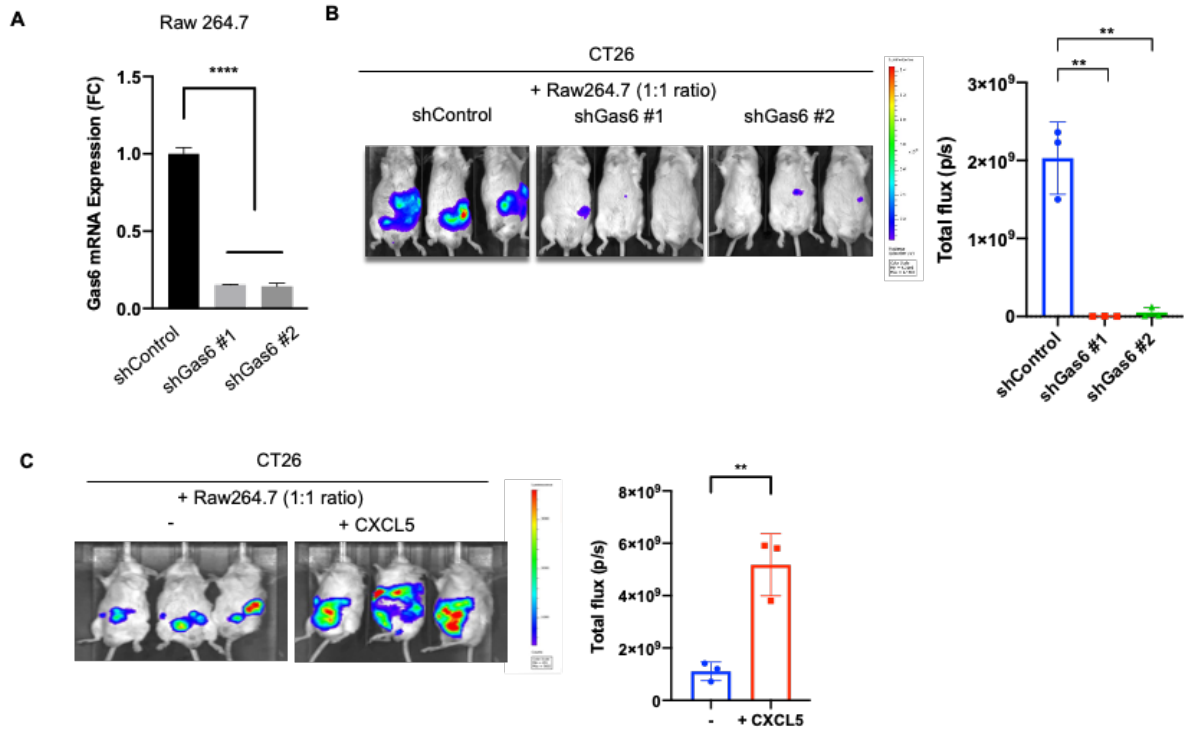


Figure 35: Gas6 secreted by macrophages promotes tumor growth.

(A) RT-qPCR shows GAS6 shRNA knockdown efficiency in Raw264.7 cells. $n=3$ biological replicates. $***P<0.001$. two-tailed t-test. **(B)** Representative in vivo bioluminescence-based images of BalB/CJ mice at day 20 post-orthotopic co-injection of CT26 cells (1×10^5 cells) and macrophage cell line Raw264.7 (1×10^5 cells) with shControl or shGAS6. Total flux measurement of the end point. $**P<0.01$. two-tailed t-test. **(C)** Representative in vivo bioluminescence-based images of BalB/CJ mice at day 20 post-orthotopic co-injection of CT26 cells (1×10^5 cells) and macrophage cell line Raw264.7 (1×10^5 cells) pre-treated with 100 ng of CXCL5 for 48 h before injection. Total flux measurement of tumors was done at the end point. $**P<0.01$. two-tailed t-test.

Chapter 7: Conclusions, discussion, and future direction

Chapter 7: Conclusions, discussion, and future direction

7.1. Conclusions and discussion

In this study, we performed the first large-scale genome analysis to identify SE genes for APC mutations, which are found in the vast majority of CRC patients and play a critical role in initiating tumorigenesis. Using synthetic essentiality as a conceptual framework, genomic loss-of-function analyses identified TDO2 as a key downstream effector specifically for APC-deficient cancers. Increased TDO2 mediates kynurenine pathway (KP) and generates excessive Kyn, which activates AhR pathway. We established that TDO2-Kyn-AhR axis increases the dependency of APC-null CRC cells on glycolysis and promotes cancer cell proliferation and growth. The axis also drives expression of CXCL5 which promotes recruitment of immune suppressive TAMs into the TME. These TAMs also secrete Gas6, which binds to Axl expressed on the cancer cells to further promote proliferation and growth of cancer cells, forming a synergistic interaction between cancer cells and TAMs (Fig. 36).

The functions of TDO2 have been studied primarily in the context of neurological diseases due to its expression in neuronal tissues and its roles in neurotransmitter production. Recent studies have revealed TDO2 overexpression in multiple cancer types and its role in facilitating tumorigenic signaling via KP (D'Amato et al., 2015)(D'Amato et al., 2015; Ott et al., 2015; van Baren and Van den Eynde, 2015). Another key KP enzyme IDO1 is also highly expressed in various tumors and is known to suppress anti-tumor immunity. However, IDO1 was not a

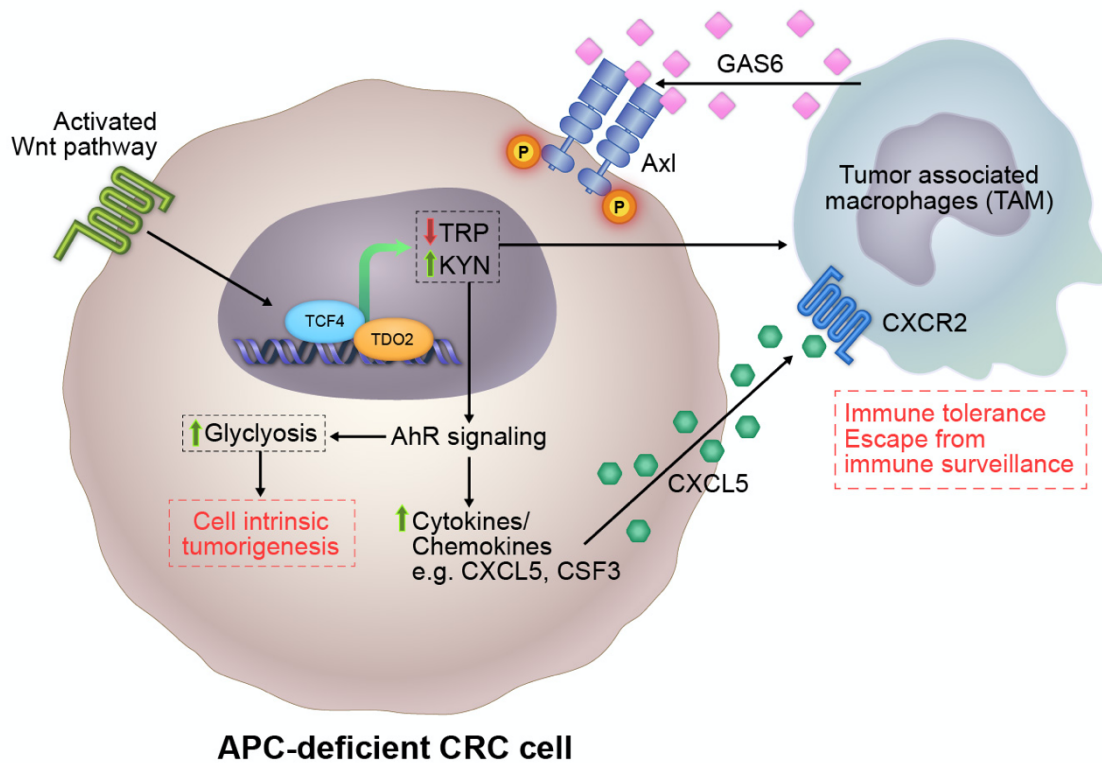


Figure 36: Working model

APC-deficiency activates a TCF4-TDO2-AhR-CXCL5-GAS6-AXL circuit that impacts multiple cancer hallmarks and immune responses.

critical dependency for APC-deficient CRC cells which suggests non-redundant, context-specific roles of these two key KP enzymes; moreover, TDO2 and IDO1 are differentially regulated (i.e. AhR can transcriptionally regulate IDO1 but not TDO2) (Puccetti, 2014). In addition to known transcriptional regulatory mechanisms governing TDO2 activity include hemes and glucocorticoid hormones (Badawy, 2017), our studies revealed that the WNT transcription factor TCF4 can upregulate TDO2, but not IDO1, expression in APC-deficient CRC cells. Specifically, AhR can regulate *IDO1*, but not *TDO2*, expression (Puccetti, 2014). In contrast, transcriptional regulatory mechanisms governing *TDO2*, but not *IDO1*, expression include hemes and glucocorticoid hormones (Badawy, 2017), as well as the WNT transcription factor TCF4 specifically in APC-deficient CRC cells (this study).

Our findings showing that TDO2-Kyn-AhR axis regulates glycolysis as a cancer cell intrinsic mechanism are consistent with previous findings that AhR can directly regulate genes involved in energy metabolism such as lipid and cholesterol synthesis (Gabriely et al., 2017). In APC-deficient CRC, we established that AhR regulates glucose uptake and overall glycolytic flux by regulating glycolysis genes including SLC2A1, HK1/2, PFKL, LDHA, and ALDOA. Experimentally, we showed knockdown of TDO2 and AhR downregulated those genes in APC-mutant cells. Tumor cell glycolysis pathway is directly targeted in t APC-deficient CRC tumor cells, we analyzed the expression of multiple glycolysis-related genes (GO Biological Process-Glycolysis Geneset) in the TCGA COAD dataset using the Oncomine platform. Colon adenocarcinoma which shows significantly lower APC expression as

expected (relative to normal colon and cecum) exhibits higher expression of glycolytic genes.

Importance of KP and AhR signaling in regulating tumor immunity is well-established in the context of both physiological and pathological conditions. In mice, AhR is critical for function and maintenance of innate T cells in the the gastrointestinal tract (Stange and Veldhoen, 2013). In stress conditions, whole body knockout of AhR exhibit impaired differentiation and function of T helper 17 cells and regulatory T cells to environmental toxins (Quintana et al., 2008, Stange and Veldhoen, 2013). In cancer, previous studies of AhR support both pro- and anti-tumorigenic roles. Whole body knockout of AhR in APC^{min} mice resulted in increased cecal tumors and no change in small intestinal tumors (Kawajiri et al., 2009), underscoring the context-specific actions of AhR in cancer. This may relate to 1. Non-ligand dependent roles of AhR such as degradation of β -catenin, 2. Effects of AhR on non-cancer cell types, 3. Tissue-specific biology. Different cancer types, regulatory mechanisms for AhR by its modulators such as ARNT, HSP90, XAP2, diverse agonists/antagonists, and direct immune modifying roles of AhR both in cancer cells and immune cells could be accounted for the discrepancy.

Here, we identified tumor-promoting roles of AhR in the context of APC-mutant context mediated by APC-TCF4-TDO2-AhR pathway and infiltrated immune cells. In mice, whole body knockout of AhR exhibit impaired differentiation and function of T helper 17 cells and regulatory T cells to environmental toxins (Quintana et al., 2008, Stange and Veldhoen, 2013). AhR is also critical for function and maintenance of innate T cells in the the gastrointestinal tract (Stange and Veldhoen,

2013). However, previous studies on AhR support both its pro- and anti-tumorigenic roles. Whole body AhR knockout in APC^{min} mice developed more cecal tumors (Kawajiri et al., 2009), suggesting ligand-independent roles of AhR which is degradation of β -catenin. Different cancer types, regulatory mechanisms for AhR by its modulators, diverse agonists/antagonists, and immune modifying roles directly by AhR both in cancer cells and immune cells could be accounted for dual roles of AhR.

Beyond the known immune suppressive activity of TAMs, our work revealed a role for TDO2 in supporting the growth of cancer cells in vivo. Specifically, we observed that, while TDO2 depletion in APC-null cancer cells show a profound decrease in phosphorylated Axl in tumors in vivo, pointing to increased Gas6 availability in the TME compared with cell culture settings. We determined that TAMs represent a major source of Gas6 compared with all other tumor-infiltrating immunocytes; moreover, macrophages derived from bone-marrow or peripheral blood do not express Gas6 (Loges et al., 2010). Activated Axl promotes diverse cellular processes including cancer cell survival via AKT, proliferation, EMT, migration, and invasion (Gay et al., 2017). Our cytokine rescue experiment data showed complete rescue by enforced expression of CXCL5 upon TDO2 depletion in APC-KO cells (Fig. 30B), suggesting tumorigenic functions of Gas6/Axl contribute to cancer cell growth. Moreover, Gas6/Axl can stabilize β -catenin (Jin et al., 2017), which enables cancer cells and TAMs to form a reinforcing paracrine loop. In pancreatic and ovarian cancer models, inhibition of Gas6/Axl pathway combined with chemotherapies has been shown to be synergistic (Kariolis et al., 2017). Correspondingly, previous work in GBM models has shown that combined Axl

inhibitor and immune checkpoint blockade inhibitor treatment showed better anti-tumor activity (Sadahiro et al., 2018).

Our human CRC profile analysis corresponds well with our murine findings, showing positive correlation between TAM abundance and TDO2 expression levels. In CRC, pro-tumorigenic TAMs are known to support tumor progression and limit the efficacy of immunotherapy (Peranzoni and Donnadieu, 2019, Pathria et al., 2019, Liu and Cao, 2015). In glioblastoma, Kyn produced by glioma cells has been shown to recruit TAMs by binding to AhR and promote CD8 T cell dysfunction via expression CD39 in TAMs (Takenaka et al., 2019). Analysis of recent failed clinical trial targeting IDO1 with Epacadostat in combination with anti-PD1 antibody in melanoma showed that immune checkpoint blockade, BRAF inhibitors, and chemotherapy serves to upregulate IDO1 expression which may overcome coverage by the IDO1 inhibitor dose used. Studies also showed that cancer cells upregulate ABC transporters which might further reduce the availability of IDO1 inhibitor in the TME.

Our findings expand the list of possibilities of compensatory mechanisms. We speculate that TDO2 upregulation could serve to sustain the Trp metabolism and KP-AhR pathway despite the IDO1 inhibition, underscoring the importance of understanding the tumorigenic roles of TDO2 and the genotypic context in which it operates (Opitz et al., 2020). In conclusion, identifying synthetic essential genes in CRC harboring APC deficiencies will improve the understanding of CRC tumor initiation and also pave the way for developing new treatment strategies for this intractable cancer.

7.2 Future directions

Considering the roles of TDO2 in regulating immune responses in APC-KO tumors, identifying optimal combination therapies of TDO2i and immune checkpoint inhibitors (ICIs) to improve the treatment of CRC would be in great importance. Using the iKAP model, engineered with inducible Kras oncogenic mutation (KRAS*) activating model and loss of APC and p53, provides an ideal platform for studying the combination treatment with TDO2i, since iKAP spontaneous tumors mirror the natural tumor incidences in CRC patients and iKAP tumors develop more aggressively. Assessing T cell checkpoint in iKAP CRC tumors under TDO2 inhibitor treatment with single cell sequencing or immunohistochemistry would allow us to gain insights on which immune-modulatory molecules should be intervened with TDO2.

Functions of infiltrated TAMs in APC-KO tumors could be further assessed in the context of T cell suppressive functions. Limitations in dividing macrophage populations into M1 and M2-like macrophages have been reported, showing the complex and reversible nature of macrophage subtypes. Transcriptomic analysis of infiltrated macrophages in CRC tumors and investigating whether their gene expression patterns, or states change by different APC status, TDO2 depletion, or Kyn supplementation would be greatly informative for deeper understanding of macrophage biology.

BIBLIOGRAPHY

- AMIR, E. D., DAVIS, K. L., TADMOR, M. D., SIMONDS, E. F., LEVINE, J. H., BENDALL, S. C., SHENFELD, D. K., KRISHNASWAMY, S., NOLAN, G. P. & PE'ER, D. 2013. viSNE enables visualization of high dimensional single-cell data and reveals phenotypic heterogeneity of leukemia. *Nature Biotechnology*, 31, 545-+.
- ANDERSSON, P., MCGUIRE, J., RUBIO, C., GRADIN, K., WHITELAW, M. L., PETTERSSON, S., HANBERG, A. & POELLINGER, L. 2002. A constitutively active dioxin/aryl hydrocarbon receptor induces stomach tumors. *Proc Natl Acad Sci U S A*, 99, 9990-5.
- BADAWY, A. A. 2017. Kynurenine Pathway of Tryptophan Metabolism: Regulatory and Functional Aspects. *Int J Tryptophan Res*, 10, 1178646917691938.
- BALL, H. J., JUSOF, F. F., BAKMIWEWA, S. M., HUNT, N. H. & YUASA, H. J. 2014. Tryptophan-catabolizing enzymes - party of three. *Front Immunol*, 5, 485.
- BODMER, W. F., BAILEY, C. J., BODMER, J., BUSSEY, H. J., ELLIS, A., GORMAN, P., LUCIBELLO, F. C., MURDAY, V. A., RIDER, S. H., SCAMBLER, P. & ET AL. 1987. Localization of the gene for familial adenomatous polyposis on chromosome 5. *Nature*, 328, 614-6.
- BOUTIN, A. T., LIAO, W. T., WANG, M., HWANG, S. S., KARPINETS, T. V., CHEUNG, H., CHU, G. C., JIANG, S., HU, J., CHANG, K., VILAR, E., SONG, X., ZHANG, J., KOPETZ, S., FUTREAL, A., WANG, Y. A., KWONG, L. N. & DEPINHO, R. A. 2017. Oncogenic Kras drives invasion and maintains metastases in colorectal cancer. *Genes Dev*, 31, 370-382.

BROWN, J. M., RECHT, L. & STROBER, S. 2017. The Promise of Targeting Macrophages in Cancer Therapy. *Clin Cancer Res*, 23, 3241-3250.

BROWN, M., BLACK, J. R., SHARMA, R., STEBBING, J. & PINATO, D. J. 2016. Gene of the month: Axl. *J Clin Pathol*, 69, 391-7.

CAMPESATO, L. F., BUDHU, S., TCHAICHA, J., WENG, C. H., GIGOUX, M., COHEN, I. J., REDMOND, D., MANGARIN, L., POURPE, S., LIU, C., ZAPPASODI, R., ZAMARIN, D., CAVANAUGH, J., CASTRO, A. C., MANFREDI, M. G., MCGOVERN, K., MERGHOUB, T. & WOLCHOK, J. D. 2020. Blockade of the AHR restricts a Treg-macrophage suppressive axis induced by L-Kynurenine. *Nat Commun*, 11, 4011.

CERVENKA, I., AGUDELO, L. Z. & RUAS, J. L. 2017. Kynurenines: Tryptophan's metabolites in exercise, inflammation, and mental health. *Science*, 357.

CHEN, J., ROCKEN, C., LOFTON-DAY, C., SCHULZ, H. U., MULLER, O., KUTZNER, N., MALFERTHEINER, P. & EBERT, M. P. 2005. Molecular analysis of APC promoter methylation and protein expression in colorectal cancer metastasis. *Carcinogenesis*, 26, 37-43.

CHEN, P., ZHAO, D., LI, J., LIANG, X., LI, J., CHANG, A., HENRY, V. K., LAN, Z., SPRING, D. J., RAO, G., WANG, Y. A. & DEPINHO, R. A. 2019. Symbiotic Macrophage-Glioma Cell Interactions Reveal Synthetic Lethality in PTEN-Null Glioma. *Cancer Cell*, 35, 868-884 e6.

CHEN, S. P., TSAI, S. T., JAO, S. W., HUANG, Y. L., CHAO, Y. C., CHEN, Y. L., WU, C. C., LIN, S. Z. & HARN, H. J. 2006. Single nucleotide polymorphisms of the

APC gene and colorectal cancer risk: a case-control study in Taiwan. *BMC Cancer*, 6, 83.

CHEN, T. J. & KOTTECHA, N. 2014. Cytobank: providing an analytics platform for community cytometry data analysis and collaboration. *Curr Top Microbiol Immunol*, 377, 127-57.

COMINGS, D. E., MUHLEMAN, D., DIETZ, G. W., JR. & DONLON, T. 1991. Human tryptophan oxygenase localized to 4q31: possible implications for alcoholism and other behavioral disorders. *Genomics*, 9, 301-8.

D'AMATO, N. C., ROGERS, T. J., GORDON, M. A., GREENE, L. I., COCHRANE, D. R., SPOELSTRA, N. S., NEMKOV, T. G., D'ALESSANDRO, A., HANSEN, K. C. & RICHER, J. K. 2015. A TDO2-AhR signaling axis facilitates anoikis resistance and metastasis in triple-negative breast cancer. *Cancer Res*, 75, 4651-64.

DIETRICH, C. & KAINA, B. 2010. The aryl hydrocarbon receptor (AhR) in the regulation of cell-cell contact and tumor growth. *Carcinogenesis*, 31, 1319-28.

DIKOVSKAYA, D., SCHIFFMANN, D., NEWTON, I. P., OAKLEY, A., KROBOTH, K., SANSOM, O., JAMIESON, T. J., MENIEL, V., CLARKE, A. & NATHKE, I. S. 2007. Loss of APC induces polyploidy as a result of a combination of defects in mitosis and apoptosis. *J Cell Biol*, 176, 183-95.

DOMANSKA, U. M., BOER, J. C., TIMMER-BOSSCHA, H., VAN VUGT, M. A., HOVING, H. D., KLIPHUIS, N. M., ROSATI, S., VAN DER POEL, H. G., DE JONG, I. J., DE VRIES, E. G. & WALENKAMP, A. M. 2014. CXCR4 inhibition enhances radiosensitivity, while inducing cancer cell mobilization in a prostate cancer mouse model. *Clin Exp Metastasis*, 31, 829-39.

FEARNHEAD, N. S., BRITTON, M. P. & BODMER, W. F. 2001. The ABC of APC. *Hum Mol Genet*, 10, 721-33.

FEARON, E. R. 2011. Molecular genetics of colorectal cancer. *Annu Rev Pathol*, 6, 479-507.

FISCHER, A. S. & SIGAL, M. 2019. The Role of Wnt and R-spondin in the Stomach During Health and Disease. *Biomedicines*, 7.

GIANNAKIS, M., HODIS, E., JASMINE MU, X., YAMAUCHI, M., ROSENBLUH, J., CIBULSKIS, K., SAKSENA, G., LAWRENCE, M. S., QIAN, Z. R., NISHIHARA, R., VAN ALLEN, E. M., HAHN, W. C., GABRIEL, S. B., LANDER, E. S., GETZ, G., OGINO, S., FUCHS, C. S. & GARRAWAY, L. A. 2014. RNF43 is frequently mutated in colorectal and endometrial cancers. *Nat Genet*, 46, 1264-6.

GOUNARI, F., CHANG, R., COWAN, J., GUO, Z., DOSE, M., GOUNARIS, E. & KHAZAIE, K. 2005. Loss of adenomatous polyposis coli gene function disrupts thymic development. *Nat Immunol*, 6, 800-9.

GRODEN, J., THLIVERIS, A., SAMOWITZ, W., CARLSON, M., GELBERT, L., ALBERTSEN, H., JOSLYN, G., STEVENS, J., SPIRIO, L., ROBERTSON, M. & ET AL. 1991. Identification and characterization of the familial adenomatous polyposis coli gene. *Cell*, 66, 589-600.

GUTIERREZ-VAZQUEZ, C. & QUINTANA, F. J. 2018. Regulation of the Immune Response by the Aryl Hydrocarbon Receptor. *Immunity*, 48, 19-33.

HAO, H. X., XIE, Y., ZHANG, Y., CHARLAT, O., OSTER, E., AVELLO, M., LEI, H., MICKANIN, C., LIU, D., RUFFNER, H., MAO, X., MA, Q., ZAMPONI, R., BOUWMEESTER, T., FINAN, P. M., KIRSCHNER, M. W., PORTER, J. A.,

SERLUCA, F. C. & CONG, F. 2012. ZNRF3 promotes Wnt receptor turnover in an R-spondin-sensitive manner. *Nature*, 485, 195-200.

HERRERA, L., KAKATI, S., GIBAS, L., PIETRZAK, E. & SANDBERG, A. A. 1986. Gardner syndrome in a man with an interstitial deletion of 5q. *Am J Med Genet*, 25, 473-6.

HORNBECK, P. V., ZHANG, B., MURRAY, B., KORNHAUSER, J. M., LATHAM, V. & SKRZYPEK, E. 2015. PhosphoSitePlus, 2014: mutations, PTMs and recalibrations. *Nucleic Acids Res*, 43, D512-20.

ISHIKAWA, T. O., TAMAI, Y., LI, Q., OSHIMA, M. & TAKETO, M. M. 2003. Requirement for tumor suppressor Apc in the morphogenesis of anterior and ventral mouse embryo. *Dev Biol*, 253, 230-46.

JOSLYN, G., RICHARDSON, D. S., WHITE, R. & ALBER, T. 1993. Dimer formation by an N-terminal coiled coil in the APC protein. *Proc Natl Acad Sci U S A*, 90, 11109-13.

KANAI, M., FUNAKOSHI, H., TAKAHASHI, H., HAYAKAWA, T., MIZUNO, S., MATSUMOTO, K. & NAKAMURA, T. 2009. Tryptophan 2,3-dioxygenase is a key modulator of physiological neurogenesis and anxiety-related behavior in mice. *Mol Brain*, 2, 8.

KAWASAKI, Y., SATO, R. & AKIYAMA, T. 2003. Mutated APC and Asef are involved in the migration of colorectal tumour cells. *Nat Cell Biol*, 5, 211-5.

KAWASAKI, Y., SENDA, T., ISHIDATE, T., KOYAMA, R., MORISHITA, T., IWAYAMA, Y., HIGUCHI, O. & AKIYAMA, T. 2000. Asef, a link between the tumor suppressor APC and G-protein signaling. *Science*, 289, 1194-7.

KINZLER, K. W., NILBERT, M. C., SU, L. K., VOGELSTEIN, B., BRYAN, T. M., LEVY, D. B., SMITH, K. J., PREISINGER, A. C., HEDGE, P., MCKECHNIE, D. & ET AL. 1991. Identification of FAP locus genes from chromosome 5q21. *Science*, 253, 661-5.

KOHLER, E. M., DERUNGS, A., DAUM, G., BEHRENS, J. & SCHNEIKERT, J. 2008. Functional definition of the mutation cluster region of adenomatous polyposis coli in colorectal tumours. *Hum Mol Genet*, 17, 1978-87.

KOINUMA, K., YAMASHITA, Y., LIU, W., HATANAKA, H., KURASHINA, K., WADA, T., TAKADA, S., KANEDA, R., CHOI, Y. L., FUJIWARA, S. I., MIYAKURA, Y., NAGAI, H. & MANO, H. 2006. Epigenetic silencing of AXIN2 in colorectal carcinoma with microsatellite instability. *Oncogene*, 25, 139-46.

KOO, B. K., SPIT, M., JORDENS, I., LOW, T. Y., STANGE, D. E., VAN DE WETERING, M., VAN ES, J. H., MOHAMMED, S., HECK, A. J., MAURICE, M. M. & CLEVERS, H. 2012. Tumour suppressor RNF43 is a stem-cell E3 ligase that induces endocytosis of Wnt receptors. *Nature*, 488, 665-9.

LIANG, T. J., WANG, H. X., ZHENG, Y. Y., CAO, Y. Q., WU, X., ZHOU, X. & DONG, S. X. 2017. APC hypermethylation for early diagnosis of colorectal cancer: a meta-analysis and literature review. *Oncotarget*, 8, 46468-46479.

LIAO, W., OVERMAN, M. J., BOUTIN, A. T., SHANG, X., ZHAO, D., DEY, P., LI, J., WANG, G., LAN, Z., LI, J., TANG, M., JIANG, S., MA, X., CHEN, P., KATKHUDA, R., KORPHAISARN, K., CHAKRAVARTI, D., CHANG, A., SPRING, D. J., CHANG, Q., ZHANG, J., MARU, D. M., MAEDA, D. Y., ZEBALA, J. A., KOPETZ, S., WANG,

- Y. A. & DEPINHO, R. A. 2019. KRAS-IRF2 Axis Drives Immune Suppression and Immune Therapy Resistance in Colorectal Cancer. *Cancer Cell*, 35, 559-572 e7.
- LIU, C., LI, Y., SEMENOV, M., HAN, C., BAEG, G. H., TAN, Y., ZHANG, Z., LIN, X. & HE, X. 2002. Control of beta-catenin phosphorylation/degradation by a dual-kinase mechanism. *Cell*, 108, 837-47.
- LIU, Y. & CAO, X. 2015. The origin and function of tumor-associated macrophages. *Cell Mol Immunol*, 12, 1-4.
- LIU, Y., LIANG, X., DONG, W., FANG, Y., LV, J., ZHANG, T., FISKESUND, R., XIE, J., LIU, J., YIN, X., JIN, X., CHEN, D., TANG, K., MA, J., ZHANG, H., YU, J., YAN, J., LIANG, H., MO, S., CHENG, F., ZHOU, Y., ZHANG, H., WANG, J., LI, J., CHEN, Y., CUI, B., HU, Z. W., CAO, X., XIAO-FENG QIN, F. & HUANG, B. 2018. Tumor-Repopulating Cells Induce PD-1 Expression in CD8(+) T Cells by Transferring Kynurenine and AhR Activation. *Cancer Cell*, 33, 480-494 e7.
- LIU, Y., SUN, J., YU, J., GE, W., XIAO, X., DAI, S. & XIANG, Q. 2019. LncRNA CACS15 accelerates the malignant progression of ovarian cancer through stimulating EZH2-induced inhibition of APC. *Am J Transl Res*, 11, 6561-6568.
- LOGES, S., SCHMIDT, T., TJWA, M., VAN GEYTE, K., LIEVENS, D., LUTGENS, E., VANHOUTTE, D., BORGEL, D., PLAISANCE, S., HOYLAERTS, M., LUTTUN, A., DEWERCHIN, M., JONCKX, B. & CARMELIET, P. 2010. Malignant cells fuel tumor growth by educating infiltrating leukocytes to produce the mitogen Gas6. *Blood*, 115, 2264-73.
- MAJOR, M. B., CAMP, N. D., BERNDT, J. D., YI, X., GOLDENBERG, S. J., HUBBERT, C., BIECHELE, T. L., GINGRAS, A. C., ZHENG, N., MACCOSS, M. J.,

ANGERS, S. & MOON, R. T. 2007. Wilms tumor suppressor WTX negatively regulates WNT/beta-catenin signaling. *Science*, 316, 1043-6.

MANTOVANI, A., SOZZANI, S., LOCATI, M., ALLAVENA, P. & SICA, A. 2002. Macrophage polarization: tumor-associated macrophages as a paradigm for polarized M2 mononuclear phagocytes. *Trends Immunol*, 23, 549-55.

MAO, D. D., GUJAR, A. D., MAHLOKOZERA, T., CHEN, I., PAN, Y., LUO, J., BROST, T., THOMPSON, E. A., TURSKI, A., LEUTHARDT, E. C., DUNN, G. P., CHICOINE, M. R., RICH, K. M., DOWLING, J. L., ZIPFEL, G. J., DACEY, R. G., ACHILEFU, S., TRAN, D. D., YANO, H. & KIM, A. H. 2015. A CDC20-APC/SOX2 Signaling Axis Regulates Human Glioblastoma Stem-like Cells. *Cell Rep*, 11, 1809-21.

MARTINELLI, E., MARTINI, G., CARDONE, C., TROIANI, T., LIGUORI, G., VITAGLIANO, D., NAPOLITANO, S., MORGILLO, F., RINALDI, B., MELILLO, R. M., LIOTTI, F., NAPPI, A., BIANCO, R., BERRINO, L., CIUFFREDA, L. P., CIARDIELLO, D., IAFFAIOLI, V., BOTTI, G., FERRAILOLO, F. & CIARDIELLO, F. 2015. AXL is an oncotarget in human colorectal cancer. *Oncotarget*, 6, 23281-96.

MAZZONI, S. M. & FEARON, E. R. 2014. AXIN1 and AXIN2 variants in gastrointestinal cancers. *Cancer Lett*, 355, 1-8.

MENG, B., WU, D., GU, J., OUYANG, S., DING, W. & LIU, Z. J. 2014. Structural and functional analyses of human tryptophan 2,3-dioxygenase. *Proteins*, 82, 3210-6.

MORIN, P. J., KINZLER, K. W. & SPARKS, A. B. 2016. beta-Catenin Mutations: Insights into the APC Pathway and the Power of Genetics. *Cancer Research*, 76, 5587-5589.

MORRISON, E. E., WARDLEWORTH, B. N., ASKHAM, J. M., MARKHAM, A. F. & MEREDITH, D. M. 1998. EB1, a protein which interacts with the APC tumour suppressor, is associated with the microtubule cytoskeleton throughout the cell cycle. *Oncogene*, 17, 3471-7.

MOSER, A. R., SHOEMAKER, A. R., CONNELLY, C. S., CLIPSON, L., GOULD, K. A., LUONGO, C., DOVE, W. F., SIGGERS, P. H. & GARDNER, R. L. 1995. Homozygosity for the Min allele of Apc results in disruption of mouse development prior to gastrulation. *Dev Dyn*, 203, 422-33.

MULLER, A. J., MANFREDI, M. G., ZAKHARIA, Y. & PRENDERGAST, G. C. 2019. Inhibiting IDO pathways to treat cancer: lessons from the ECHO-301 trial and beyond. *Semin Immunopathol*, 41, 41-48.

NATHAN, C. F., MURRAY, H. W., WIEBE, M. E. & RUBIN, B. Y. 1983. Identification of interferon-gamma as the lymphokine that activates human macrophage oxidative metabolism and antimicrobial activity. *J Exp Med*, 158, 670-89.

NOVELLASDEMUNT, L., ANTAS, P. & LI, V. S. 2015. Targeting Wnt signaling in colorectal cancer. A Review in the Theme: Cell Signaling: Proteins, Pathways and Mechanisms. *Am J Physiol Cell Physiol*, 309, C511-21.

OLSON, T. S. & LEY, K. 2002. Chemokines and chemokine receptors in leukocyte trafficking. *Am J Physiol Regul Integr Comp Physiol*, 283, R7-28.

ORCHARD, G., MARTIN, J. G., VOGELSTEIN, R. J. & ETIENNE-CUMMINGS, R. 2013. Fast neuromimetic object recognition using FPGA outperforms GPU implementations. *IEEE Trans Neural Netw Learn Syst*, 24, 1239-52.

OSHIMA, M., OSHIMA, H., KITAGAWA, K., KOBAYASHI, M., ITAKURA, C. & TAKETO, M. 1995. Loss of Apc heterozygosity and abnormal tissue building in nascent intestinal polyps in mice carrying a truncated Apc gene. *Proc Natl Acad Sci U S A*, 92, 4482-6.

OTT, M., LITZENBURGER, U. M., RAUSCHENBACH, K. J., BUNSE, L., OCHS, K., SAHM, F., PUSCH, S., OPITZ, C. A., BLAES, J., VON DEIMLING, A., WICK, W. & PLATTEN, M. 2015. Suppression of TDO-mediated tryptophan catabolism in glioblastoma cells by a steroid-responsive FKBP52-dependent pathway. *Glia*, 63, 78-90.

PAOLINO, M., CHOIDAS, A., WALLNER, S., PRANJIC, B., URIBESALGO, I., LOESER, S., JAMIESON, A. M., LANGDON, W. Y., IKEDA, F., FEDEDA, J. P., CRONIN, S. J., NITSCH, R., SCHULTZ-FADEMRECHT, C., EICKHOFF, J., MENNINGER, S., UNGER, A., TORKA, R., GRUBER, T., HINTERLEITNER, R., BAIER, G., WOLF, D., ULLRICH, A., KLEBL, B. M. & PENNINGER, J. M. 2014. The E3 ligase Cbl-b and TAM receptors regulate cancer metastasis via natural killer cells. *Nature*, 507, 508-12.

PATE, K. T., STRINGARI, C., SPROWL-TANIO, S., WANG, K., TESLAA, T., HOVERTER, N. P., MCQUADE, M. M., GARNER, C., DIGMAN, M. A., TEITELL, M. A., EDWARDS, R. A., GRATTON, E. & WATERMAN, M. L. 2014. Wnt signaling directs a metabolic program of glycolysis and angiogenesis in colon cancer. *EMBO J*, 33, 1454-73.

PATHRIA, P., LOUIS, T. L. & VARNER, J. A. 2019. Targeting Tumor-Associated Macrophages in Cancer. *Trends Immunol*, 40, 310-327.

PILOTTE, L., LARRIEU, P., STROOBANT, V., COLAU, D., DOLUSIC, E., FREDERICK, R., DE PLAEN, E., UYTENHOVE, C., WOUTERS, J., MASEREEL, B. & VAN DEN EYNDE, B. J. 2012. Reversal of tumoral immune resistance by inhibition of tryptophan 2,3-dioxygenase. *Proc Natl Acad Sci U S A*, 109, 2497-502.

PINATO, D. J., CHOWDHURY, S. & STEBBING, J. 2016. TAMing resistance to multi-targeted kinase inhibitors through Axl and Met inhibition. *Oncogene*, 35, 2684-6.

PRENDERGAST, G. C. 2011. Cancer: Why tumours eat tryptophan. *Nature*, 478, 192-4.

PUC CETTI, P. 2014. On the Non-Redundant Roles of TDO2 and IDO1. *Front Immunol*, 5, 522.

RAWSON, J. B., MANNO, M., MRKONJIC, M., DAFTARY, D., DICKS, E., BUCHANAN, D. D., YOUNGHUSBAND, H. B., PARFREY, P. S., YOUNG, J. P., POLLETT, A., GREEN, R. C., GALLINGER, S., MCLAUGHLIN, J. R., KNIGHT, J. A. & BAPAT, B. 2011. Promoter methylation of Wnt antagonists DKK1 and SFRP1 is associated with opposing tumor subtypes in two large populations of colorectal cancer patients. *Carcinogenesis*, 32, 741-7.

ROSENBLUH, J., NIJHAWAN, D., COX, A. G., LI, X., NEAL, J. T., SCHAFER, E. J., ZACK, T. I., WANG, X., TSHERNIAK, A., SCHINZEL, A. C., SHAO, D. D., SCHUMACHER, S. E., WEIR, B. A., VAZQUEZ, F., COWLEY, G. S., ROOT, D. E., MESIROV, J. P., BEROUKHIM, R., KUO, C. J., GOESSLING, W. & HAHN, W. C. 2012. beta-Catenin-driven cancers require a YAP1 transcriptional complex for survival and tumorigenesis. *Cell*, 151, 1457-73.

ROSZER, T. 2015. Understanding the Mysterious M2 Macrophage through Activation Markers and Effector Mechanisms. *Mediators Inflamm*, 2015, 816460.

SCHNEIDER, C., KING, R. M. & PHILIPSON, L. 1988. Genes specifically expressed at growth arrest of mammalian cells. *Cell*, 54, 787-93.

SCHRAMME, F., CROSIGNANI, S., FREDERIX, K., HOFFMANN, D., PILOTTE, L., STROOBANT, V., PREILLON, J., DRIESSENS, G. & VAN DEN EYNDE, B. J. 2020. Inhibition of Tryptophan-Dioxygenase Activity Increases the Antitumor Efficacy of Immune Checkpoint Inhibitors. *Cancer Immunol Res*, 8, 32-45.

SESHAGIRI, S., STAWISKI, E. W., DURINCK, S., MODRUSAN, Z., STORM, E. E., CONBOY, C. B., CHAUDHURI, S., GUAN, Y., JANAKIRAMAN, V., JAISWAL, B. S., GUILLORY, J., HA, C., DIJKGRAAF, G. J., STINSON, J., GNAD, F., HUNTLEY, M. A., DEGENHARDT, J. D., HAVERTY, P. M., BOURGON, R., WANG, W., KOEPPEN, H., GENTLEMAN, R., STARR, T. K., ZHANG, Z., LARGAESPADA, D. A., WU, T. D. & DE SAUVAGE, F. J. 2012. Recurrent R-spondin fusions in colon cancer. *Nature*, 488, 660-4.

SIEBER, O., LIPTON, L., HEINIMANN, K. & TOMLINSON, I. 2003. Colorectal tumourigenesis in carriers of the APC I1307K variant: lone gunman or conspiracy? *J Pathol*, 199, 137-9.

STAFFORD, J. H., HIRAI, T., DENG, L., CHERNIKOVA, S. B., URATA, K., WEST, B. L. & BROWN, J. M. 2016. Colony stimulating factor 1 receptor inhibition delays recurrence of glioblastoma after radiation by altering myeloid cell recruitment and polarization. *Neuro Oncol*, 18, 797-806.

STEIN, M., KESHAV, S., HARRIS, N. & GORDON, S. 1992. Interleukin 4 potently enhances murine macrophage mannose receptor activity: a marker of alternative immunologic macrophage activation. *J Exp Med*, 176, 287-92.

STORMO, G. D. 2013. Modeling the specificity of protein-DNA interactions. *Quant Biol*, 1, 115-130.

SU, L. K., KINZLER, K. W., VOGELSTEIN, B., PREISINGER, A. C., MOSER, A. R., LUONGO, C., GOULD, K. A. & DOVE, W. F. 1992. Multiple intestinal neoplasia caused by a mutation in the murine homolog of the APC gene. *Science*, 256, 668-70.

SUBRAMANIAN, A., TAMAYO, P., MOOTHA, V. K., MUKHERJEE, S., EBERT, B. L., GILLETTE, M. A., PAULOVICH, A., POMEROY, S. L., GOLUB, T. R., LANDER, E. S. & MESIROV, J. P. 2005. Gene set enrichment analysis: a knowledge-based approach for interpreting genome-wide expression profiles. *Proc Natl Acad Sci U S A*, 102, 15545-50.

SUZUKI, H., WATKINS, D. N., JAIR, K. W., SCHUEBEL, K. E., MARKOWITZ, S. D., CHEN, W. D., PRETLOW, T. P., YANG, B., AKIYAMA, Y., VAN ENGELAND, M., TOYOTA, M., TOKINO, T., HINODA, Y., IMAI, K., HERMAN, J. G. & BAYLIN, S. B. 2004. Epigenetic inactivation of SFRP genes allows constitutive WNT signaling in colorectal cancer. *Nat Genet*, 36, 417-22.

TAKENAKA, M. C., GABRIELY, G., ROTHHAMMER, V., MASCANFRONI, I. D., WHEELER, M. A., CHAO, C. C., GUTIERREZ-VAZQUEZ, C., KENISON, J., TJON, E. C., BARROSO, A., VANDEVENTER, T., DE LIMA, K. A., ROTHWEILER, S., MAYO, L., GHANNAM, S., ZANDEE, S., HEALY, L., SHERR, D., FAREZ, M. F.,

PRAT, A., ANTEL, J., REARDON, D. A., ZHANG, H., ROBSON, S. C., GETZ, G., WEINER, H. L. & QUINTANA, F. J. 2019. Control of tumor-associated macrophages and T cells in glioblastoma via AHR and CD39. *Nat Neurosci*, 22, 729-740.

TAKETO, M. M. 2006. Wnt signaling and gastrointestinal tumorigenesis in mouse models. *Oncogene*, 25, 7522-30.

TANIGUCHI, H., YAMAMOTO, H., HIRATA, T., MIYAMOTO, N., OKI, M., NOSHO, K., ADACHI, Y., ENDO, T., IMAI, K. & SHINOMURA, Y. 2005. Frequent epigenetic inactivation of Wnt inhibitory factor-1 in human gastrointestinal cancers. *Oncogene*, 24, 7946-52.

TIGHE, A., JOHNSON, V. L. & TAYLOR, S. S. 2004. Truncating APC mutations have dominant effects on proliferation, spindle checkpoint control, survival and chromosome stability. *J Cell Sci*, 117, 6339-53.

VAN DER FLIER, L. G., SABATES-BELLVER, J., OVIING, I., HAEGEBARTH, A., DE PALO, M., ANTI, M., VAN GIJN, M. E., SUIJKERBUIJK, S., VAN DE WETERING, M., MARRA, G. & CLEVERS, H. 2007. The Intestinal Wnt/TCF Signature. *Gastroenterology*, 132, 628-32.

VAN ENGELAND, M., DERKS, S., SMITS, K. M., MEIJER, G. A. & HERMAN, J. G. 2011. Colorectal cancer epigenetics: complex simplicity. *J Clin Oncol*, 29, 1382-91.

WALTERS, M. J., EBSWORTH, K., BERAHOVICH, R. D., PENFOLD, M. E., LIU, S. C., AL OMRAN, R., KIOI, M., CHERNIKOVA, S. B., TSENG, D., MULKEARNS-HUBERT, E. E., SINYUK, M., RANSOHOFF, R. M., LATHIA, J. D., KARAMCHANDANI, J., KOHRT, H. E., ZHANG, P., POWERS, J. P., JAEN, J. C., SCHALL, T. J., MERCHANT, M., RECHT, L. & BROWN, J. M. 2014. Inhibition of

CXCR7 extends survival following irradiation of brain tumours in mice and rats. *Br J Cancer*, 110, 1179-88.

WATANABE, T., WANG, S., NORITAKE, J., SATO, K., FUKATA, M., TAKEFUJI, M., NAKAGAWA, M., IZUMI, N., AKIYAMA, T. & KAIBUCHI, K. 2004. Interaction with IQGAP1 links APC to Rac1, Cdc42, and actin filaments during cell polarization and migration. *Dev Cell*, 7, 871-83.

WIMMEL, A., GLITZ, D., KRAUS, A., ROEDER, J. & SCHUERMANN, M. 2001. Axl receptor tyrosine kinase expression in human lung cancer cell lines correlates with cellular adhesion. *Eur J Cancer*, 37, 2264-74.

WU, G., MA, Z., HU, W., WANG, D., GONG, B., FAN, C., JIANG, S., LI, T., GAO, J. & YANG, Y. 2017. Molecular insights of Gas6/TAM in cancer development and therapy. *Cell Death Dis*, 8, e2700.

XING, Y., CLEMENTS, W. K., LE TRONG, I., HINDS, T. R., STENKAMP, R., KIMELMAN, D. & XU, W. 2004. Crystal structure of a beta-catenin/APC complex reveals a critical role for APC phosphorylation in APC function. *Mol Cell*, 15, 523-33.

XU, J., ESCAMILLA, J., MOK, S., DAVID, J., PRICEMAN, S., WEST, B., BOLLAG, G., MCBRIDE, W. & WU, L. 2013. CSF1R signaling blockade stanches tumor-infiltrating myeloid cells and improves the efficacy of radiotherapy in prostate cancer. *Cancer Res*, 73, 2782-94.

YE, M., ZHANG, Y., GAO, H., XU, Y., JING, P., WU, J., ZHANG, X., XIONG, J., DONG, C., YAO, L., ZHANG, J. & ZHANG, J. 2018. Activation of the Aryl Hydrocarbon Receptor Leads to Resistance to EGFR TKIs in Non-Small Cell Lung

Cancer by Activating Src-mediated Bypass Signaling. *Clin Cancer Res*, 24, 1227-1239.

ZHANG, Y., GUO, L., LI, Y., FENG, G. H., TENG, F., LI, W. & ZHOU, Q. 2018. MicroRNA-494 promotes cancer progression and targets adenomatous polyposis coli in colorectal cancer. *Mol Cancer*, 17, 1.

ZHAO, D., LU, X., WANG, G., LAN, Z., LIAO, W., LI, J., LIANG, X., CHEN, J. R., SHAH, S., SHANG, X., TANG, M., DENG, P., DEY, P., CHAKRAVARTI, D., CHEN, P., SPRING, D. J., NAVONE, N. M., TRONCOSO, P., ZHANG, J., WANG, Y. A. & DEPINHO, R. A. 2017. Synthetic essentiality of chromatin remodelling factor CHD1 in PTEN-deficient cancer. *Nature*, 542, 484-488.

VITA

Rumi Lee was born in Republic of Korea. She received the degree of Bachelor of Science with a major in Life Sciences from Korea University in March of 2012. She received the degree of Master of Science with a major in Molecular Biology and worked as a graduate researcher for one year at the same school. In August of 2015 she entered The University of Texas MD Anderson Cancer Center UTHHealth Graduate School of Biomedical Sciences.

Permanent address:

18 Soratae-Gil, Anseong-Si

Gyeonggi-Do

Republic of Korea 17530